Integrity Of Packages And Contents Subject To Handling And Distribution Hazards

PhD Thesis

School of Engineering and Manufacture
De Montfort University
July 1998

Author: Jianyuan Sun

The following pages have been redacted at the request of the University;

Published papers after page 194

Abstract

The use of loosely packed items in rigid or semi-rigid containers is widespread. These packages are very often handled by high speed equipment and put in different environmental conditions which includes the possibility of mechanical damage, due to shock, impact and compression. So care must be taken that damage does not occur to both package and contents. The development of analytical and simulation techniques for investigating the dynamic behaviour of a package subject to handling and distribution hazards is becoming more possible by the use of a wide range of available software.

The modelling of the dynamic behaviour of packaging systems during handling and transport is achieved by mathematical analysis where possible and supported by computer simulation. The analysis was carried out for a range of body properties in order to test the results against experimental data. Investigations into the applied package force/motion and subsequent package impact and deformation were carried out with a view to gaining an understanding of the forces involved. The dynamic analysis was undertaken using commercially available software but it is necessary to develop special techniques to enable it to be applied to this type of problem.

Corrugated fibreboard containers subjected to internal and external loading will be subjected to stress, strain, deflection, and buckling to side panels. A Finite Element method of analysis of the panel was developed. The reaction of the panel to loading can be observed by means of this method. The failure of the container due to the loading can be predicted and the variability of the material and the panel can be changed arbitrarily to test and analyze different packaging designs.

Corrugated fibreboard and container elements were treated as engineering structures so the engineering concepts of stress, stain, equilibrium and compatibility could be applied. A Finite Element method using the ANSYS code made it possible to analyze

the structure behaviour and helps to partly solve the design optimization process for a corrugated container.

The project includes four main aspects:

1 Finite Element analysis of the corrugated fibreboard and container elements subjected to internal and external load.
2 Corrugated fibreboard material tests.
3 Modelling of a package-contents system
4 Simulation of the products-cushion-package system

The main area of research that is described in this thesis is concerned with developing the analytical and experimental methods to model and analyze the behaviour of packaging. This enables the size of the cushioning structure to be minimized and the cushioning and package material to be selected appropriately. The final stage of this project was to develop the techniques for the prediction of the susceptibility to damage to packaging systems particularly during the design stage, and to develop a comprehensive technique for the design and justification of the package system.

Acknowledgements

I wish to thank De Montfort University and the Department of Mechanical and Manufacturing for providing an atmosphere of learning and research, without whose support, this project would not possible.

My sincere appreciation goes to my supervisor Professor Jeffery Knight, the Head of the Department for his employing, supervision, and encouragement. I am very grateful to Dr. Hugh Newlyn, my second supervisor, for his guidance, encouragement, and keen interest.

Special thanks go to RASNA (UK) for experience and knowledge of Mechanica software Applied Motion.

Finally, I would like to thank Mr Lee Brown, Mr Colin Haslett, and Mr Bob Burdett for their help; also my thanks go to Dr Xu Wang for offering the references and all members of the Department of Mechanical and Manufacturing Engineering who have helped and assisted with this work.

Contents

Glossary of Terminology

Glossary A. Abbreviations

BCT	Box compression test
CD	Cross machine direction
CSSC	Centre special slotted container
DOF	Degree of freedom
ECT	Edge crush test
FR	Flexural rigidity
MD	Machine direction
RSC	Regular slotted container
WCS	World co-ordinate system

Glossary B. Important Symbols

c	Damping coefficient
b_t	Distance between liner supports
d_0	Equivalent linear displacement
d_b	Maximum available displacement
d_m	Maximum displacement of packaged article
D	Flexural rigidity
D_x	Flexural rigidity in machine direction
D_y	Flexural rigidity in cross machine direction

Glossary of terminology

E	Young's modulus
F_c	Coulomb friction
F_s	Static friction
g	Acceleration of gravity
G	Value of acceleration in terms of multiples of gravity 'g'
G_0	Maximum acceleration in terms of multiples of gravity 'g' under linear cushioning
G_m	Maximum acceleration of packaged article in terms of multiples of gravity 'g'
G_s	Shear modulus
I	Second moment of area of cross section
k, k_0, k_2, k_a	Spring stiffnesses
k_b	Buckling coefficient
m_2	Mass of the packaged article
M_x, M_y	Moment acting on any section of a plate parallel to the XOZ and YOZ planes
P	Force acted on packaged article
P_m	Maximum force acted on packaged article
q_{dt}	Relative velocity between sliding surface
Q_x	Shearing force along X direction
t_c	Thickness of a plate or corrugated fibreboard
t_f	Thickness of fibreboard liner
U_k	Coefficient of sliding friction

Glossary of terminology

U_{ratio}	U_s/U_k
U_s	Coefficient of static friction
V_{latch}	The velocity where static friction transfers to coulomb friction
W_2	Weight of packaged article
β_2	Fraction of critical damping
γ_{xy}, γ_{yz}	Shearing strain in any section of a plate parallel to XOY, YOZ planes
ε_x, ε_y	Strain in X and Y direction
η	Plasticity reduction factor for elastic modulus
E_t	Plastic modulus
λ	Slenderness ratio
σ_x, σ_y	Stress in X and Y direction
σ_{cr}	Critical buckling stress
$\sigma_{cr,el}$	Critical compressive stress
τ_{xy}	Shearing stress in any section of a plate parallel to XOY plane
ν	Poisson's ratio

Chapter 1

Introduction

1.1 Background

The importance of packaging within industrial and commercial environments is becoming increasingly significant. Packaging, along with better transportation, has made it possible to centralize production facilities and take advantage of the economies of large-scale operation. The product and the package are becoming so interdependent that they cannot be considered one without the other. The amount of money being spent in USA for packaging exceeded $52 billion in 1984[1]. The production of corrugated board, the dominant transport packaging, is approaching 25 billion m^2/year in Europe in 1996[2]. The growth of packaging has to some extent outrun the technology. The people in this area must lean heavily on periodicals to keep abreast of the rapid changes, and they often have to develop their own disciplines to suit the situation at hand. It has also become necessary to borrow from the other sciences to supplement the meagre knowledge that has been accumulated in this field, and the skill of the packaging designer in making intelligent decisions depends on knowledge of many fields and experience within the packaging industry.

People with the responsibility for making recommendations and influencing decision making need all the knowledge and skill they can muster, since packaging accounts for an increasing share of the cost of goods. Furthermore, they should approach their task with an open mind and a broad perspective if they are to take full advantage of the great variety of materials and techniques that are available. It is to miss the opportunities that exist for true accomplishments in a dynamic and progressive field if one is to become preoccupied with routine solutions to problems.

The knowledge related to packaging which has come into existence might be considered as the foundation for a technology which will take its place with the older established sciences. Food technology, for example, is getting increasing attention, it is largely concerned with the preservation of foods by packaging and processing, with the emphasis on maintaining quality in addition to simply preserving the product. Chemical engineering, industrial engineering, and mechanical engineering are also focusing a large share of their efforts in this direction. Out of this will eventually come a unifying system for applying the fragmentary operations of each of these disciplines to the total problem of delivering goods to the point of use with maximum efficiency.(see Figure 1.1)

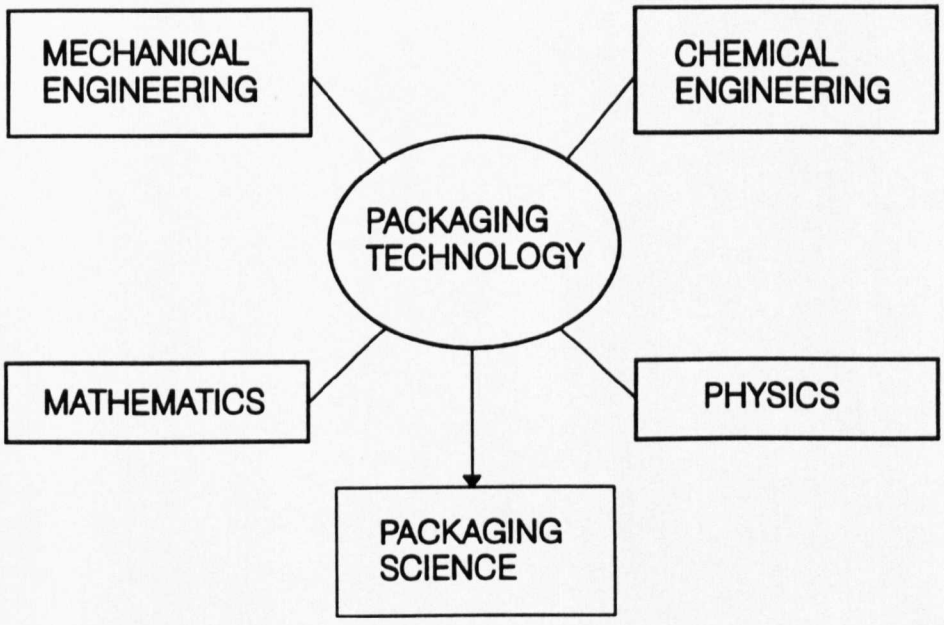

Figure 1.1 Packaging Technology

Current methods for the handling and distribution of goods are such an essential factor in package design that there is a need for more modern techniques to be used for analysis in order to increase the efficiency of production and distribution.

Some studies investigating the impact behaviour of rigid or semi-rigid packages have already been reported in the literature. So far, however, most of these investigations have concentrated on methods for evaluating the quality of these containers, which include the Mullen burst test, the puncture test, the compression strength test and the fixed and floating test[17,18,19]. There is still a strongly felt need for a further understanding of the mechanical behaviour of containers subjected to external force or impact, especially with contents inside.

1.2 Research objectives

The main aim of this research was to develop techniques for evaluating the susceptibility to damage of a package and content subject to handling and distribution hazards, to minimize the size of cushion structure, and to choose the appropriate packaging material, with a view to making recommendations to handling machinery designers that will improve the security and integrity of the package and contents. The hazards are limited to the most important mechanical damage due to shock, impact, compression. To achieve this aim the following objectives have to be met:

1 To develop the techniques for modelling the interaction between content/content and content/package. This is to be achieved by mathematical analysis supported by computer simulation.

2 Analysis of the dynamics of a package with discrete content to be carried out using the interaction results achieved in 1.

3 To develop the computer simulation techniques for the product-cushion-package system with real characteristics and properties, and to simulate the environmental conditions as accurately as possible. The characteristics of the system can be selected arbitrarily and changed easily so that the simulation techniques will play an integral role in design procedure.

4 To develop the analytical tools and simulation models for testing of the structure and mechanical behaviour, and for design of corrugated fibreboard and container.

1.3 The layout

The scope of development of packaging and the relevant and current research in the area is given in the 'Literature Survey and Review of Packaging' chapter. A state of the art account of packaging is also given in this chapter. The definitions of packaging is given in the 'Specifications and Functions of Packaging' chapter, which is intended to give a description of the performance requirements and the functions of packaging, such as containment and protection.

The basic knowledge of corrugated fibreboard and container is presented in 'FEA of Structural Behaviour of Corrugated Fibreboard Container' chapter, a Finite Element Analysis of corrugated fibreboard and container is given in this Chapter, in which the deformation, stress, strain and buckling of the fibreboard and container are investigated. The experimental work of fibreboard and container element is also presented in this Chapter.

In 'Modelling of the Collision between Package and Contents' chapter, an analysis and simulation of a package-content system is presented, in which both rigid and flexible impact behaviour of the system are investigated. The kinematics and dynamics of the

package-contents system is investigated in the 'Simulation of the Interaction between A Package and Its Contents' chapter. Some simulation techniques for 2D and 3D models are developed in this chapter. A model of the package with cushion and content is set up in 'A Model of Product-Cushion-Package System' chapter. The drop test is carried out by computer simulation, the measure of the damage to the packaging system is discussed, the methods of cushioning are also investigated. In 'Analysis of A Packaging System' chapter, the cushioning with different elasticity is discussed and simulated, the affects of cushioning, damping, friction on the product are investigated. Finally comes the 'Conclusion and Further Work' chapter.

Chapter 2

Literature Survey and Review of Packaging

2.1 Introduction

Packaging has many faces. Its more familiar forms include metal and corrugated containers, flexible packets and paper cartons. There are three broad categories that require very different technologies for their accomplishment: (1) consumer packaging, (2) industrial packaging, and (3) military packaging. The first is concerned generally with small units in large numbers. Industrial packaging, in contrast, is usually made up from a large and heavier unit. The third category is a highly specialized type of protective packaging in which all the elements have been worked out and documented in the most intricate detail.

2.2 Transportation and Handling Environment

Packaging engineers and designers would be in a better position to allow for the "transportation and handling environment" if they had a more detailed knowledge of the hazards involved and a better definition of these vague and general terms. The "environment" encompasses storing, materials handling, and shipping. Each of these involves time, temperature, relative humidity, and weather conditions such as rain, snow, and condensate moisture. Transportation involves a variety of modes, rail, truck, air, and ship, or combinations of these. Each mode in turn subjects package and contents to different combinations of vibration, shock inputs, etc., and each commodity or product has a different degree of susceptibility to these conditions. Of all aspects of the "environment", handling is the most difficult to define and describe.

A combination of growing awareness of the need for information, increasing

availability of mechanical and electronic measurement devices, and the advent of computers to process the resulting data has in recent years produced a body of literature in this area, a brief survey of which is given below. What is now available suffices to give a reasonable clear outline of the nature and magnitude of the factors involved.

2.3 Scope of corrugated packaging

2.3.1 The history of corrugated fibreboard package

The most common type of package being used commercially today is the corrugated box. The first patents for making corrugated paper were recorded in England in 1856. The first to use a box made of double-lined corrugated board was a cereal manufacturer, who in 1903 got acceptance in the official freight classification for this type of shipping container. By the end of World War I about 20 percent of the boxes were corrugated or solid fibreboard, and 80 percent were of wood construction. By the end of World War II these figures were reversed[1]. In the 1950s and 1960s corrugated board showed very high growth rates throughout Europe. Production increased on average by some 13 percent annually[2]. The UK consumption of corrugated fibreboard used in packaging in 1985 was valued at £746m. It added up to 1, 545, 000 tonnes and covered an area of 2, 865, 000 m^2[3].

2.3.2 Classification and standard grades of corrugated fibreboard

The research on the performance of corrugated fibreboard became necessary in 1914 when the use of them for shipping began to grow. To control damage during transportation, some rules, regulations, and specifications were established[4]. Various methods for evaluating the quality of corrugated board were developed. These include the Mullen burst test(see section 4.3.1 for definition), the puncture test, the short

column edge crush test, and the flat crush test. These procedures were used by boardmakers to evaluate the quality of board based on weight, thickness, and Mullen burst test. It was assumed that container performance was determined by these factors alone.

Although these attributions were convenient for use in establishing a grade structure, they were not directly related to corrugated package performance. This fact has been the centre for debate over changing the test methods for evaluating corrugated package performance. Various researchers like Scott[5] and King[6] all agreed that the currently required measures of basis weight, calliper, and Mullen burst test should be accompanied by a short column edge crush test, if not entirely replaced by it. Justification for regarding edgewise compression as the best currently available measure of corrugated fibreboard quality is based on several observations: 1. It is the most important input into the widely recognized box compression strength prediction formula of McKee, Gander and Wachhuta[7]. 2. It is the board property which has the closest relationship with box performance as determined in the international and intercontinental transport trials conducted by the Swedish Packaging Research Institute[6]. 3. Work at the Institute of Paper Chemistry has shown corrugated fibreboard box panels subject to internal pressure(as from the box contents bulging the panels outwards) result in compression type failure. This provides evidence that board compression strength is important apart from its contribution to box compression strength.

Currently, the Uniform Freight Classification Committee[8] does not require compression strength values. Most companies, however, do require an edge crush test in their specification for corrugated packages. In Europe, the edge crush test is fully accepted as the criterion of corrugated package performance[9].

2.3.3 Box compression strength and edgewise strength

Even with all of these material specifications, however, box compression strength(BCT) is the most commonly used test to assess stacking capacity of the packaging. It depends on the size and shape of the box, and the distribution of load on the top of the box. Simplified empirical formula (see section 4.3.2) developed by McKee [7] allows the calculation of BCT from the edge crush strength(ECT) of the material, flexural rigidity in machine direction(MD) and cross direction(CD) of the material and the perimeter of the container(Z). This formula has been widely accepted and is currently in use. The BCT has also been studied at length under various conditions. Tests have been performed with corrugated packages conditioned to hot and cold temperature extremes as well as high and low relative humidities[10]. Cavlin[11] devised a new method for measuring the ECT of paper. He designed an instrument to avoid buckling of the test strip. Standard methods for deriving ECT of corrugated board have been made. Amongst the significant contributions to the literature on the subject are papers by Stott[12], Eriksson[13,14] and Kroeschell[15]. Stockmann[16] and Peterson[17] developed a new method for measuring the intrinsic edgewise compressive strength of paper which is, not a structure, but an intrinsic physical property of the material.

McKee[18] described that top-load compression strength of a vertical flute, corrugated box depends largely on the edgewise compression strength of the combined board in the cross-machine direction and to a considerable extent on the flexural stiffness in both principle directions of the combined board. Flexural stiffness is the ability to resist bending. Differences in compression strength of A, B, and C flute boxes are mainly due to the differences in flexural stiffness of these constructions. The definition of A, B and C flute is given in section 4.2.4. Flexural stiffness depends primarily on the modulus of elasticity and calliper of the liners and on the square of the combined board calliper. One of the many beneficial effects to emerge from

McKee's work was the realization that the correct method to measure flexural stiffness is by the four-point rather than the three-point beam test. Another was the proof that calliper of combined board is highly correlated with flexural stiffness.

2.4 Dynamics and performance of packaging system

The need to protect packaged products against "shock", one of the hazards of transportation and handling environment, has long been recognized. Hence "cushioning" was, therefore, the earliest subject to receive attention. The pioneer effort and the first fundamental work was that of Mindlin[19]. An early paper,"Application of the Properties of Cushioning Materials in the Design of Cushion", which included work in corrugated fibreboards was published by Kellicutt.

From the earliest days to present, the armed services had both the incentive and the means to investigate the problem of shock inputs in various transportation modes. Weiner gave a paper on "Military Packaging in the United States"[20]. Among other things, it included a table (Table 2.1) showing shock loads experienced for various types of transport and associated vibration frequencies[21].

2.4.1 Dynamics of packaging system

Mechanical damage is a common occurrence in the transportation of packaged articles. The causes of failure are generally inadequate protective cushioning, lack of strength of the outer container, or occasional abnormal weakness of the packaged articles. The first and second of these problems are the most common. The ability of a corrugated fibreboard box to protect its contents is related to its compression strength. The corrugated container industry has been manufacturing corrugated fibreboard according to bursting strength and basis weight specifications. These specifications do not accurately reflect the ability of a box to meet performance

requirements in the distribution environment. Singh[22] investigated the effect of package weight and the handling environment on the reduction in compression strength of corrugated fibreboard containers. The mean compression strength and corresponding deflection values for three box sizes were evaluated as a function of drop height and package gross weight after handling. The compression strength decreased as the package weights increased and as the drop heights increased. He also analyzed the compression of single-wall corrugated packages by using fixed and floating test platens[23]. It is found that the difference between the compression strength using fixed and floating platen methods to be small compared to the normal variation in compression strength between two identical boxes.

Table 2-1 Shock loads and vibration frequencies for various types of transport

Type of transport	Shock loads, g	Vibration frequencies, Hz
Air		
Normal	2 to 3	60 to 200
Maximum	8	
Road		
Rough surface	6	1 to 15
Maximum	8	
Rail		
Normal travel	1 to 1.25	2.5 to 7.5 on bed
Switching	7 to 12	50 to 65 on frame
Bumping	20	
Ship	1	5 to 25

There should also be consideration given to the dynamic loading that occurs during normal distribution and product handling. It is found that the compression strength of corrugated boxes increased after exposure to vibration in a stack. He attributes this to the evening of the corner heights due to vibration which allows each corner to offer equal strength. It is reported an 8% increase in top-to-bottom compression strength

due to vibration. Singh also investigated the effect of mechanical shocks on the compressive strength of corrugated containers. The results show that as much as 75% of the original compressive strength can be lost after multiple handling.

Sayir[24] studied experimentally the impact behaviour of corrugated sheets of short fibre-reinforced cement on the basis of measured time function of impact force and structure displacement. The results were compared with those obtained from a newly developed model which simulates not only the local dynamics of the impact of a rigid spherical object on a thin flat elastic plate but also considers coupled membrane modes of motion due to the curvature of the corrugated structure. Butler[25] described that the impact tests on containers are carried out using either a large drop test facility or a compression air gun known as the Horizontal Impact Facility(HIF). Mindlin[19] developed the theoretical analysis of packaging cushioning. He was assuming that the outer container is adequate, the survival of a packaged article in a drop test still depends on a large number of factors descriptive of the mechanical properties of both cushioning medium and the package item.

2.4.2 Structure performance of fibreboard container

Corrugated fibreboard and the container can be classified as complex structures to which the engineering concepts of stress, strain, equilibrium, and compatibility can be applied. Fox[26,27,28] has successfully demonstrated that the corrugated fibreboard can be treated using the conventional methods of engineering mechanics. Engineering analysis will provide a basic understanding that will enable designers to predict container performance in advance of actual fabrication and testing of their designs. Furthermore, fundamental properties that govern container performance can be identified. Then efforts can be focused on controlling and improving these key properties for optimum enhancement of performance. He believes that the

performance characteristics of containers are influenced by their fibrous components, the mechanical and physical properties of the linerboard and medium, the structural properties of the combined board, and the container design.

Peterson[29-33] pointed out that the key property that governs container performance is linerboard compressive strength. Production control of compressive strength and product specifications based on the compressive characteristics will directly reflect container performance characteristics. Performance was studied for three loading modes, internal load, external load, and internal plus external load. The basic approach has been to derive mathematical models of the container panels under these loading conditions and then verify these models with experimental tests.

The engineering approach will provide the basis for developing a unified container performance and failure theory. This theory will give the analyst three powerful abilities: 1. Performance can be predicted for containers made of conventional liner and medium and conventional in design. 2. Fundamental properties that govern container performance can be identified. 3. The theoretical model will suggest how containers should be configured to obtain optimum performance for specific end use.

2.5 State of the art

Most of the progress in packaging in the past has been by trial-and-error methods. There is a great need for a more reliable basis for decision making, and this can come only from research in sufficient depth to give a solid foundation to the techniques required. Some studies of the static and dynamic stress involved with the handling and physical transfer of packaged merchandise have been made by various researchers [32,33,34], especially on determining the various parameters used in the formula by McKee[8]. Koning[34] developed a theoretical model defining the relationship between the linerboard characteristics and the corrugated container. In development

of the model, the most important linerboard characteristics must be determined. These include maximum strength, modulus of elasticity, and the overall shape of the stress-strain curve.

Recent works [32,33,34,35,36] have however underlined the limits of the use of the relationship and showed the need for advanced modelling using the orthotropic plate instability theory. Plooy[35] was engaged in an investigation of the inter-relationships between strength properties of liner, fluting, corrugated board and the resultant box, with the objective of making the best economic use of raw materials for manufacture of corrugated container.

Technical data from transport studies indicate quantitatively the stresses involved vary significantly. Studies reported by the U.S. National Safe Transit Association provide package designers with helpful quantitative data on the relative comparative stress involved in distribution.

Most of the studies on packaging, at present, are based on testing and experimental method. This can lead to lack of predictability and limited exploration. So the use of computer software and simulation analysis is becoming necessary and important. Fortunately there are some researchers who have been working in this area using CAD and computer simulation. Geibler[37] presented a method of calculating mechanical loadings on a product-package system by CAD. A finite element analysis is used to determine the frequency response that characterizes the damping behaviour of the cushion structure. More recently, the research by Pommier[38] has introduced a Finite Element Method using computer software to partly solve the optimization process of the components of corrugated fibreboard container.

2.6 Summary

It can be seen that the use of corrugated fibreboard has a long history. A great amount of work has been carried out on investigating the behaviour of the containers subject to different loading. Some representative work reported is reviewed here in order to set up the background for this research.

The rules, regulations and specifications were established to control damage during transportation and handling. These will be discussed in Chapter 3 and Chapter 4. Among them the box compression strength has been identified as the most important test to assess the stacking capacity of the container.

The analysis of the possible mechanical damage of the packaged content is focused on the properties of the cushioning and the container. The study of the structural performance of the container material makes it possible to consider how the container should be configured to obtain optimum performance for special end use.

It also can be seen that computerized analysis methods for packaging design are urgently needed and require a great amount of work to be successful.

Chapter 3

Specifications and Functions of Packaging

3.1 Packaging specification

The specification is the document against which packaging materials or components should be ordered, supplied and verified[39]. It is a technical definition of a package and/or packing process. It should communicate enough information so that the supplier can make it, and a manufacturing department can use it for packaging. Specifications can be drawn up in several ways:

a) By specifying the style and size of the package, the grade of materials from which it shall be made, tolerances and other details of manufacture.

b) By specifying the performance requirements of the materials which are used to manufacture the package.

c) By specifying the handling and machinery(process) requirements.

d) By defining the requirements in terms of total package performance in distribution and storage.

Generally specifications can take two forms, Materials Specification and Performance Specification. A combination of these two specification formats providing a good recommended or preferred material in combination with performance criteria often provides all parties with the most acceptable arrangement. These are often reinforced by general specifications referring for instance to storage and handling conditions, and slot depth for corrugated containers. In addition, specification for the procedures detailing packing requirements , palletisation, pallet load labelling and, quality assurance may also be required.

3.1.1 The performance requirement

Packaging requirements are drawn up to insure, as far as possible, that a package will perform its function, ie contain, protect and communicate the product[1].

Containment is concerned with containing and presenting a product in a form which is convenient to manufacturers, carriers, distributes and customers. It will be influenced by factors such as filling, packing and unpacking, handling, movement, storage, dispensing, and after-use by the final recipient.

Protection is concerned with providing the product with a package of sufficient resilience, durability and resistance to withstand the environment and prevent product damage.

Communication is concerned with providing the relevant information about the product image, storage, distribution, destination and use.

Performance in distribution and storage is concerned for the most part with the containment and protection functions of the package.

Definition of these performance requirements necessitates a thorough understanding of the distribution and storage systems and the factors affecting the containment and protection functions.

3.1.2 Factors affecting containment and protection

Containment and protection are influenced by general environmental conditions which include five main groups: Mechanical, Climatic and Physical, Chemical, Biological and Human. The mechanical group includes impact and compression and these are the

factors to be investigated by this research.

Besides the environmental conditions, the size, shape, and weight of the outer container can have considerable effect on the hazards encountered during processes, and different methods of handling and transport.

The likelihood of a hazard exceeding a certain level is also most important. For example, the chances of a package being dropped from above a given height must be considered when providing protection against drops and assigning a performance level on a specification. Protection against and specification for the very rare or accidental drop from a great height may not justify the increased cost of the package; and a small percentage of damaged goods can often be tolerated, and may be preferable to increasing the cost of the package. Protection is required against the normal hazards and not those which occur during mishandling.

3.2 Functions of packaging

No matter which way the purpose of packaging is analyzed, the answers should always be the same. The function of a packaging system is basically to contain, carry, and dispense. Shells and the skins of animals served as packages for these purposes for primitive man. As time went on, other requirements were added, such as to protect and measure, and later to communicate and to display. People have now entered into an era in which the package is called upon to motivate, promote, glamorise, and sometimes to build up the contents.

3.2.1 Containment

To transfer a particular product, for example a powder, from the place of manufacture to the point of use requires some kind of container. At the manufacturing stage the

product is usually in a bulk tank of some type. It then becomes necessary to subdivide it into more convenient units for transportation and handling. Without the means to contain a powder product it would be impossible to transport it beyond the point of origin. At the retail level, it is usually necessary to reduce the size of the units even further to accommodate the demands of the trade.

3.2.2 Carry

There is a system which has been widely accepted that includes a reduction in size of the units produced at the manufacturing plant. The production is put into small boxes or bottles, which is then gathered into groups and further repacked into cases for shipment out of the manufacturing plant. Thus reducing the size of the unit to be handled at each stage. The function of carrying is accomplished more effectively toward the point of ultimate use.

3.2.3 Measurement

The advances that have been made in prepackaging goods have produced some additional benefits. One of these is the opportunity to standardize the quantity of material in a package to obviate dealing with arbitrary amounts of goods. The package therefore becomes a measuring device in addition to its other functions.

3.2.4 Protection

Using the package for the purpose of protection is a significant aspect. If a product is damaged during distribution due to the improper packaging, the manufacturer will suffer economically.

3.2.5 Communication

The function of communication of packaging has become an important factor. Symbols, marks, and slogans are used to help the manufacturer communicate with the consumer. They may also take the form of instructions, warnings and, guarantees. This is especially effective since the message remains with the product through all stages of transportation, barter and consumption.

Chapter 4

FEA of Structural Behaviour of Corrugated Fibreboard Container

4.1 Introduction

The corrugated fibreboard container within the packaging industrial is becoming increasingly significant[2,3]. The study of corrugated fibreboard and containers has been targeted to develop a better understanding of the structure and mechanical behaviour in order that corrugated container performance can be predicted.

Corrugated fibreboard and containers were treated as engineering structures so the engineering concepts of stress, strain, equilibrium and compatibility can be applied. Use of the finite element method using the ANSYS code makes it possible to analyze the structural behaviour and partly solve the design optimization process of corrugated containers.

In the case of corrugated fibreboard it is justifiable to assume the simplifications associated with the applied elasticity approach on thin plate behaviour[56]. Essentially, this approach neglects through thickness of the plate including shear strain. In addition, linear elastic behaviour is assumed for the material, which allows the use of the existing metal-based analysis procedures, after minor modification to allow for orthotropy of material properties for the analysis of corrugated fibreboard structures.

4.2 The basics of corrugated fibreboard and containers

4.2.1 Box construction

The proper name for a fibre shipping container, if you want to be precise, is a box

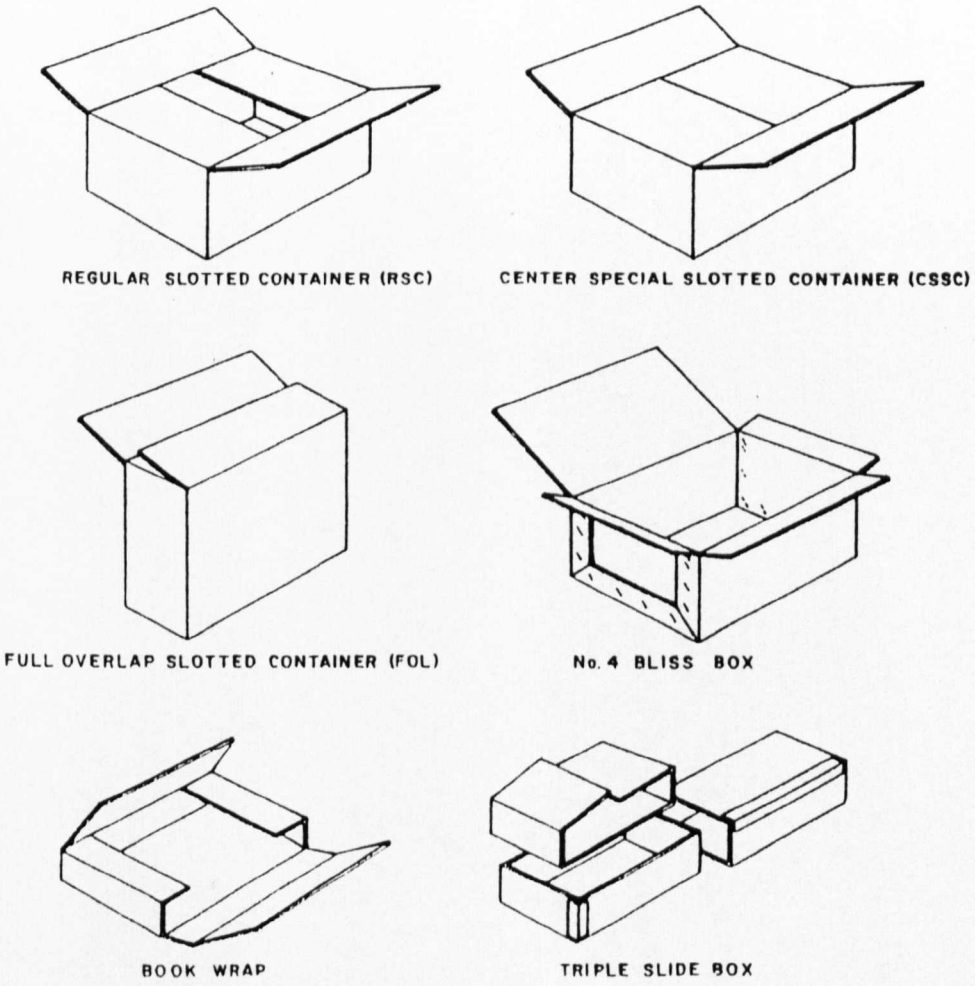

Figure 4.1 Styles of corrugated boxes

rather than a carton or a case. The most frequently used style of box is the "regular slotted container", generally referred to as an RSC, in which all the box including the flaps is manufactured from a single piece of fibreboard and is shipped flat to the user's plant(See Figure 4.1). Corrugated fibreboard is either single-faced, that is, a flat sheet of paper to which has been glued another sheet of corrugated paper (or "medium" as it is known), or double-faced, in which case a flat sheet is glued to both sides of the corrugated medium. It is also possible to get double-wall or treble-wall board by alternating additional layers of corrugated and flat sheets. The flat sheets, or facings, will vary in thickness according to the strength required, but the corrugated medium is nearly always 0.23 mm in thickness and weighs 12.66 kg/100 m^2.

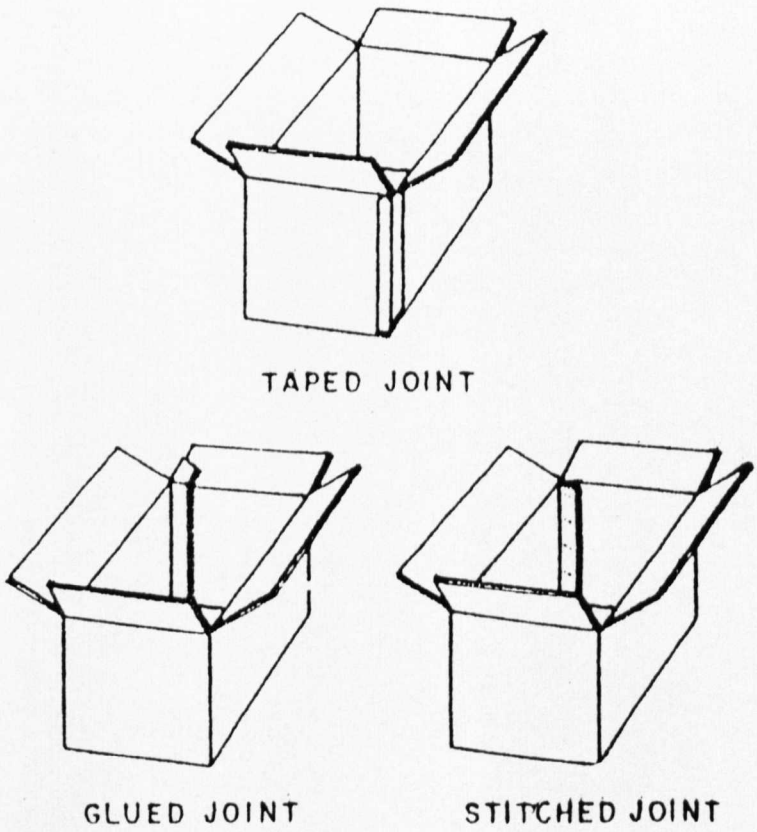

Figure 4.2 Manufacturer's joint styles

Both outer facings are usually the same weight, but occasionally they are "unbalanced". Such an unbalanced sheet has a tendency to warp and may be difficult to handle, either in the box maker's plant or at the point of assembly. For this reason it is to be avoided unless there is a very good reason for using it.

4.2.2 Manufacturer's joint:

The ends of the box blank are brought together and joined by what is called the "box manufacturer's joint". Three methods for making the joints are commonly used: taped joints, glued joints, and wire-stitched joints(See Figure 4.2). The cost is about the same for all three. The tape that is used for making a taped manufacturer's joint is different from the tape that is applied to the flaps in closing the box, and it is considerably stronger. A taped joint makes a box that is smooth inside and out, but it is not as strong as a stitched or glued joint. The glued joint is the strongest of all, in most instances.

One disadvantage of a glued joint or a stitched joint is that it will have a hump with a sharp edge where it overlaps. Although the corrugations are crushed at this point in the manufacturing process, the extra thickness will sometimes cause excessive abrasion of the contents. If this is a problem, the lap can be put on the outside. Another disadvantage of stitches is that they will sometimes rust.

4.2.3 Corrugations

Normally the direction of the corrugations in a box is vertical, to provide the maximum stacking strength. Interior corrugated parts generally have the corrugations vertical also, although a liner will sometimes have the corrugations in the horizontal direction to withstand the shock from sliding down chutes and from being carried on conveyors, or from damage in transport. Actually the difference in the strength of

vertical and horizontal corrugations is not very great; table 4.1 shows that B-flute board really has more stacking strength horizontally.

Table 4.1 Stacking strength with horizontal corrugations or stacking on side

A-flute horizontal	80 percent of A-flute vertical
B-flute horizontal	120 percent of B-flute vertical
C-flute horizontal	90 percent of C-flute vertical

4.2.4 Flute selection

The corrugated fibreboard has been divided into different flute types as A, B, C flute. The flute types are defined by their height and the number of flutes per unit length. Based on these properties, the take up factor is determined. The take up factor defines the length of medium material used in a corrugated board structure compared with the length of facings (Table 4.2). The A flute corrugated fibreboard has more paperboard per inch of width than either B or C flute made of corresponding materials. Take-up factors of approximately 1.54, 1.36, and 1.48 have been reported for A, B, C flute respectively according to Kellicutt and Landt[38]. As A-flute is the thickest of the three boards, more corrugating medium is required to form the flutes than in either B or C flute. Similarly, C flute corrugated board requires more material than Bflute board. Thus if one considers just the amount of material present, it would be expected that A flute would be slightly stronger than C flute and C flute slightly stronger than B flute. But this is contrary to empirical data.

Table 4.2 Flute configurations in corrugated board

Flute	Flute height (mm)	No. of flutes(m/per)	Take up factor
A	4.70	110	1.54
C	3.61	129	1.48
B	2.46	154	1.36

Maitenfort[41] reported the results of an interlaboratory evaluation of the short column crush test. This evaluation revealed that for equal weight components, the

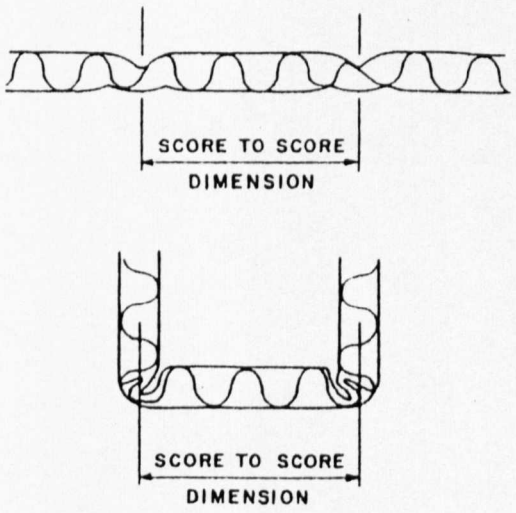

Figure 4.3 Allowance for scoring

edgewise compressive strength of B flute specimens was higher than C flute, which in turn was higher than A flute. McKee and others [7] also recognized this trend and stated that there was "theoretical grounds for expecting the edgewise compression strength of combined board to be in the order of B flute greater than C flute and C flute greater then A flute.".

Whether A, B, or C flute is used depends upon the type of contents, particularly their fragility, density, and self-supporting characteristics. If top-to-bottom compressive resistance is important, as in the case of nonsupporting products stacked to a great height in the warehouse, A flute is the proper choice. Fragile articles also will receive better cushioning from A flute fibreboard, except in cases of high density that may indicate a higher flat crush value. (See Table 4.3) For greater crush resistance, B flute, with more lines of contact between the corrugated medium and the facing, is a better choice. It also has greater strength at the score line, where canned foods have a tendency to tear out, and better end-to-end crush resistance. For very small boxes, B flute folds more easily and makes a neater-looking package. For interior parts, A flute is usually more serviceable because of its greater thickness and better cushioning properties, but the density of the contents must be taken into account to prevent complete collapse of the corrugations under impact.

A compromise between A and B which is growing in popularity is a C flute construction. This gives reasonable good stacking strength and a fair amount of stiffness. For average types of loads it is a good choice, and it often is easier to get because of its wide use.

Table 4.3 Flat crush value

Flute	Flat crush (N/m^2)
A	310.1
B	392.7
C	344.5

4.2.5 Scoring allowances

When corrugated fibreboard is scored and folded at right angles, the centre line of the sheet will intersect the score line; that is, half the thickness of the board will be on one side of the score line and half will be on the other side.(See Figure 4.3) Therefore, when the sheet is folded into a rectangle to form a box, the inside dimensions will be less than the score-to-score dimensions by an amount equal to one thickness of board. Likewise, the outside dimensions will be greater than the score-to-score dimensions by one thickness of board. For a given inside dimension, the scores should be one thickness farther apart. When the board is folded on the score lines, the scoring dimension falls in the centre of the wall that is formed.

4.2.6 Optimizing package dimensions

Every shipping container has a combination of dimensions which minimizes the amount of board required to enclose a specific volume. For a regular slotted container the relationship of length:width:depth (L:W:D) is known to be 1:0.5:1,according to Maltenfort[48], a fact which is periodically rediscovered and reported in the literature. Unfortunately, it is seldom necessary to select the shape of the box without regard to

stacking, palletizing, handling,etc. Therefore, minimum board area is frequently not synonymous with "optimum" box, and finding the optimum board area formula is, however, part of every box designer's basic information. The subject is properly covered by Maltenfort[43,44,45].

Minimizing board area can also affect shipping container performance. In looking for a shipping container that will stack properly in a warehouse, give the product the needed protection, lend itself to palletizing, and go through an automatic sealing line, people may find that use of the maximum amount of board, rather than the minimum, is really the most economical when you consider all factors. At other times you have to compromise between the minimum board area and maximum performance. In each instance, you must take into account the needs of the product. Clearly, if you have a fragile product packed in an regular slotted container and stack the boxes end-to-end(because in this direction you get the most compression strength), then you must choose a box as nearly square as possible, rather than one with a small a ratio(a=W/L) Maltenfort[46-48]. This is true because the width dimension is the most critical in end-to-end compression.

You must also consider that optimizing package dimension to minimize board requirements can affect the appearance of the box. Thus if your merchandising requirements are adversely affected by the redimensioning process, or perhaps the over-all appearance is less pleasing to the eye, then you may well choose to sacrifice the minimum board area savings. In any event, in the redimensioning process you must take into account the full function of the package.

4.3 Test of Corrugated Fibreboard and Container

An essential part of any packaging program is the testing and evaluation of the

complete packaged unit, as well as the various components. It is good economics to determine the optimum design in the beginning and to maintain uniform performance throughout the life of the package. A good test program will indicate the results to be expected in the field, and good management demands an objective evaluation of every step in the packaging operation.

There are many different kinds of tests, but one of the main categories is preshipment testing of new packages to determine their resistance to the hazards of transportation and storage. The most primitive method of evaluation is the staircase technique. By tumbling a package down a flight of stairs it is possible to find the principle weakness in a shipping unit. This is one of the oldest known preshipment tests, and it is still being used in some places.

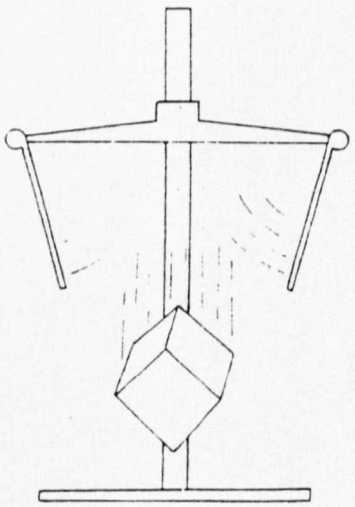

Figure 4.4 Drop tester

A number of testing machines have been developed which are intended to simulate shipping hazards and which will give reproducible results. There are "drop testers" which facilitate accurate positioning and precise distances for edge and corner drops. (See Figure 4.4) Typical tests would be on a bottom corner, bottom edge, flat bottom, flat end and vertical edge, for a total of five drops. A package is positioned on a drop table, either flat or at an angle, at the desired height. A latch is released to allow the table to swing out of the way, under spring pressure, permitting the package to fall freely onto a hard surface.

A "vibration tester" is a table which can be oscillated at various frequencies. The usual method is to adjust the frequency until the package starts to leave the table. (See Figure 4.5.)An average test would be 45 minutes at 230 cycles per minute. Package is placed loosely on shaker table. Frequency of vibration is increased until the package starts to leave the table, as determined by sliding a piece of paperboard

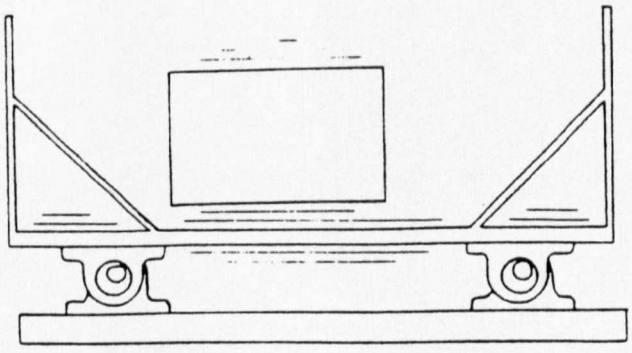

Figure 4.5 Vibration machine

under the package as it bounces. Test is continued at this frequency for the required time.

An "incline-impact tester" is designed to duplicate the effects of rail transport handling. The results are similar to the drop test, but the shocks are applied only to the flat surface. A package is placed on a dolly on a sloping runway, pulled up a 10^0 incline for the required distance, and allowed to ride down until it strikes a solid wall. (See Figure 4.6) A typical test would be one impact on each of the six sides from a distance of 1.5m up the incline(9.7 kph at impact).

In addition, commercial laboratories and some academic laboratories have more sophisticated equipment which can perform drop tests onto surfaces with different hardnesses and resiliencies, and vibration can be cycled through various frequencies, called a "sweep". This may be important if there is a natural or resonant frequency in the package itself or its contents which could be amplified. Strain gauges and accelerometers may be used to provide a permanent record.

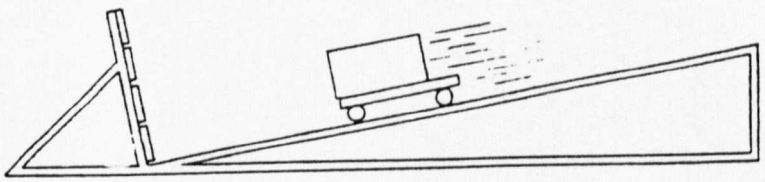

Figure 4.6 Inclined-impact tester

Stacking or compression tests are easy to set up, since such a test requires only an applied load over a period of time. For storage in a warehouse, a single package should be able to withstand its own weight multiplied by the number of tiers in a normal warehouse situation for 30 days or more. For a test of one hour the load should be three times as much, to allow for fatigue and variations in humidity. If an average-size box compresses more than 50 mm,. or the sidewall bulges more than 6 mm, the box is close to failure.

4.3.1 The existing tests

There are many kinds of tests for many different purposes. The concern here is with tests to be used in the development of the package structure. Quality control is a highly specialized area which makes use of probabilities and statistics to apply limited information to large amounts of material. Process tests are used to judge the merits of materials or structures in the course of their fabrication, so that adjustments can be made toward a more suitable end product.

The following contains a brief description of some of the methods used for evaluation of package and packaging materials.

1. **Drop**. A Fibreboard box, prepared as for shipment, is dropped on one bottom corner at the joint, on the three edges radiating from this corner, and on the three flat faces adjacent to this corner.
2. **Compression**. A fibreboard box is sealed as though for shipment, usually without contents. A uniformly distributed load is gradually increased until sudden buckling occurs.
3. **Flat crush**. At least ten tests pieces of material of width 12.7 mm and of length 150 mm are cut, the length being in the machine direction. Flat crush resistance is the

maximum force that a test piece will withstand before the flutes collapse.

4. **Incline impact**. A dolly is pulled up a 10^0 incline until it is 914 mm above the floor. a package is placed on the dolly and allowed to ride down until it strikes a solid wall at floor level. This is to determine the resistance to horizontal impact.

5. **Burst(Mullen test)**. Pressure required to force a rubber diaphragm through a round hole against a specimen of fibreboard firmly clamped around the edges of the hole. Results are reported as Mullen units.

6. **Puncture**. Test pieces from a representative sample of board are subjected to puncture by a triangular pyramid puncture head attached to a pendulum. The energy required to force the puncture head completely through the test piece, i.e. to make the initial puncture and to tear and bend open the board, can be measured.

7. **Vibration**. Placing of the test package on a vibration table and vibration it using a frequency varying at a constant rate between 3 and 100 Hz. The atmospheric conditions, the duration of the test, the peak acceleration, the attitude of the package and its method of restraint are predetermined.

8. **Fatigue**. Number of cycles of fluctuating stress, below the elastic limit of the material, that will produce failure.

4.3.2 Review of Box Compression

The literature and amount of information available on the subject of box compression is extensive. The first to see corrugated board as an engineering material was T. A. Carlson at the USA Forest Products Laboratory, as early as 1939. Kellicutt and Landt[49] considerably extended his work and were the first to shed light on the problems of the safe stacking life of corrugated boxes and the effect of relative humidity on box compression. To a large extent this work was ahead of its time, and for many years the industry relied on empirical "standards" developed by independent test laboratories. Since only a few of the largest companies had test facilities for

doing this kind of testing. Essentially these standards related box perimeter to box compression, with separate curves for various "grades" classified according to burst strength. Further modifications were made with respect to flute, basic box shape, amount of printings, etc. The standards were developed for top-to-bottom and end-to-end compression and applied to double board.

The next step forward came in the early 1950's with the realization that what was needed were relationships between box dimensions, flute contours, and a true material strength parameter. The pioneering effort in this area was in developing the Concora Liner Test(CLT) which , in conjunction with a knowledge of the flute contour and the box dimensions, made it possible to undertake "compression estimation" within a reasonable degree of accuracy[42]. This development covers horizontal as well as vertical flute boxes, top-to-bottom, end-to-end, and side-to-side testing, double face as well as double wall.

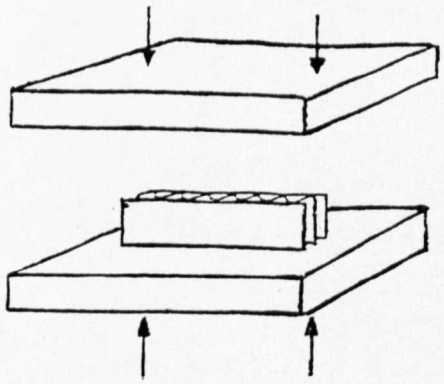

Figure 4.7 The ECT test of corrugated board

During the period of 1961-1963 McKee and his co-workers at the Institute of Paper Chemistry published their researches relating combined board column crush, flexural stiffness and box perimeter to top-to-bottom compression.

The need for and the use of "compression estimation" is not as well understood or appreciated as it should be. In the design of corrugated shipping containers it is essential to know beforehand the ability of a given material combination, size, and flute construction to carry a required load and /or stack with a known weight to a desired height in a warehouse. A comparison between an actual compression test and a predicted(estimated) value permits an objective assessment of box quality and fabrication efficiency.

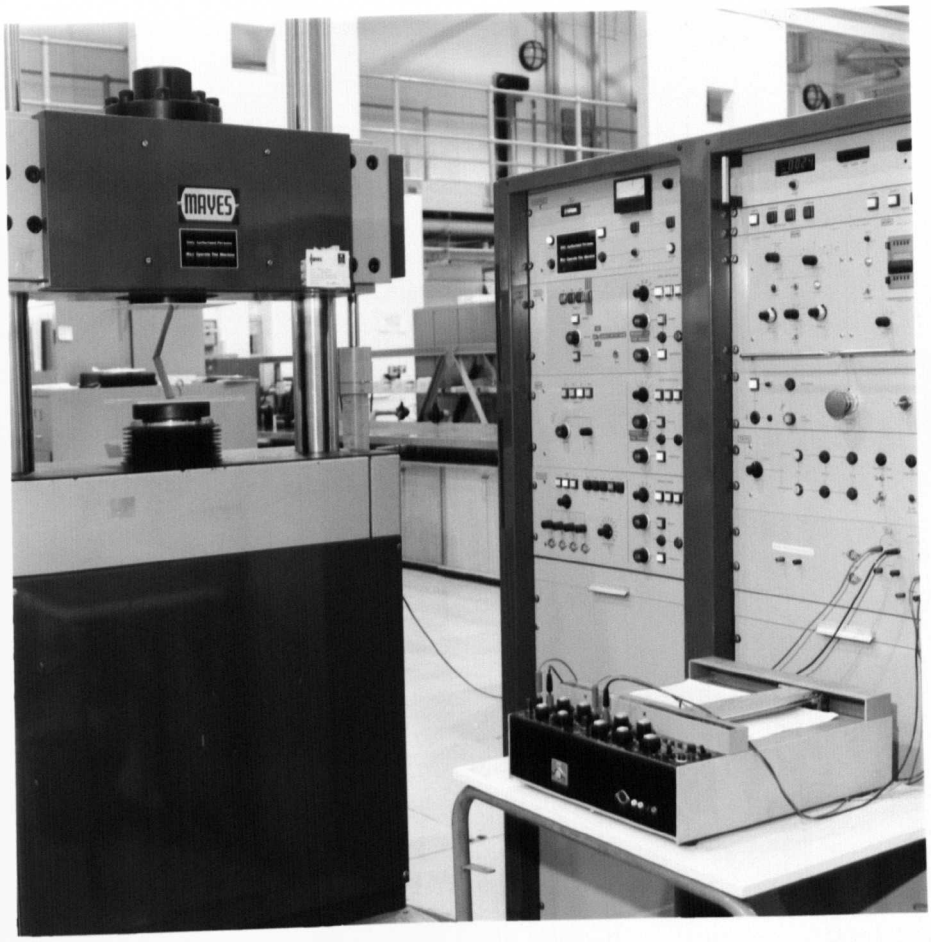

Figure 4.8 The testing machine

A key property that governs the container performance is linerboard compressive strength or Box Compression Test(BCT). BCT is the most commonly used test to assess stacking capacity of packaging. The knowledge of the vertical compression strength of a container according to its dimensions and to the various paper types it is made of, is the root of the problem of board container optimum design. Within the scope of container BCT prediction, McKee's formula has been widely accepted :

$$BCT = 9.025 P_t^{0.746} (\sqrt{D_x D_y})^{0.254} Z^{0.492} \quad (4.1)$$

Where

P_t- ECT, edgewise crush strength test per unit length of loaded edge of combined board (N/m);

D_x - flexural rigidity per unit width of combined board in machine direction(Nm);

D_y- Flexural rigidity per unit width of combined board in cross-machine direction(Nm);

Z - container perimeter(m).

Many studies reported by Mckee[18], Koning[34], and Carlsson[36] have been undertaken in order to analytically determine the various parameters used in this formula, such as P_m and the D_x and D_y. Some studies carried out by Plooy [35] and Pommier[50] have indicated the limits of use of this relationship and showed the need for advanced modelling using the orthotropic plate instability theory. Figure 4.7 shows a simple example of the ECT test of corrugated board suggested by Eriksson[13]..

4.3.3 Edge Crush Test

According to the McKee's compression strength formula (equation 4.1), Edge Crush

Strength (ECT) of corrugated board is one of the main properties needed to calculate the loading capacity of corrugated boxes. The other main property, according to McKee, is flexural rigidity. ECT is dependent on the properties of the components used in combined board manufacture but is also affected by conversion and finishing operations. The latter is not surprising because box compression depends on the inherent qualities of the components being retained in these operations. Thus, both container board qualities and manufacturing quality are factors in achieving adequate ECT.

The relation between ECT and component characteristics has been analyzed in two main ways. The first and simplest approach is to consider that ECT is primarily dependent on the edgewise compressive strengths of the components used in making the board. This approach gives good prediction accuracies, if based on appropriate statistical weighting factors obtained from proper sampling and testing.

The second approach is to treat the combined board as a structure comprised of narrow, flat plate elements of liner between flute tips and curved plates. These plate elements may become unstable and buckle, limiting the achievable ECT. This is more likely to occur in the case of lightweight grades.

The practical way to test the edge crush strength of corrugated board is to place a test piece between the platens of a compression tester with the flutes perpendicular to the platens as shown in Figure 4.7. The test piece is subjected to an increasing compression force until it breaks down. The maximum force that the test piece can withstand without breaking is reported as the edge crush test(ECT) or strength of the material, expressed as force per unit length[7].

The test equipment used for tests in this study is Mayes Universal Testing Machine, Model MPU 250. It is shown in Figure 4.8. Its loading range is between 0.1 to 500

KN.

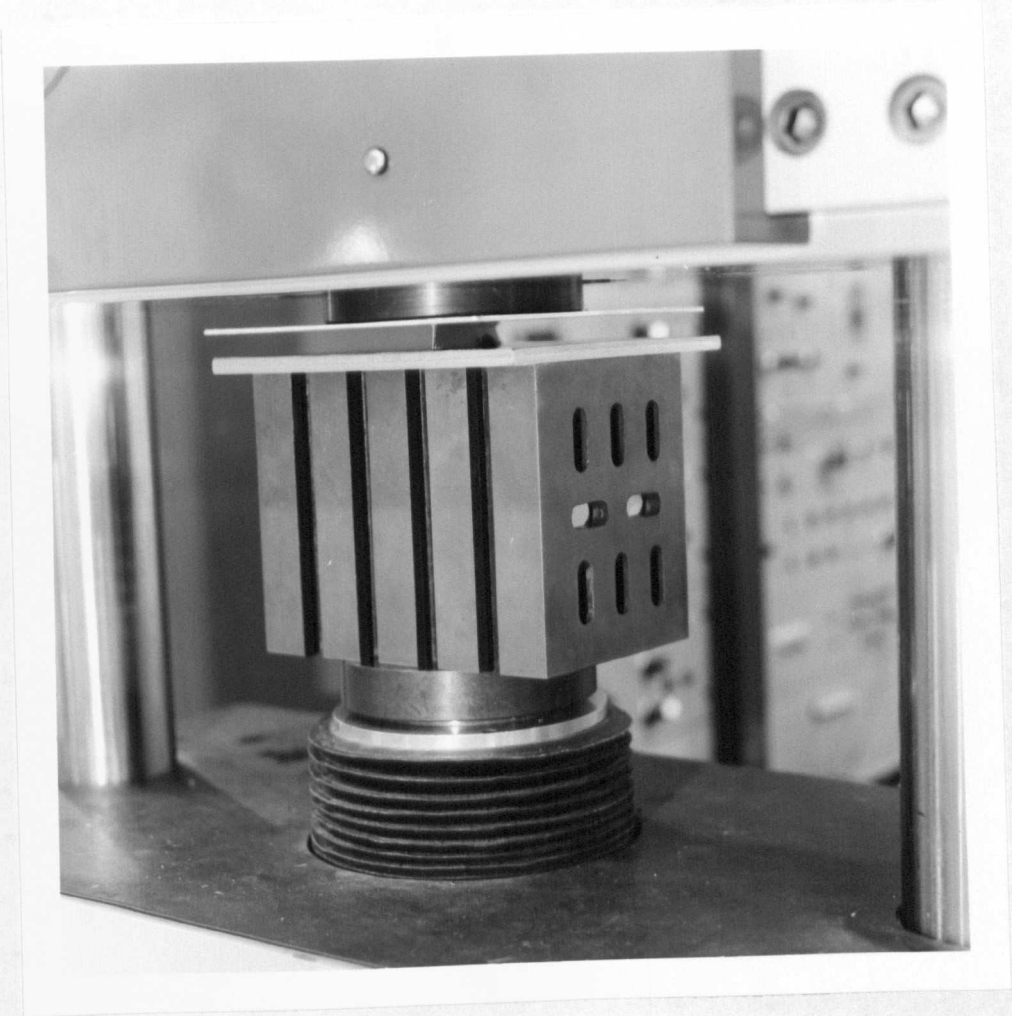

Figure 4.9 Edge crush test

The test pieces used in group one of this study are 3 mm in thickness, with the height less than 10 times the thickness, as 24 mm and the length 200 mm. The results are shown in table 8.3. For group 2 the specimen length is 100 mm, the remaining dimensions are the same as group 1. The results are shown in Table 4.4. As mentioned before, the edge crush test value is normally given as force per unit length. Because of this, the length of the test pieces does not influence the result of edge crush test. This is verified by comparing Table 4.3 and Table 4.4. Practical handling of test pieces during cutting and testing, as well as the dimensions of the testing platens, will serve to limit the length of test pieces. Figure 4.9 shows the situation of edge crush test.

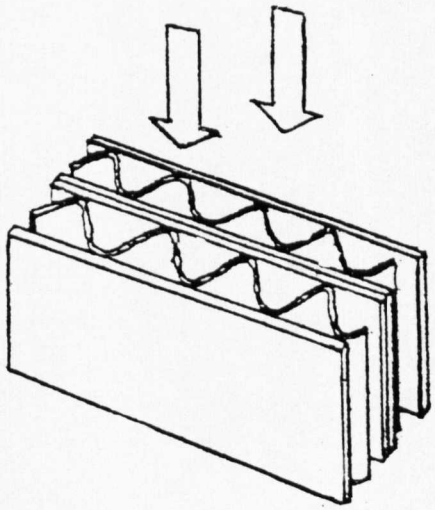

Figure 4.10 Width of test piece

In order to investigate the influence of the width on ECT, two test pieces were placed close together as shown as Figure 4.10. This investigation produced no differences in the edge crush values when testing two pieces as compared with testing one single piece. See Table 4.5, group 3. Consequently, there appears to be no reason to increase the width of test pieces by putting two pieces close together when testing.

Tests also show that the corner-shaped test pieces with short column gave the same edge crush test values as normal rectangular test pieces. See Table 4.6, group 4. The angle of the corner does not affect the ECT level.(See Figure 4.11)

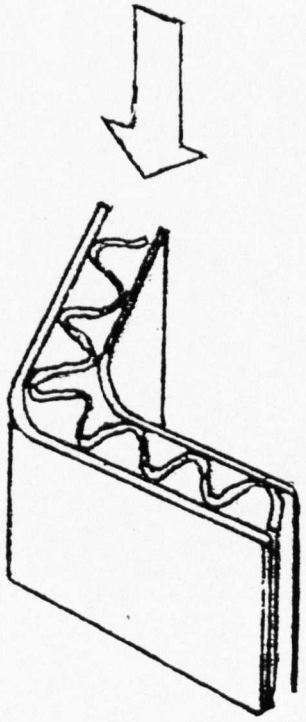

Figure 4.11 Corner-shaped test piece

Table 4.3 ECT for group 1

	Test1	Test2	Test3
Loading(KN)	0.8	0.8	0.8
ECT(KN/m)	4	4	4

Table 4.4 ECT for group 2

	Test 1	Test 2	Test 3
Loading(KN)	0.4	0.4	0.4
ECT(KN/m)	4	4	4

Table 4.5 ECT for group 3

	Test1	Test2	Test3
Loading(KN)	0.8	0.8	0.8
ECT(KN/m)	4	4	4

Table 4.6 ECT for group 4

	Test1	Test2	Test3
Loading(KN)	0.4	0.5	0.4
ECT(KN/m)	4	5	4

4.3.4 Buckling Failure Test

In the literature, many references deal with the height of the test pieces [7, 16,42]. The most important information to be gained from these references is the fact that the breakdown of a test piece shows different mechanisms, depending on the height of the test piece. With a short height compared with the thickness of the board(i.e., the height is not more than 10 times the thickness), there is pure compression or crushing of the test pieces. With a tall height of the test piece (i.e., the height is more than 40 to 50 times the thickness), the breakdown will be buckling, according to Euler theories reported by Stockmann[16]. With a medium height of the test piece, the breakdown is also buckling. Lower force is required for buckling than for the crushing breakdown of the test piece.

The test method for buckling of corrugated board is to place a test piece between the platens of a compression tester with the flutes perpendicular to the platens. The test piece is subjected to an increasing compression force until it buckles. The maximum force that the test piece can withstand before buckling is acquired. The specimen for buckling test, as group 5, is a long column test piece of 200*200 mm^2, the thickness is 3 mm. The result of tests of group 5 is shown in Table 4.7. The buckling tests of

long and medium column are shown in Figure 4.12 and Figure 4.13.

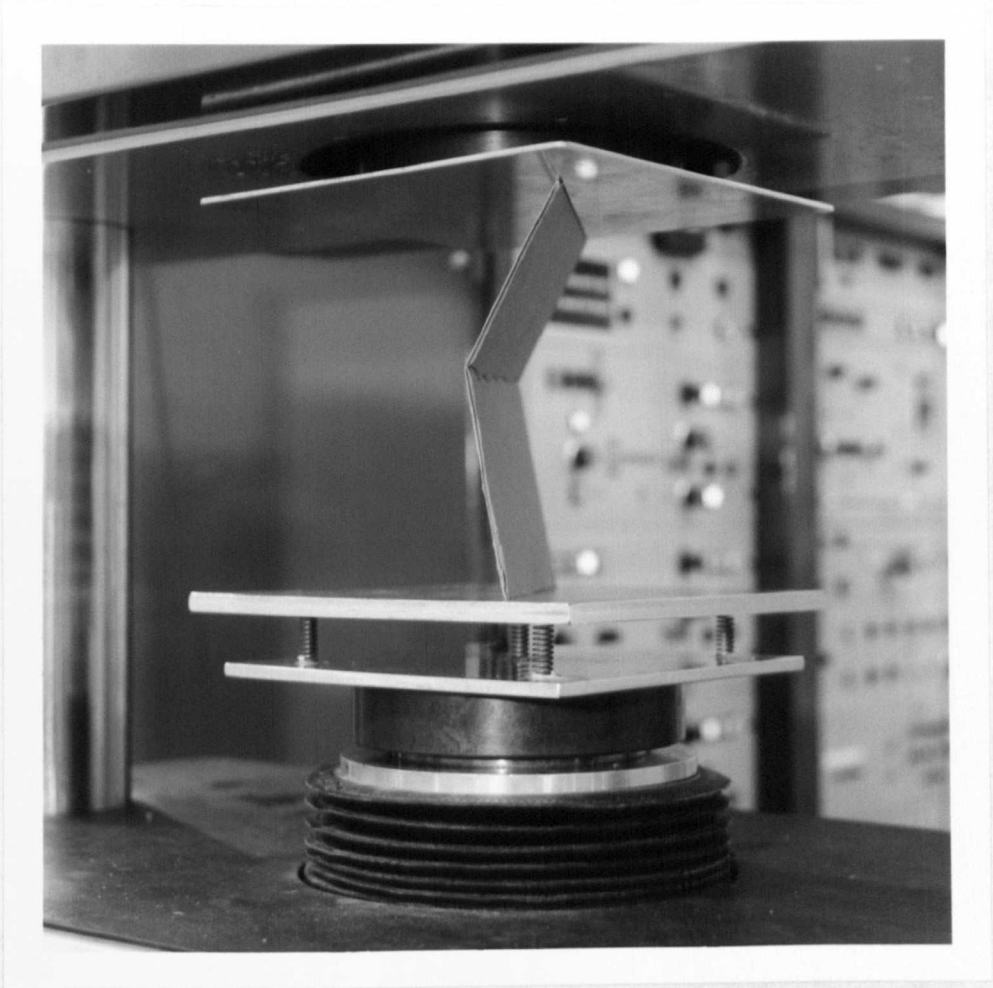

Figure 4.12 Buckling test of long column

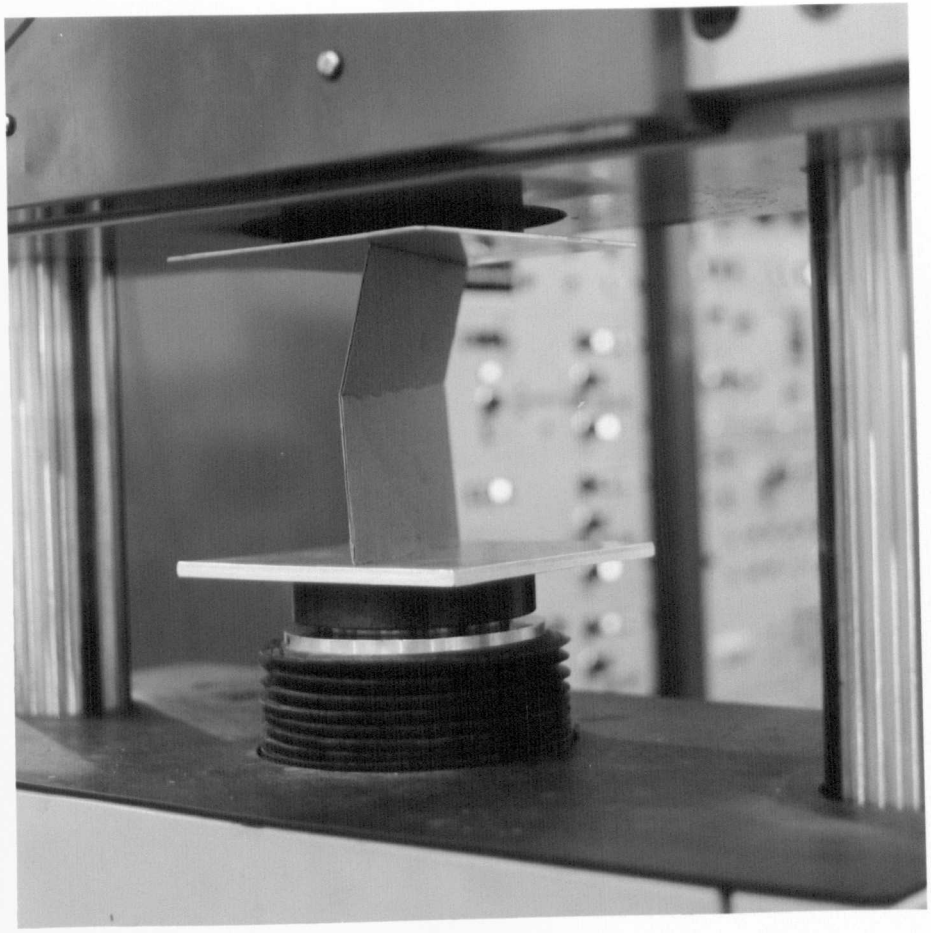

Figure 4.13 Buckling test of medium column

Table 4.7 Test of buckling for long column

	Test1	Test2	Test3
Buckling(KN)	0.2	0.2	0.2

The result of the test of medium column , 200*90mm^2 , as group 4, is shown in Table 4.8.

Table 4.8 Test of buckling for medium column

	Test1	Test2	Test3
Buckling(KN)	0.3	0.4	0.4

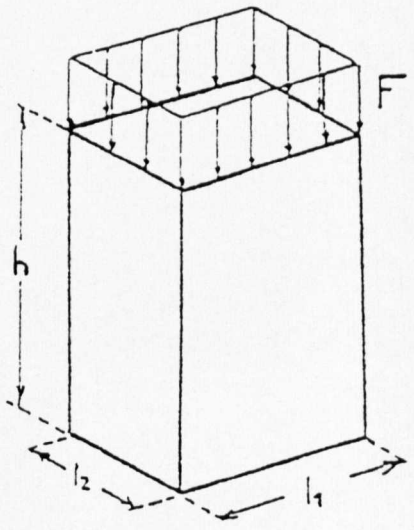

Figure 4.14 Box uniformly compressed

Buckling tests for corner-shaped (right angle) test pieces were also carried out in this study. The problem of symmetry makes it possible to select only a quarter of the structure. (See Figure 4.14) The specimen height h used was 90 mm and 200 mm respectively. The results are shown in Table 4.9 and Table 4.10.

Table 4.9 Buckling test of a quarter medium column

	Test1	Test2	Test3
Buckling(KN)	0.6	0.6	0.5

Table 4.10 Buckling test of a quarter long column

	Test1	Test2	Test3
Buckling(KN)	0.4	0.4	0.4

4.3.5 Box Compression Test

A quarter of a box of 200*200*200 mm^3 was put onto the compression machine for top-to-bottom compression test as shown in Figure 4.15. The box is unsealed and the board is double-face. it is generally agreed that a box should accept its full compression load and fail before it deflects too much.

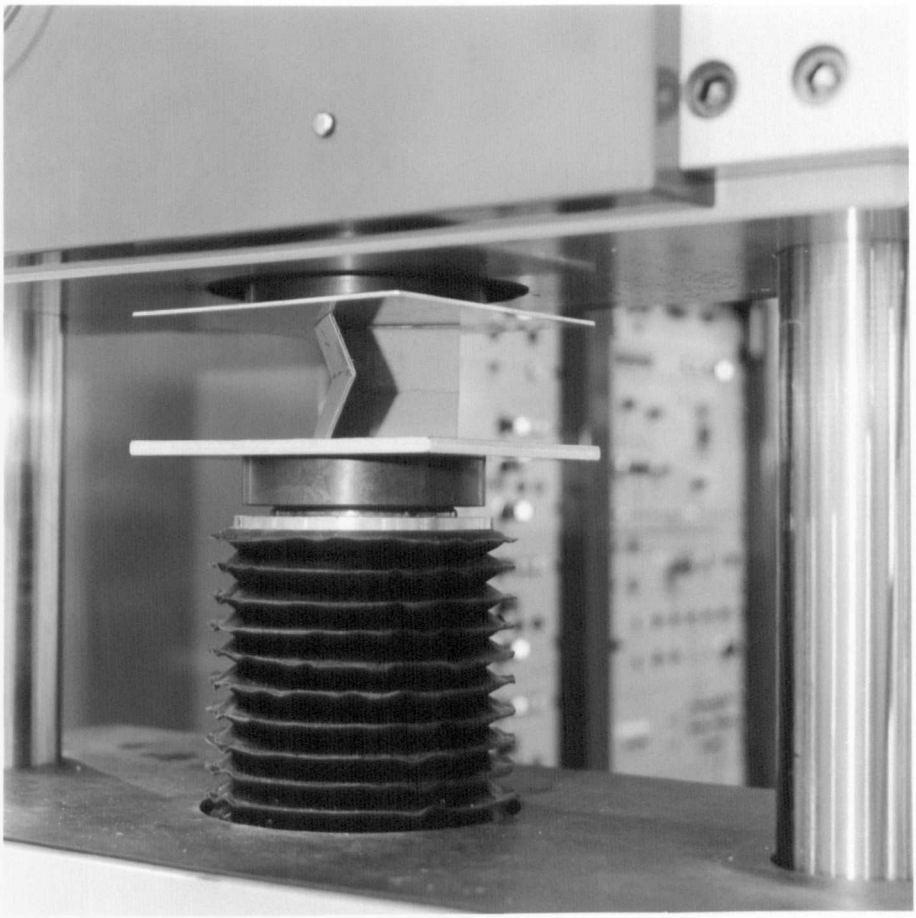

Figure 4.15 Test on the quarter of the structure

4.4 Structure Configuration and Loading Type for Computer Analysis

Corrugated fibreboard employed in this study consists of two liners of equal thickness, stiffness, and strength. They are separated by a corrugated medium, which is supposed to provide sufficient strength and stiffness so as to maintain full in-plane and bending displacement compatibility between the two liners (see Figure 4.16). The structure of the corrugated medium is assumed as V-shaped or linear between liners. Plane sections are assumed to remain plane and perpendicular to the midplane after loading.

Container loading has been divided into three major categories: internal, external and a combination of internal plus external loading modes. The internal loading has been further divided into three classes consisting of uniform, ramp, and point loading distribution.(see Figure 4.17)

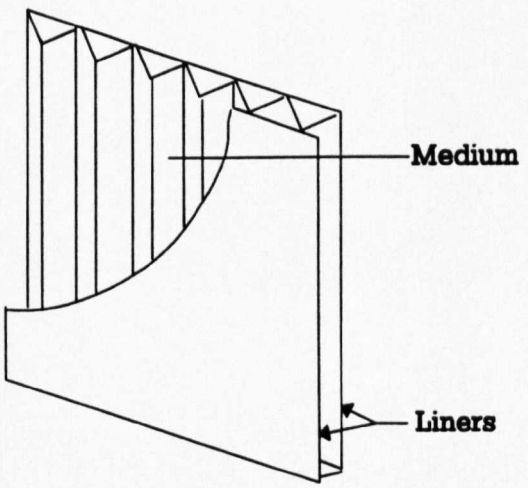

Figure 4.16 The structure of corrugated fibreboard

4.5 FE method and analysis

In order to predict the damage to the container it was necessary to generate a mathematical model for the panels. As presented above, a lot of different mathematical approaches were used to predict the stress, strain, deformation and buckling. Early work was mostly carried out using experimental equations.

For corrugated fibreboard with a complex profile, three dimensional mathematical modelling is required and Finite Element Analysis should be very useful as has been proven in other engineering structural problems.

4.5.1 The Finite Element Method

The Finite Element method is one of the most powerful numerical technique available today for analysis of complex structural and mechanical system. It is used to obtain

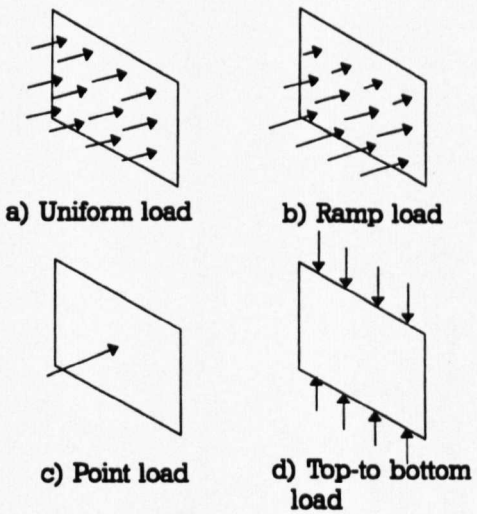

Figure 4.17 Load code

numerical solutions to a wide range of problems. The Finite Element method can be used for both static and dynamic analysis.

The classical method of analysis in elasticity involves the study of an infinitesimal element of an elastic body. Relationships between stress, strain and displacement for the infinitesimal element are developed that are usually in the form of differential equations that apply to each point in the body. These equations must be solved subject to appropriate boundary conditions. In other words, the approach is to define and solve a classical boundary value problem in mathematics. Problems in engineering usually involve very complex shapes and boundary conditions. Consequently, for such cases, the equations cannot be solved exactly, but must finally be solved by approximate methods; for example, by truncated series, finite differences, numerical integration, etc. All these approximate methods require some form of discretization of the solution.

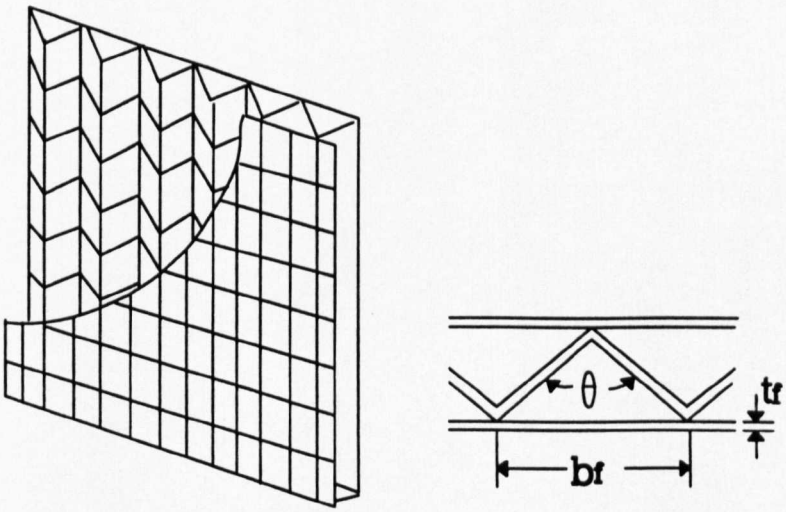

Figure 4.18 Finite element model for simulation

The formulation of Finite Element solutions recognizes at the outset that discretization

is likely to be required. The first step in application of the method is to discretize the domain into an assemblage of a finite number of finite size elements (or subregions) that are connected at specified node points. The quantities of interest (usually nodal displacements) are assumed to vary in a particular fashion over the element. This assumed element behaviour leads to relatively simple integral equations for the individual elements. The integral equations for an element are evaluated to produce algebraic equations in terms of the displacements of the node points. The algebraic equations for all elements are assembled to achieve a system of equations for the structure as a whole. Appropriate numerical methods are then used to solve this system of equations.

4.5.2 Computing Hardware

The major limitation on the accuracy of finite element models in general is the mesh size and the number of elements used. These factors themselves depend on the maximum cpu time that can be used on a particular computer and the memory file space available. Another factor of the overall speed of job completion is the job turnaround time which depends on the ease of use of the operating system and the available editors.

The computer used for the finite element calculations of the project was the Sun 10/LX work station, It was installed with the finite element package ANSYS 5. The computer uses Solaris 2.3/2.5 as its operating system. For each computer the memory is 48 megabytes and they share a common disc space which is 12 gigabytes for installing packages.

4.5.3 Computing Software

The theory of stress, strain, and buckling for corrugated fibreboard is discussed in following sections. Several finite element packages are available commercially, each with its own advantages and disadvantages. The requirement for the project was the ability to solve large deformation, non-linear buckling and stress-strain problems. The package which was available in our laboratory, ANSYS, has the above ability and so was chosen as the modelling software.

In the category of structural analysis, in ANSYS two main analysis types were used for this project. They are static analysis and buckling analysis. The static analysis is used to determine displacements, stresses, strain, and forces in the structure due to loads that do not induce significant inertia and damping effects. Both linear and nonlinear are available. Among the nonlinearities that can be included are plasticity, stress stiffening, large deflection, large strain, etc. The kinds of loading that can be applied in a static analysis include externally applied forces and pressures, steady-state inertia forces (such as gravity or rotational velocity), imposed (non-zero) displacements, and temperatures (for thermal strain).

The buckling analysis is used to calculate the buckling loads and determine the buckling mode strains due to a response spectrum or random vibrations. Two techniques are available in ANSYS program for predicting the buckling load and buckling mode shape of a structure: nonlinear buckling analysis, and eigenvalue (or linear) buckling analysis.

Nonlinear buckling analysis is usually the more accurate approach. This technique employs a nonlinear static analysis with gradually increasing loads to seek the load level at which the structure becomes unstable. The structure can include features such as initial imperfections, plastic behaviour, gaps, and large-deflection response.

Eigenvalue buckling analysis predicts the theoretical buckling strength of an ideal linear elastic structure.

4.5.4 The Finite Element model

A corrugated fibreboard container subjected to internal and external loading will subject to stress, strain, deflection, and buckling to the side panel. A FE method of analysis of the panel is developed.

The reaction of the panel to such loading can be observed by means of this method. The failure of the container due to the loading can be predicted and the variables of material and panelproperties can be changed to test and analyze different packaging designs.

Finite element modelling of corrugated fibreboard has been carried out using commercially available software, ANSYS 5. The analysis used 4-nodes shell elements which have both bending and membrane capabilities. Both in-plane and normal loads are permitted. The element has six degrees of freedom at each node. Stress stiffening and large deflection capabilities are also included. Orthotropic material properties were used.

The development of the finite element model is shown in Figure 4.18. Both the single panel of the container and a quarter of the side-panel of the box were considered. The effect of connecting panels on the behaviour of the panel is controlled by the artificially prescribed displacement boundary conditions for the panel, such as either a simply supported boundary or a clamped boundary.

The successful finite element analysis depends on the meshing procedure for the structure to a large extent, since it contains two layers of liner and a corrugated

medium and since they are separately modelled portions of the model, they have to be combined into one.

4.6 Load-deformation relation and stress

The simulative solutions of the stress, deflection and buckling for a 20*20cm^2 panel have been obtained. These were compared with analytical and experimental results reported by Peterson[30-33] and found to be compatible.

4.6.1 Uniform load

Stress is predicted to be biaxial of tensile or tension-compression nature in the middle of the panel for uniform internal load according to Fox[27] and Peterson[30-33], as shown in Figure 4.19a. The simulation result from this study are shown in Figure 4.19b and it is similar to the result from experimental photoelasticity conducted by Peterson[30-33]. The overall stress distribution is identified by colour fringes and their order and location with respect to one another. A constant colour line is a line of constant stress level, and a uniform colour area indicates an area of constant stress level.

It is seen from the figures that the state of stress near the corner comprises a compressive stress perpendicular to the diagonal and the tensile stress parallel to the diagonal. There is a trend for failure to occur through propagation of a crease along the diagonal from the corner region toward the centre of the panel and outward to the corner of the panel. The ultimate load of the panel is reached when the geometry of the failure pattern develops into a kinematically unstable mechanism according to Peterson.

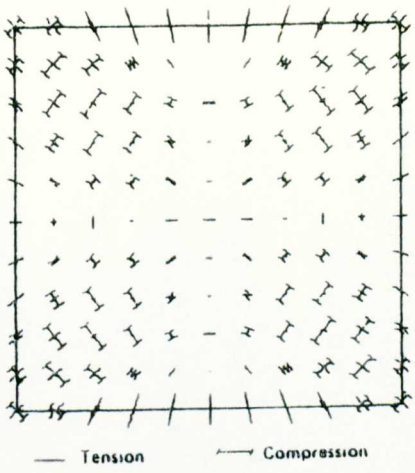

a Tension-compression under uniform load

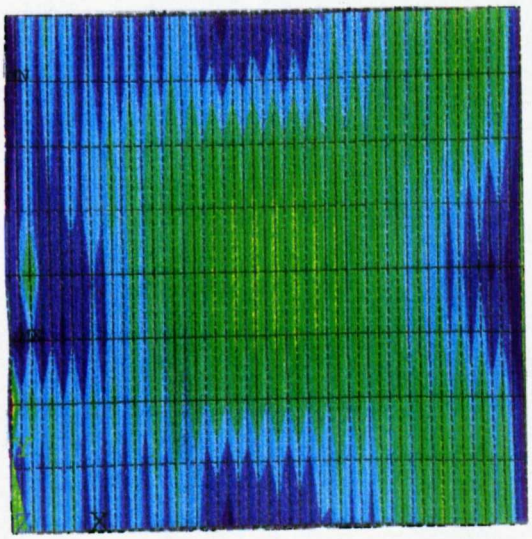

b Stress field from simulation

Figure 4.19 Stress patterns for uniform load

4.6.2 Point load

The stress distribution for a point load is similar to the case of uniform load. The FEA simulation output(Figure 4.20) from this study can be compared with experimental photostress fringe pattern from Peterson's work[30-33]. In this case the failure should occur on the diagonal but not in the corner as suggested by Peterson. Failure would be caused by a compressive crease forming in the inside liner and along the diagonal of the panel. A box subjected to a point load, which is sufficient to cause failure, does in fact fail at these expected locations and along the diagonals according to Peterson.

4.6.3 Ramp load

Ramp load, when a container is filled with a liquid or power product, the stress will be greater at the bottom. The critical biaxial stress state is located in the bottom corner region. The failure is due to the compressive stress component of biaxial stress state occurring in the inside liner. Stress distribution from a simulation(Figure 4.21) can be compared to those from experimental results done by Peterson[30-33]. Failure should occur near the lower corner of the panel.

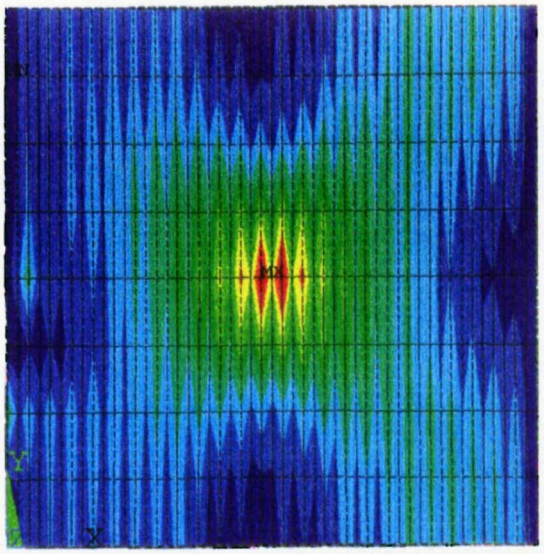

Figure 4.20 Stress pattern for point load

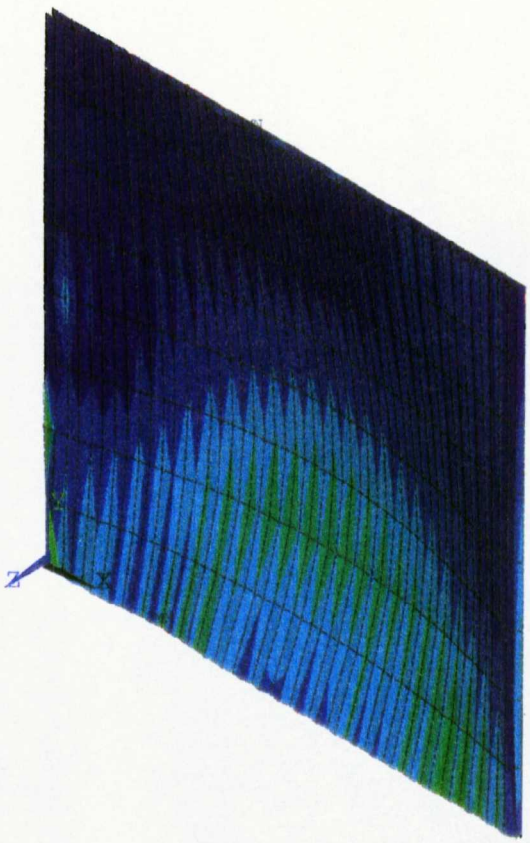

Figure 4.21 Stress pattern for ramp load

4.7 Buckling analysis

Stacking capability is one of the most important end use requirements for corrugated fibreboard containers. Its stacking performance is classified by its degree of resistance against collapse under a top-to-bottom load. With a top-to-bottom load, edgewise compressive stresses are uniformly distributed along the perimeter of the container. At a critical load the side panels of the container will buckle elastically. The regions in the vicinity of the vertical edges, however, remain essentially straight. These corner regions will, therefore, carry the bulk of the top-to-bottom load in the buckled state.

If the top-to-bottom load continues to rise, compressive stresses within corner regions will eventually reach the compressive strength of the combined board, and a collapse of the container will initiate there.

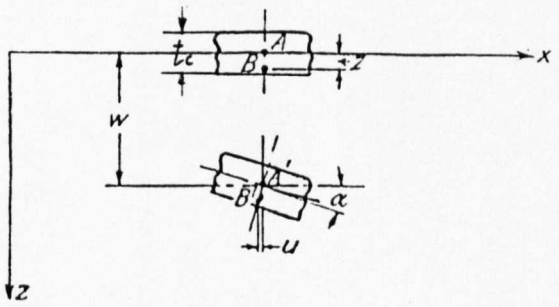

This diagram is not to scale and is drawn to illustrate the parameters

Figure 4.22 Definition of thin plate

4.7.1 Buckling and bending of thin plates

When the thickness of an elastic body is small compared with the other dimensions, it is called thin plate. Let t_c be the thickness of the plate. The plane parallel to the faces of the plate and bisecting the thickness of the plate, in the undeformed state, is called the middle plane of the plate according to Wang[40].

Choosing the coordinate axes so that the x and y axes are in the middle plane of the plate and the z axis is perpendicular to the middle plane. If a thin plate is bent with small deflection, *i.e.*, when the deflection of the middle plane is small compared with the thickness t_c the following assumptions can be made.

1. The normals of the middle plane before bending are deformed into the normals of the middle plane after bending.

2. The stress σ_z is small compared with the other stress components and may be neglected in the stress-strain relations

3. The middle plane remains unstrained after bending.

Consider a section of the plate parallel to the xz plane as shown in Figure 4.22 which is presented in [40]. After bending, a point A on the middle plane is deflected to A' with a deflection w. According to the first assumption, a point on the normal to the undeformed middle plane, such as B, which is at a distance z from A, is now displaced to B', which is on the normal to the middle plane after bending. From Figure 4.22, it is observed that the displacement of the point B' in the x direction is:

$$u=-z\alpha \tag{4.2}$$

Since the deflection is small, $\alpha \approx \tan\alpha = \partial w/\partial x$ and

$$u=-z\frac{\partial w}{\partial x} \tag{4.3}$$

Similarly, the displacement of the point B' in the y direction is

$$v=-z\frac{\partial w}{\partial y} \tag{4.4}$$

The assumption that the normals of the middle plane before bending are deformed into the normals of the middle plane after bending is equivalent to assuming that the shearing strains γ_{xz} and γ_{yz} are zero.

$$\epsilon_x=\frac{\partial u}{\partial x} \qquad \epsilon_y=\frac{\partial v}{\partial y} \qquad \gamma_{xy}=\frac{\partial u}{\partial x}+\frac{\partial v}{\partial y} \tag{4.5}$$

From the definition of strain,

$$\epsilon_x=-z\frac{\partial^2 w}{\partial x^2} \qquad \epsilon_y=-z\frac{\partial^2 w}{\partial x^2} \qquad \gamma_{xy}=-2z\frac{\partial^2 w}{\partial x \partial y} \tag{4.6}$$

By making use of the relations of equation (4.3) and (4.4), the above equation can be obtained as,

$$\epsilon_x=\frac{1}{E}(\sigma_x-\nu\sigma_y) \qquad \epsilon_y=\frac{1}{E}(\sigma_y-\nu\sigma_x) \qquad \gamma_{xy}=\frac{1}{G_s}\tau_{xy} \tag{4.7}$$

According to assumption 2, the stress-strain relations for a thin plate in bending are

$$\begin{aligned}\sigma_x&=\frac{E}{1-\nu^2}(\epsilon_x+\nu\epsilon_y)\\ \sigma_y&=\frac{E}{1-\nu^2}(\epsilon_y+\nu\epsilon_x)\\ \tau_{xy}&=G_s\gamma_{xy}=\frac{E}{2(1+\nu)}\gamma_{xy}\end{aligned} \tag{4.8}$$

Substituting equation (4.6) into the above formulas, then

$$\begin{aligned}\sigma_x&=-\frac{Ez}{1-\nu^2}\left(\frac{\partial^2 w}{\partial x^2}+\nu\frac{\partial^2 w}{\partial y^2}\right)\\ \sigma_y&=-\frac{Ez}{1-\nu^2}\left(\frac{\partial^2 w}{\partial y^2}+\nu\frac{\partial^2 w}{\partial x^2}\right)\\ \tau_{xy}&=-\frac{Ez}{1+\nu}\frac{\partial^2 w}{\partial x\partial y}\end{aligned} \tag{4.9}$$

With these relations, the bending and twisting moments per unit length acting on any section of the plate parallel to the xz and yz planes (Figure 4.22) can be obtained by integration. Thus:

$$M_x=\int_{-h/2}^{h/2}\sigma_x z dz=-\int_{-h/2}^{h/2}\frac{Ez}{1-\nu^2}\left(\frac{\partial^2 w}{\partial x^2}+\nu\frac{\partial^2 w}{\partial y^2}\right)z dz \qquad (4.10)$$

Since w is the deflection of the middle plane, it does not depend upon z. Hence

$$M_x=-\frac{E}{1-\nu^2}\left(\frac{\partial^2 w}{\partial x^2}+\nu\frac{\partial^2 w}{\partial y^2}\right)\int_{-h/2}^{h/2}z^2 dz=-D\left(\frac{\partial^2 w}{\partial x^2}+\nu\frac{\partial^2 w}{\partial y^2}\right) \qquad (4.11)$$

Where D denotes $Eh^3/12(1-\nu^2)$ and is called the flexural rigidity of the plate. Similarly

$$\begin{aligned} M_y&=\int_{-h/2}^{h/2}\sigma_y z dz=-D\left(\frac{\partial^2 w}{\partial y^2}+\nu\frac{\partial^2 w}{\partial x^2}\right)\\ M_{xy}&=M_{yx}=-\int_{-h/2}^{h/2}\tau_{xy} z dz=D(1-\nu)\frac{\partial^2 w}{\partial x\partial y}\end{aligned} \qquad (4.12)$$

Where the negative sign before the integral for M_{xy} is due to the fact that, for positive τ_{xy} and positive z, dM_{xy} is negative.

4.7.2 Boundary conditions

The boundary conditions for a rectangular plate with edges parallel to the x and y axes are considered[40] .

1. Simply Supported Edge. When a supported edge of a plate is free to rotate, it is called a simply supported edge(Figure 4.23). Thus, if the edge $x=a$ is simply supported, the deflection as well as the bending moment along the edge must be zero. That is,

$$(w)_{x=a}=0 \qquad (M_x)_{x=a}=-D\left(\frac{\partial^2 w}{\partial x^2}+\nu\frac{\partial^2 w}{\partial y^2}\right)_{x=a}=0 \qquad (4.13)$$

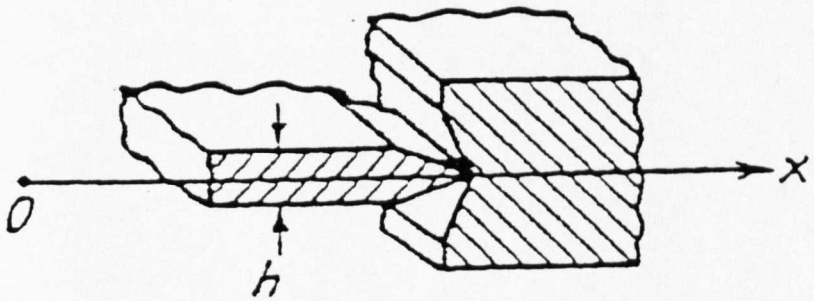

Figure 4.23 Boundary conditions

But the condition w=0 along the edge x=a means also that along this edge

$$\frac{\partial w}{\partial y}=\frac{\partial^2 w}{\partial y^2}=0 \tag{4.14}$$

The boundary conditions for a simply supported edge can therefore be written as,

$$(w)_{x=a}=0 \qquad \left(\frac{\partial^2 w}{\partial x^2}\right)_{x=a}=0 \tag{4.15}$$

2. Built-in or Clamped Edge. If the edge $x=a$ is built in or clamped, along this edge the deflection as well as the slope of the middle plane must be zero. That is,

$$(w)_{x=a}=0 \qquad \left(\frac{\partial w}{\partial x}\right)_{x=a}=0 \tag{4.16}$$

3. Free Edge. If the edge x=a is free, there must be no bending and twisting moments as well as no vertical shearing forces along the edge:

$$(M_x)_{x=a}=0 \qquad (M_{xy})_{x=a}=0 \qquad (Q_x)_{x=a}=0 \tag{4.17}$$

which requires that

$$\left(\frac{\partial^2 w}{\partial x^2}+\nu\frac{\partial^2 w}{\partial y^2}\right)_{x=a}=0 \tag{4.18}$$

it may be taken as the boundary conditions for a free edge.

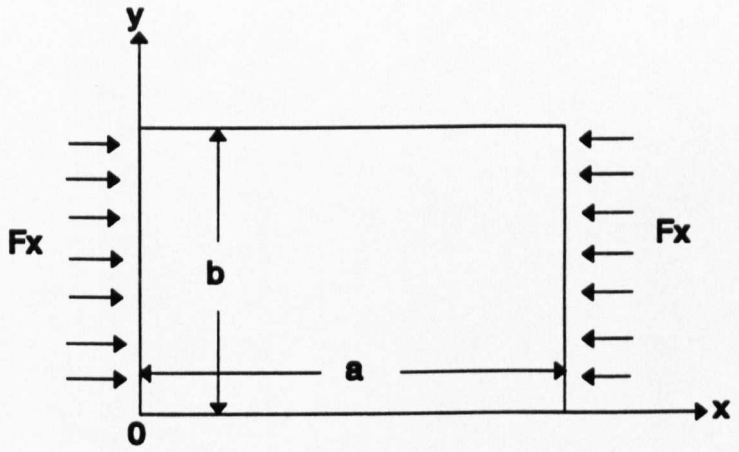

Figure 4.24 A simply supported rectangular plate

4.7.3 Buckling of simply supported rectangular plates uniformly compressed in one direction

When a flat plate is compressed in its middle plane, the flat form of equilibrium becomes unstable and the plate begins to buckle at a certain critical value of the inplane force. Let us consider a simply supported rectangular plate (Figure 4.24) compressed in its middle plane by a uniformly distributed force F_x along the sides x=0 and x=a. In such a case,

$$F_x = -constant \qquad F_y = F_{xy} = p = 0 \tag{4.19}$$

Where p is the lateral loading on the plate. According to Wang[40], the equilibrium equation in the direction perpendicular to the middle plane (z direction) is:

$$\frac{\partial^4 w}{\partial x^4} + 2\frac{\partial^4 w}{\partial x^2 \partial y^2} + \frac{\partial^4 w}{\partial y^4} = \frac{1}{D}\left(p + F_x\frac{\partial^2 w}{\partial x^2} + F_y\frac{\partial^2 w}{\partial y^2} + 2F_{xy}\frac{\partial^2 w}{\partial x \partial y}\right) \tag{4.20}$$

where D denotes $Eh^3/12(1-\upsilon^2)$ and is called the flexural rigidity of the plate. The above equation should be satisfied in this situation. By substituting $-N_x$ for N_x,

$$D\nabla^4 w + F_x\frac{\partial^2 w}{\partial x^2} = 0 \tag{4.21}$$

The boundary conditions are satisfied if:

$$w = \Sigma_{m=1}^{\infty}\Sigma_{n=1}^{\infty} A_{mn} \sin\frac{m\pi x}{a} \sin\frac{n\pi y}{b} \tag{4.22}$$

Substituting the above expression into equation (4.21),

$$\Sigma_{m=1}^{\infty}\Sigma_{n=1}^{\infty}\left[D\pi^4\left(\frac{m^2}{a^2}+\frac{n^2}{b^2}\right)^2-F_x\pi^2\frac{m^2}{a^2}\right]A_{mn}\sin\frac{m\pi x}{a}\sin\frac{n\pi y}{b}=0 \quad (4.23)$$

The trivial solution is that A_{mn} =0 or w=0. To find the nontrivial solution let

$$D\pi^4\left(\frac{m^2}{a^2}+\frac{n^2}{b^2}\right)^2-F_x\pi^2\frac{m^2}{a^2}=0 \quad (4.24)$$

or

$$F_x=\frac{\pi^2D\left(\frac{m^2}{a^2}+\frac{n^2}{b^2}\right)^2}{m^2/a^2}=\frac{\pi^2D}{b^2}\left(\frac{mb}{a}+\frac{n^2a}{mb}\right)^2 \quad (4.25)$$

This means that when F_x reaches the value given by the right-hand side of the above expression, A_{mn} and consequently w may be different from zero, which indicates the buckling of the plate. From equation (4.25), the value of F_x is smallest if n is equal to 1. This indicates that, when such a plate buckles, there can be several half waves in the direction of compression but only one half wave in the perpendicular direction. The critical load is therefore:

$$(F_x)_{cr}=\frac{\pi^2D}{b^2}\left(\frac{mb}{a}+\frac{a}{mb}\right)^2=\delta\frac{\pi^2D}{b^2} \quad (4.26)$$

where $\delta=[(mb/a)+(a/mb)]^2$ is a numerical factor the magnitude of which depends on m and the ratio a/b. The minimum value of $(F_x)_{cr}$ occurs when

$$\frac{d(F_x)_{cr}}{d(mb/a)}=\frac{2\pi^2 D}{b^2}\left(\frac{mb}{a}+\frac{a}{mb}\right)\left[1-\frac{1}{(mb/a)^2}\right)=0 \qquad (4.27)$$

or

$$\frac{mb}{a}=1 \qquad (4.28)$$

This gives the minimum value of $(F_x)_{cr}$ *as* $4\pi^2D/b^2$. As stated by Wang[40], for various values of the integer m, the magnitude of δ depends on the ratio *a/b* only. The values of δ for m=1, 2, 3, 4, 5 are plotted in Figure 4.25 against a/b ratios. Having these curves, the magnitude of the critical load and the number of half waves for any value of a/b ratio can be determined by taking the ordinate of the curve which gives the smallest δ for the given ratio of a/b. For example, for a/b=2.5, from Figure 4.25 that δ=4.133 and m=3. This indicates that the plate will buckle into three half waves in the direction of load under a buckling load of $(F_x)_{cr}=4.133\pi^2D/b^2$.

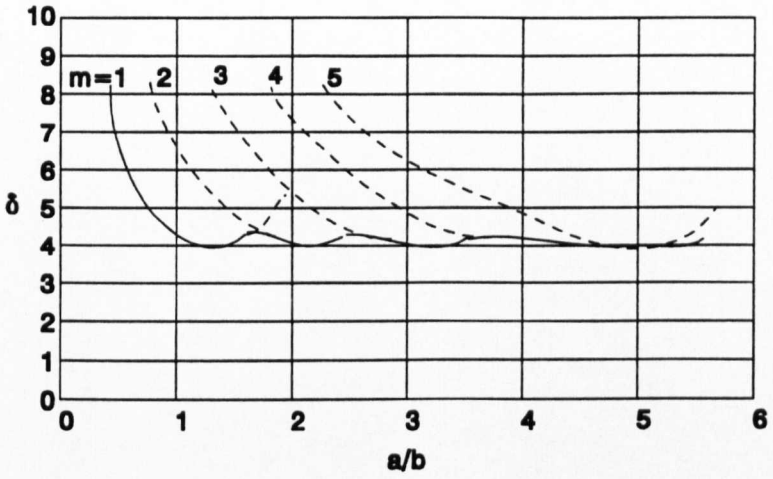

Figure 4.25 Values of δ against *a/b* ratios

4.7.4 Definition of corrugated fibreboard compressive strength

Under a top-to-bottom load acting parallel to the liners the compressive forces are uniformly distributed along the edges of the liner facings. The panel will buckle once the force F_x per unit length of fibreboard exceeds the critical limit as expressed in equation (4.26).

Because of the bonding of the liner to the tips of the flutes of the corrugating medium, the panel in the vicinity of the flute tips is prevented from buckling. Thus, like the corner regions of a container in the buckled state, the regions of linerboard in the vicinity of flute tips remain straight and will carry the bulk of the total compressive load beyond the force F_x. If the top-to-bottom load acting on a container

continues to rise, the compressive stresses within flute tip regions of the liner will reach the intrinsic edgewise compressive strength of the liner, and failure will initiate there. A high flexural rigidity, D, of the liner improves the compressive strength of the combined board because the load-bearing capacity of the centre of a buckled panel is proportional to its flexural rigidity according to equation (4.26).

Thus, to achieve optimal stacking performance of a box, the linerboard should combine high flexural rigidity with high intrinsic edgewise compressive strength. To predict, design, or specify the performance of linerboard as a structural member of a container, it is mandatory to correctly measure the two principal sheet properties, flexural rigidity and intrinsic edge compressive strength. While there are reliable methods for measuring flexural rigidity, there are considerable uncertainties how to measure compressive strength.

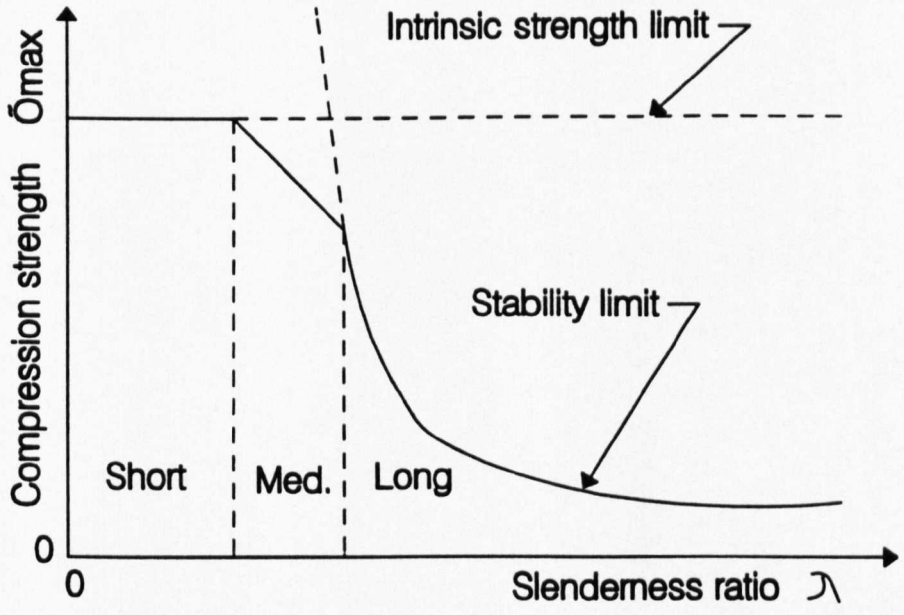

Figure 4.26 Effect of slenderness ratio on compressive strength

As mentioned above, the failure initiation of a liner as part of a container under a top-to-bottom load must be expected to occur at a site where the liner is prevented from buckling. Consequently, the measuring method should provide loading conditions that prevent buckling. To arrive at the proper measuring method it is helpful to review the behaviour of a column under a compressive load.

Figure 4.26 shows the typical trend of the dependency of the compressive strength σ_{max} of a column on its slenderness ratio λ for an arbitrary material according to Stockmann[51]. The slenderness ratio λ is defined by

$$\lambda = \frac{l}{\sqrt{I/A}} \tag{4.29}$$

where

l =free length of a column

I =second moment of area of cross-section

A =cross-sectional area

In the case of the thickness of a column with rectangular cross section, equation (4.29) becomes

$$\lambda = \frac{l}{\sqrt{qt_c^3/12qt_c}} = 2\sqrt{3}\frac{l}{t_c} \tag{4.30}$$

where t_c is the thickness of a column and q its width.

According to Figure 4.26, the compressive strength, σ_{max}, which a column can sustain without failing increases with decreasing slenderness ratio. Three ranges of column height can be recognized: long, medium, and short column.

Long column, its height/thickness ratio is larger than 40, will buckle elastically once a critical compressive stress $\delta_{cr,el}$ is reached. The Euler-equation defines this stability limit by

$$\sigma_{cr,el}=k_b\frac{\pi^2 E}{\lambda^2} \tag{4.31}$$

where E is the modulus of elasticity of the material and k_b is a buckling coefficient. Figure 4.27 presented by Moody[52] shows the buckling coefficient k_b for A, B, and C flute corrugated fibreboard. Thus, for long columns, the compressive strength, δ_{max}, is reached once the compressive stress reaches the critical stress level, $\delta_{cr,el}$. Further loading of a column will not increase the stress $\delta_{cr,el}$, but merely enhance the bending deformation. For long columns failure is an elastic buckling. The column suffers no damage.

For medium columns, compressive failure is also a buckling phenomenon. However, the buckling occurs at a critical stress level, within the plastic(nonlinear) region of the compressive stress-strain curve. A nonlinear relationship between stress and strain is caused by structure rearrangements within the material. The severity of such structure changes increases with stress level.

Short columns will fail without undergoing any bending deformation. The stress at which this bending-free failure occurs is the intrinsic compressive strength of the material. This was demonstrated by tests presented in 4.3.3.

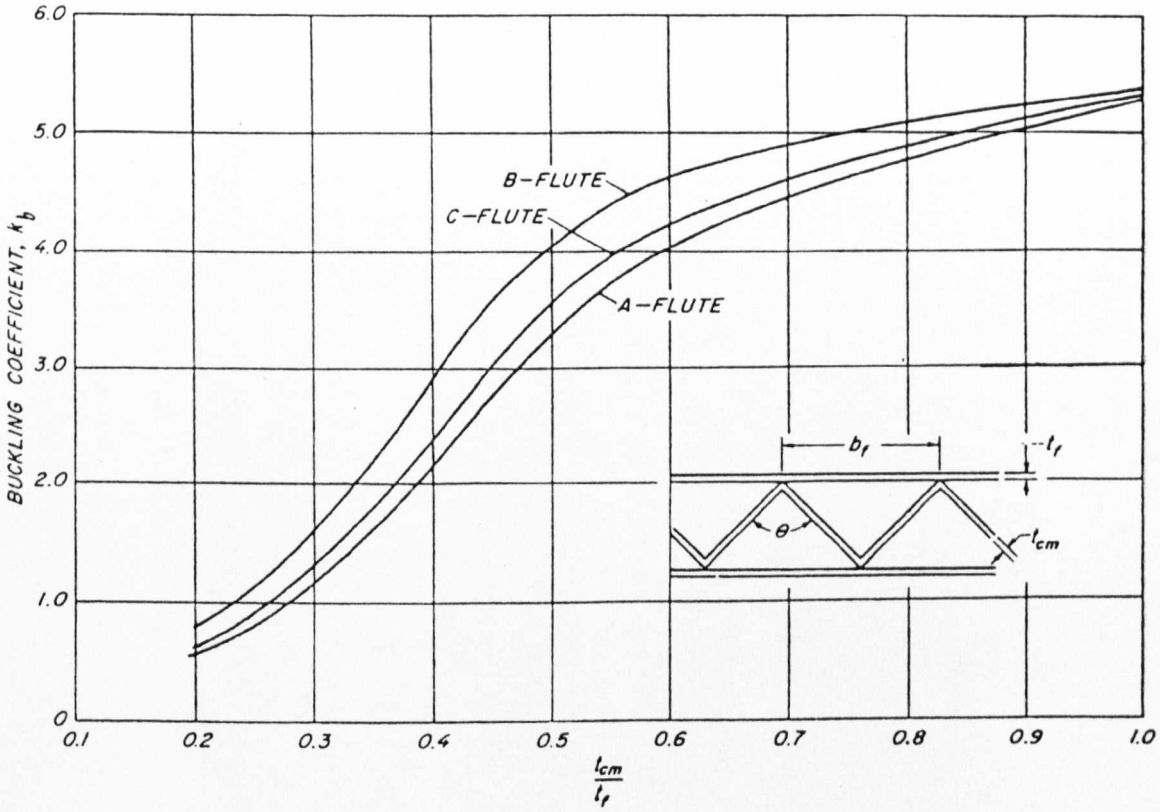

Figure 8.27 Buckling coefficient of A, B, C flute corrugated fibreboard

4.7.5 Comparison of buckling load and stress of corrugated fibreboard

Corrugated fibreboard is a sandwich plate made of paperboard. Because the height-thickness ratio for the short column crush test specimen is under 10, columnar buckling does not contribute to failure, but local buckling of the liners must be considered since they are unsupported between flute tips.

As indicated in [52] the Anderson's formula for the critical buckling stress δ_{cr} is,

$$\sigma_{cr} = \frac{k_b \pi^2 \eta E}{12(1-\nu^2)} \left(\frac{t_f}{b_f}\right)^2 \qquad (4.32)$$

Where

k_b =the buckling coefficient which is dependent upon the ratio of the thickness of the core material or corrugating medium to the facing thickness and the flute angle θ (Figure 4.27).

η =plasticity reduction factor for elastic modulus.

E =modulus of elasticity of liner.

t_f =liner thickness.

ν =poisson's ratio.

b_f =distance between liner supports.

In order to apply equation (4.32) to the corrugated fibreboard specimens, some assumptions were necessary to simplify the analysis. The flutes were assumed as V-shaped or linear between liners as shown in Figure 4.27. Though equation (4.32) is based on isotropic material, it was assumed also to apply to paperboard of the type usually used in corrugated fibreboard. Another assumption, based on Kellicutt's[49] reported values of Poisson's ratio for paperboard for the machine and cross machine direction, was that ν^2 was small and $1-\nu^2$ was nearly equal to 1. Finally, it was assumed that the short column specimens actually fail by local buckling.

To utilize this formula for predicting edgewise compressive strength, the value of the plasticity reduction factor, η, or the plastic modulus, ηE, must be known. The technique used to determine ηE and subsequently σ_{cr}, is as follow:

The plastic modulus, ηE, also called the tangent modulus of elasticity E_t, was assumed to be the slope of the tangent to the stress-strain curve at the buckling stress. Recalling that $(1-\nu^2)\approx 1$, equation (4.32) becomes

$$\sigma_{cr} = \frac{k_b \pi^2 E_t}{12} \left(\frac{t_f}{b_f}\right)^2 \tag{4.33}$$

If E is divided by both sides of this equation, it becomes

$$\frac{E}{\sigma_{cr}} = \frac{12}{k_b \pi^2} \left(\frac{b_f}{t_f}\right)^2 \frac{E}{E_t} \tag{4.34}$$

Stress-strain curves (Figure 4.28) for the paperboard components were then obtained by Moody[52] using the technique and equipment described by Setterholm[53]. As the liners and corrugated medium were the same material, the modulus of elasticity was determined and tangent modulus were determined at regular intervals of stress above the proportional limit. Values of E/δ_{cr} were then plotted as abscissas and the corresponding E/E_t as ordinates for the paperboard liners and medium as shown in Figure 4.29[52]. The value of E/δ_{cr} at the intersection of the two curves was used to determine the magnitude of the critical buckling stress.

A FE simulation of buckling analysis was carried out on a 200mm×200mm fibreboard with the assumptions that the liners and the corrugated medium were the same material and the flutes were V-shaped. Figure 4.30 shows the buckling results of a sample with 102 nodes each acted upon by a concentrated force, 20N, parallel to the panel surface. Figure 4.31 is the load-deflection relationship and Figure 4.32 is the stress distribution on the panel. From Figure 4.31 the buckling load is about half of the load range that is 10×102×(3.75/10)=382.5N, comparing with the test results shown in Table 4.7.

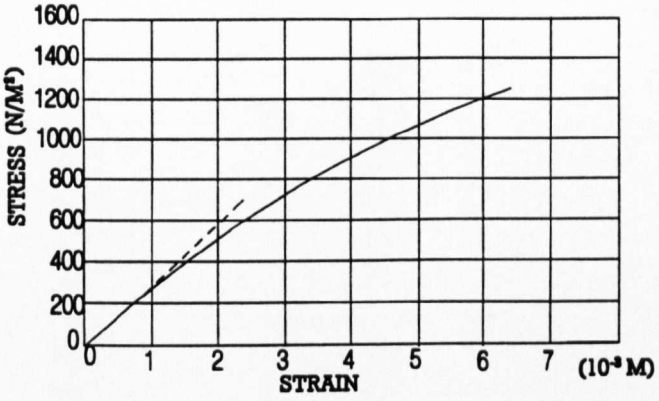

Figure 4.28 Stress-strain for facing material

Based on the knowledge of the Poisson's ratio for paperboard that ν^2 was very small and $1-\nu^2$ was nearly equal to 1. To use this formula for predicting edgewise compressive strength, the value of the plasticity reduction factor, η, or the plastic modulus, $\eta E=E_t$, must be known. From [2] $\eta=1/2.2$, $k_b=5.3$, and from the model $t_f=0.3\times10^{-3}$m, $b_f=0.8\times10^{-2}$m, $E=6.3\times10^9$ N/M^2, put these figures into equation (4.33), calculating the buckling stress is 0.174×10^8 N/m^2. The simulation result is 0.182×10^8N/m^2.

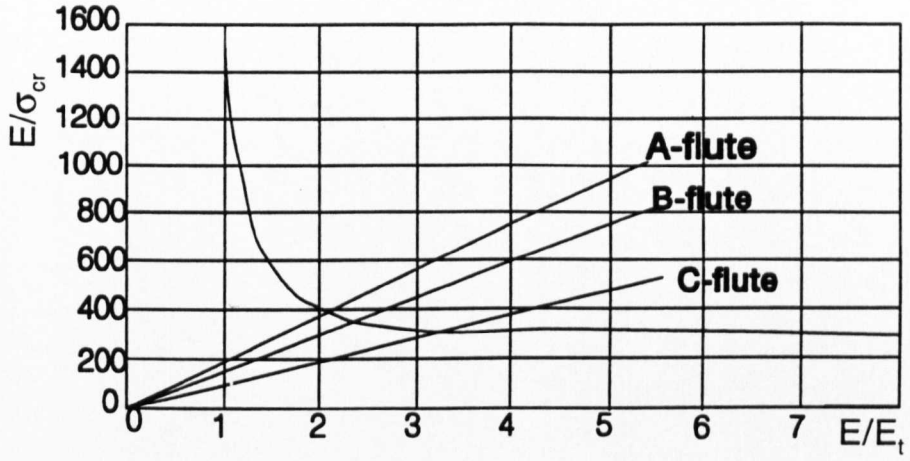

Figure 4.29 Determination of the tangent modulus for the facing materials

A comparison of the buckling stresses of a corrugated fibreboard liner between theoretical work and simulation was also carried out. For this liner k=5.3, E=6.3×10^9 N/M^2 and t=0.2mm, and l=200mm, from equation (4.30) and equation (4.31), the buckling stress is 27.4×10^3 N/m^2, the simulation buckling stress from Figure 4.33 is 22.3×10^3 N/m^2. The buckling for the liner is, from Figure 4.34, F=11×0.013×(8/10)=0.11 N. Figure 4.35 is the buckling simulation of a quarter of the side panel of a corrugated fibreboard container.

The differences of the buckling load and stresses between the simulation and theoretical analysis are mainly due to a small out -of-plane perturbation load that was

applied on the simulation model. It acted on the centre point of the panel and perpendicular to it. Since the external loading on the structure is perfectly in-plane, the out-of-plane deflections necessary to initiate buckling will not develop and the analysis will fail to predict buckling behaviour. The differences of the results between testing and simulation are probably due to the condition of samples and environmental situation such as temperature and humidity.

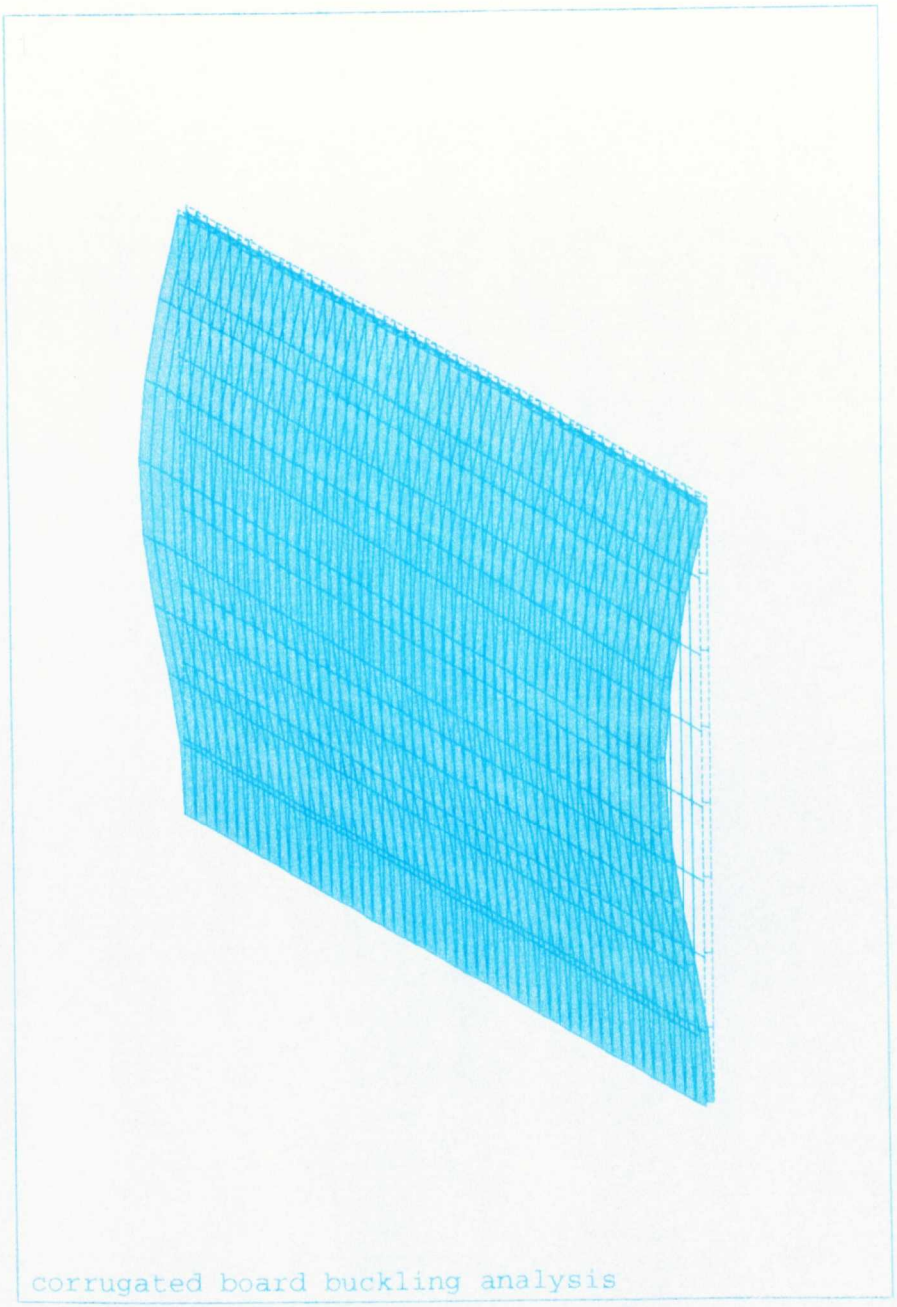

Figure 4.30 Simulation of the buckling of the corrugated fibreboard

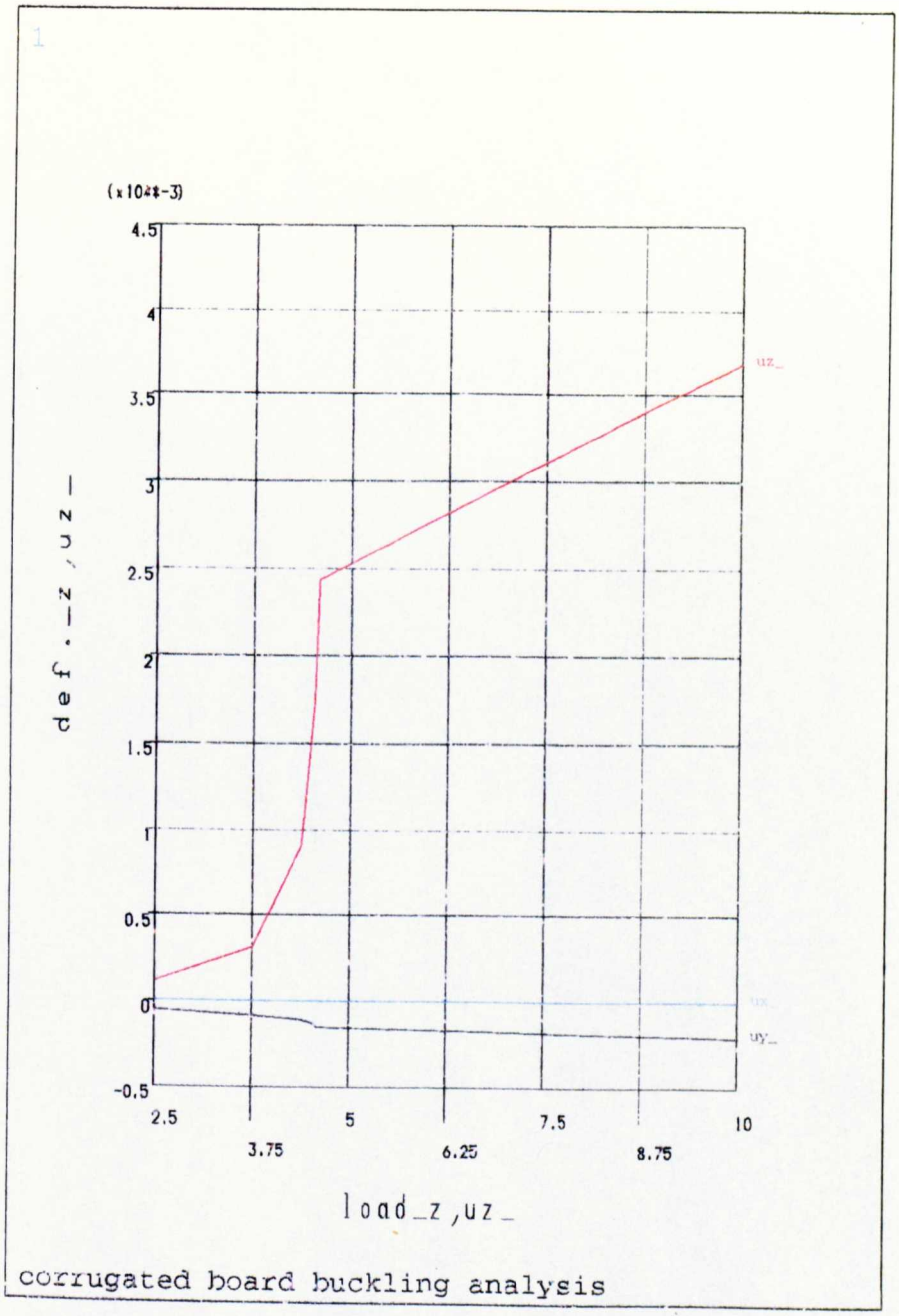

Figure 4.31 Load-deflection of the corrugated fibreboard for the buckling simulation

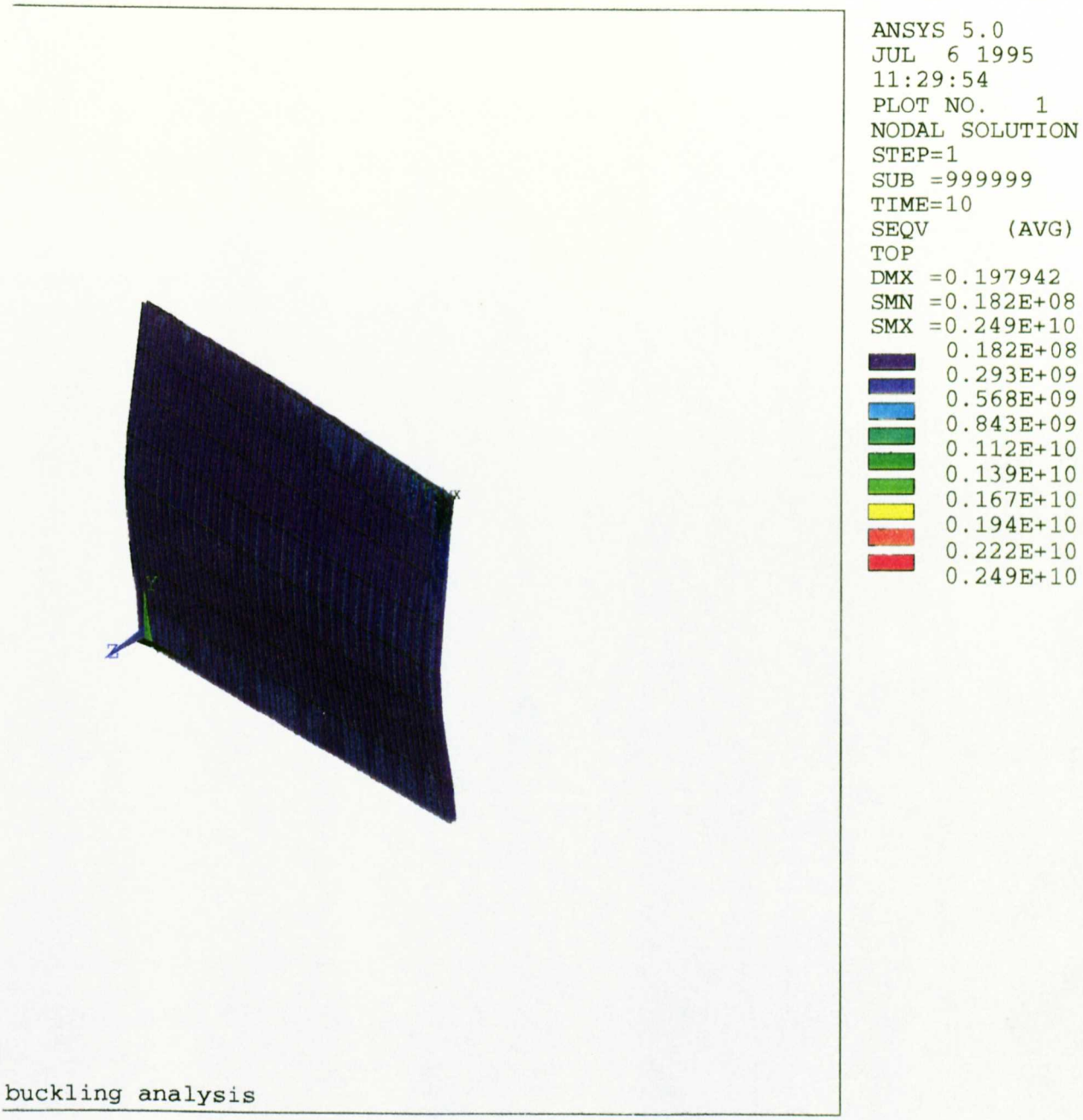

Figure 4.32 Stress distribution of corrugated fibreboard buckling simulation

4.8 Summary

A FE computer simulation approach has been employed in modelling corrugated fibreboard panel as an engineering structure. The principals of elasticity and engineering mechanics have been utilized to analyze and predict panel performance. A container panel subjected to different type of loading has been modelled and compared with existing experimental results. The container failed due to the development of compressive stresses in all cases examined by relevant studies. Paper is much weaker in compression than in tension. The FE modelling offered a easy way to determine the compressive strength and buckling load for different material, thickness, and structure of the fibreboard.

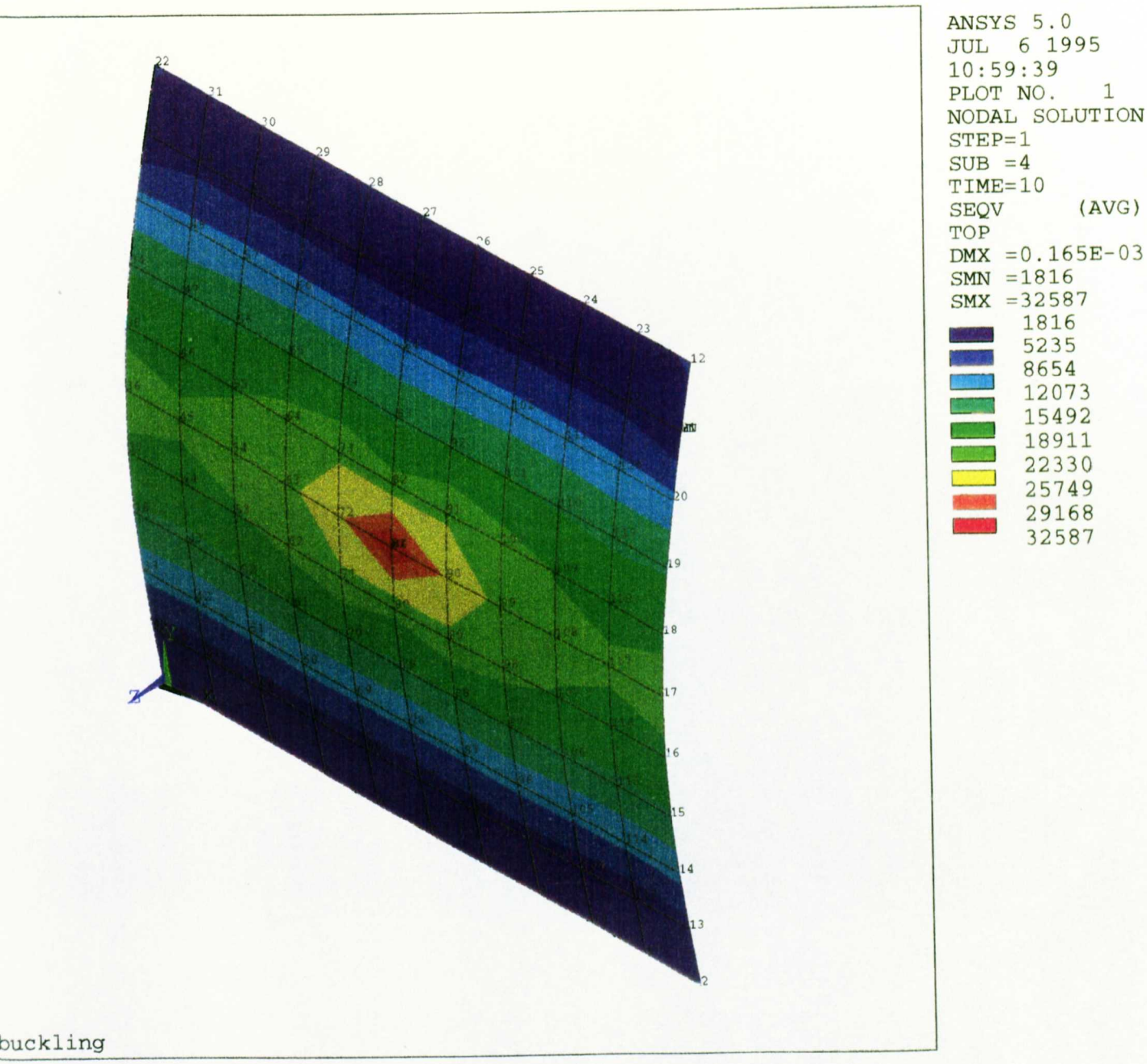

Figure 4.33 Buckling simulation of the liner paper

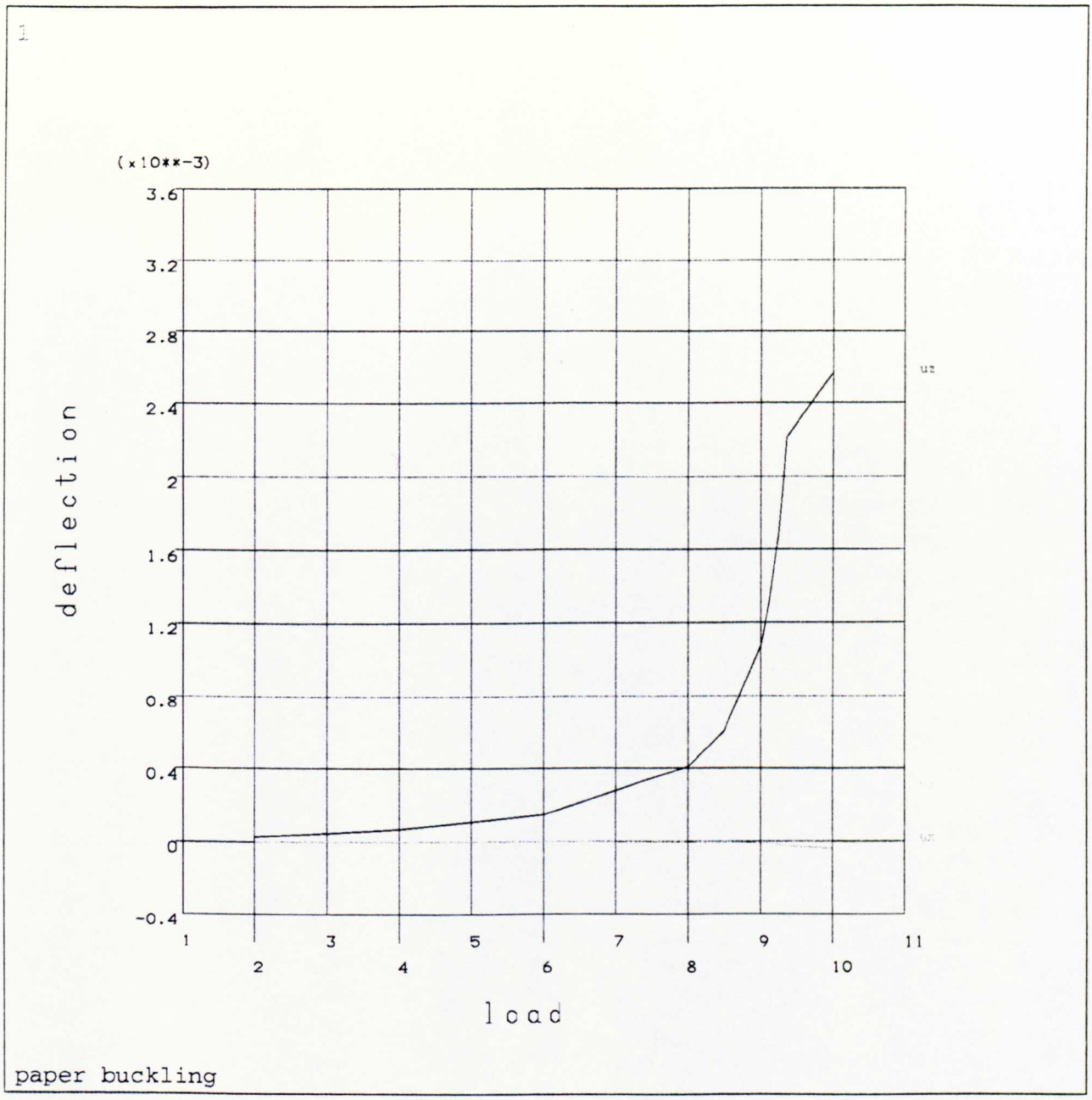

Figure 4.34 The load-displacement of the liner paper

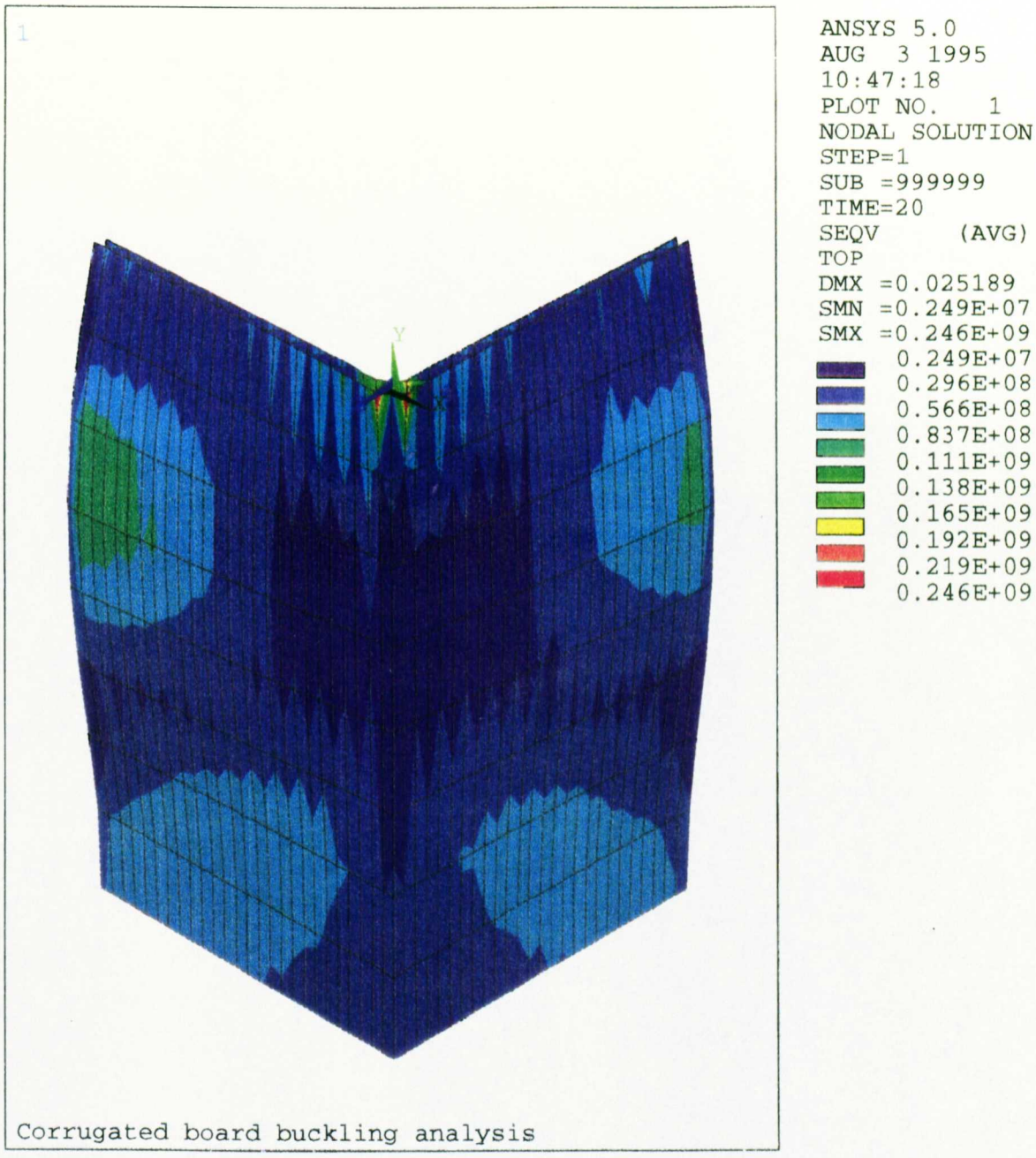

Figure 4.35 Buckling simulation of a quarter of container

Chapter 5

Modelling of the Collision between Package and Contents

5.1 Introduction

An understanding of the kinematics and dynamics of moveable packages with discrete contents is necessary in many industries, for example if the package with contents were to be processed on a high speed moving production line. Currently they are taken from the production line and then positioned by hand. In order to increase the efficiency and decrease the intensive use of labour, automation needs to be applied in these areas. There is a problem protecting the packages and contents from dynamic damage, especially when using high speed equipment. A 2D model to investigate the collision between contents and a surface was set up in order to analyze the dynamics and the deformation due to the contact as a first step in understanding the problem. The dynamics equations which govern the motion of the body were derived, and subsequently the collision was simulated on a SUN SPARC STATION using RASNA Mechanica Applied Motion software.

One of the main purposes was to investigate and evaluate the dynamic behaviour of the packet/contents and the resulting load/deformation which occurs within the system. The dynamics and structural performance of the package system are governed by many different factors. The most important factors are the external/internal forces, package rigidity and material properties. In order to analyze the behaviour of the package subjected to the action of the external forces, it is helpful to analyze a body colliding with a surface including the initial trajectory, the development of the motion, and the loading and deformation during contact.

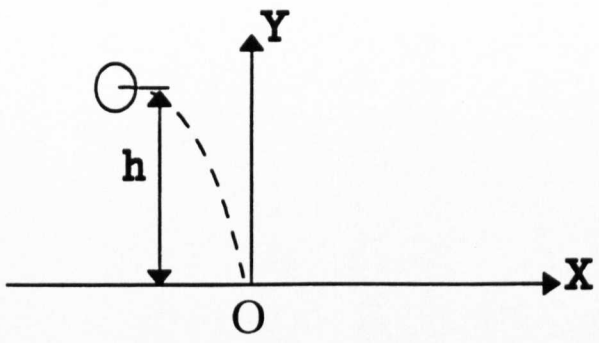

Figure 5.1 The model for collision

This chapter sets out to establish basic principles of a body colliding initially with a rigid surface, see Figure 5.1. It describes the mathematical analysis of the dynamics of the collision, and then considers the change from the rigid surface to a flexible one. The collisions were then simulated using the Mechanica Applied Motion software.

5.2 The analysis

There are several conditions to be considered when a body collides with a surface. They include the relative position between them at the beginning of the motion, the motion trajectory of the body and the angle of entrance. In this case the surface was in the horizontal position, the body was at any position above the surface and was given a velocity along the X-axis by exerting an impact at the same time the body moved as a free-drop object along the Y-axis. This motion is general and it is easy to observe the direction and the trajectory of the body after the collision.

5.2.1 Colliding

Figure 5.1 shows the initial condition of the body and the package. The body is

represented by a little circle, the bottom surface of the package is represented by the X-axis, which is considered fixed. The vertical distance between them is h. Assume that the horizontal speed of the body is v_1 and, the mass of body is m_1. A co-ordinate system XOY is created at the point of collision (Sun[56]).

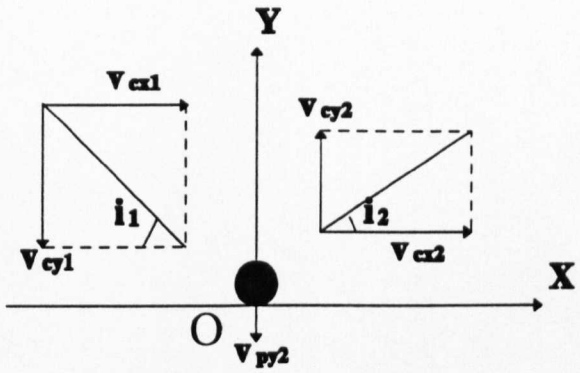

Figure 5.2 The Impact Velocity

Since the X-axis is established within the plane of contact and the Y-axis along the line of impact, the impulsive forces of deformation and restitution act only in the Y direction.

See Figure 5.2, from the principles of impact, the following equations can be written:

$$v_{cy1} = -\sqrt{2hg} \tag{5.1}$$

Where

$$v_{cy2} = -ev_{cy1} \tag{5.2}$$

v_{cy1} and v_{cy2} represent separately the velocities of the body along Y axis before and after collision. It indicates that the velocity of the body after colliding is just related to the distance h and the coefficient of restitution e.

5.2.2 After colliding

After colliding with a rigid surface, the body will bound to its original height, and keep the same speed along the X-axis. This is the condition of no energy loss. The angle of reflection of the body i_1 equals the angle of entrance i_2. The trajectory of the motion is continuous, and it can be described using the same expressions. The motion will repeat until the body moves away from the surface.

When the rigid surface is replaced with a flexible one, the body motion will decline. The degree of declination is mainly related to the material characteristics of the body and the surface, that is related to e, the coefficient of restitution. Here the trajectory of motion is described by

$$x = v_1 t \tag{5.3}$$

$$y = \frac{v_{cy2}}{v_1} x - \frac{g}{2v_1^2} x^2 \tag{5.4}$$

from which

$$y=v_{cy2}t-\frac{1}{2}gt^2 \tag{5.5}$$

where

$$v_{cy2}=ev_{cy1}=e\sqrt{2hg} \tag{5.6}$$

so

$$y=e\sqrt{2hg}x-\frac{g}{2v_1^2}x^2 \tag{5.7}$$

Equation (5.7) is the trajectory of the body after collision. It is a parabolic function.

When considering the contact with the flexible surface, the contact can be simulated using a spring and damper system leading to the governing equation on impact (Y axis is positive in a downward direction):

$$\ddot{y}+\frac{c}{m_1}\dot{y}+\frac{k}{m_1}y=g \tag{5.8}$$

where c is the damping coefficient and k is the stiffness of the spring. The solution of which is:

$$y=e^{\alpha t}(c_1\cos(\beta t)+c_2\sin(\beta t))+\mu \tag{5.9}$$

the values of α, β ,c_1, c_2 and μ can be derived from the initial conditions, Please see the appendix for references.

Assuming the boundary conditions to be

$$y=0,\ t=0,\ \dot{y}=v_{cyl} \tag{5.10}$$

and

$$\dot{y}=0,\ y=y_{max} \tag{5.11}$$

On rebound, the equation is also

$$\ddot{y}+\frac{c}{m_1}\dot{y}+\frac{k}{m_1}y=g \tag{5.12}$$

and the solution of it is in the same form as equation(5.9).

In this case the boundary conditions are:

$$t=0, \qquad y=y_{max}, \qquad \dot{y}=0 \tag{5.13}$$

The time-position relationship of the body has been calculated in part 1 of the Appendix. The energy loss during impact and rebound can be determined by evaluating the following integrals

$$WD=\int_0^t c\dot{y}dt[impact]+\int_0^t c\dot{y}dt[rebound] \tag{5.14}$$

Equating potential energy lost to the gain in kinetic energy enables the exit velocity to be determined. The ratio of exit to impact velocity will represent e the coefficient of restitution.

A comparison of calculated and computer derived values of the body position after impact is given later, see Figure 5.7.

5.3 Computer simulations

A model for demonstrating the above collisions was set up on a SUN SPARC STATION using the Mechanica Applied Motion software. Two bodies were created representing the free body and the surface. The initial conditions were set. The contact was modelled using a spring and damper to enable energy loss to be simulated.

4.3.1 Rigid surface

A body collision with a rigid surface can be simulated using a stiff spring.

$$F_{spring} = -ky \tag{5.15}$$

where

k is stiffness value

y is the deformation of the surface

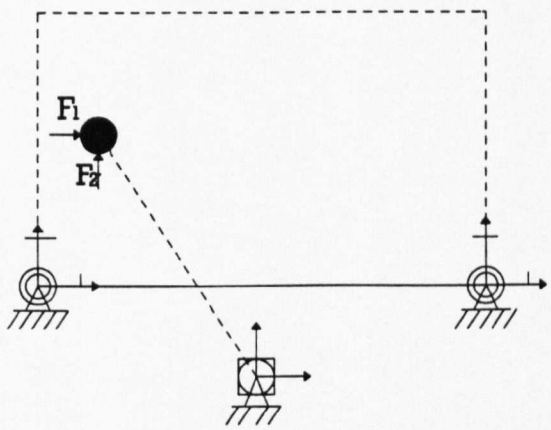

Figure 5.3 The Simulation Model of Rigid Collision

Choosing k>=10^6N/m will produce an ideal results for rigid impact. Below are the steps for modelling the rigid collision simulation using Mechanica Applied Motion software.

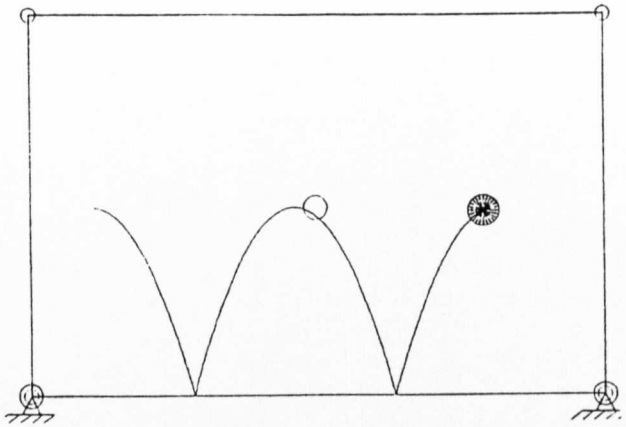

Figure 5.4 The trajectory of rigid collision

Step 1: Create a free joint between ground and the body. Create two *U*-joints between ground and the 2-D package, see Figure 5.3. The *U*-joints allows two rotational degrees of freedom and no translational degrees of freedom.

Step 2: Align *X*-axis of the two *U*-joints on the surface and make sure they are along the *X*-axis of the WCS(World Co-ordinate System) on screen, see Figure 5.3.

Step 3: Create a impulsive force F_1 on the body along *X*-axis.

Step 4: Create a measure about the body position along the impact axis. The measure is a designation of an aspect of the design that Applied Motion tracks the behaviour of during the analysis.

Step 5: Create a spring force F_2 fixed on the body by a polynomial function with the variable of position measure. Set $k=10^6$N/m. Set the condition that the force is active only when the measure<=0.

Select values of the parameters as shown in Figure 5.1 and Figure 5.3 as below, m_1=0.065kg, h=60mm, F_1=75tN(t=0.01), F_2=-$10^6 y$N. The graphical output of the simulation is shown in Figure 5.4, the motion trajectory of the body colliding with the rigid surface, is a series of separate parabolas. Because no energy loss is considered, the height of the parabolas and width remain constant, and are related to the initial velocity along the X-axis and h. Assuming smooth contact between the body and the surface, the magnitude of the impact force along the Y-axis is relative to the mass of body and the velocity V_y along Y axis. V_y is dependant on the height. The impacting force F_2 on impact is derived from the moment at impact and the impact time t.

$$F_{impact} = \frac{m_1 v_y}{t} = -\frac{m_1\sqrt{2hg}}{t} \tag{5.16}$$

Here t is affected by the material properties of body and surface, i.e. relative stiffness. Different values of F will occur as the stiffness of the materials are changed.

5.3.2 Flexible Surface

The simulation can be carried out by using a stiff spring together with damping when replacing the rigid surface with a flexible surface. See Figure 5.5. The spring force for impact is:

$$F_{spring} = -ky \tag{5.17}$$

where k and y have the same meaning as previous.

Here $k<=10^4$N/m can provide reasonable results for contents to package contact, since the two materials are not very stiff. The expression $F=-ky$ is also accurate enough for a small deformation, but it is possible to consider the influence of increasing the contact area when the deformation becomes large according to Douglas[54]. In this case a y^3 term should be added to the expression, that is:

$$F_{spring}=-ky-k_1y^3 \tag{5.18}$$

so that the force of the collision can be considered to be a function of deformation y multiplied by the surface area of a ball contacting the surface, which is proportional to y^2.

A damping force is added to simulate the dissipation of energy loss due to friction, heat exchange and deformation. The damping force is represented by

$$F_{damping}=cv \tag{5.19}$$

Where

c is the damping coefficient and

v is the separation velocity.

By changing c, different results of the collision can be obtained, and the materials properties can be simulated and observed since the dissipation of energy varies with c.

The steps for simulation of the flexible collision are as follows,

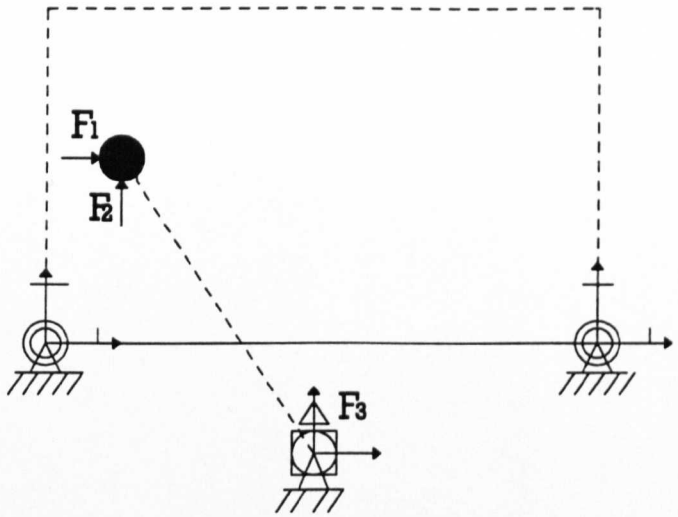

Figure 5.5 The Simulation Model of Flexible Collision

Step 1: Create a free joint between ground and the body. Create two U-joints between ground and the 2-D package.

Step 2: Align a translation axis of the free joint along with the impact axis, make sure the X-axis and Y-axis are both on the plane of impact.

Step 3: Align the local X-axis of the two U-joints along the X-axis of the WCS on the screen.

Step 4: Create an impulsive force F_1 on the body along X-axis.

Step 5: Create a DOF measure about the body position along the impact axis.

Step 6: Create a spring force F_2 fixed on the body by a polynomial function with the variable of a position measure, which is the distance between the centre of the ball and the surface. Set k=1700N/m, which is due to the increasing contact area when the deformation become large. Set the condition that the force is active only when measure<=0.

Step 7: Create a joint force F_3 which is a damper. The damper force is a function of the separation velocity. Set the condition statement to match that set in step 5 that the force is active only when measure<=0.

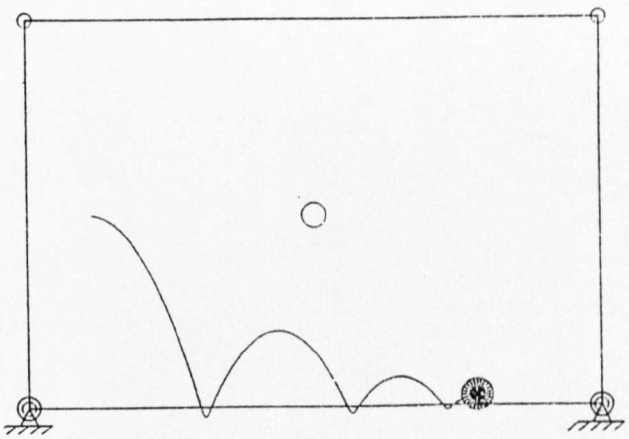

Figure 5.6 The trajectory of flexible collision

As with the rigid collision, some values of the parameters in this flexible model are chosen as m_1=0.26kg, h=60mm, F_1=75tN(t=0.01), F_2=-1700y, F_3=5vN. The graphical output of the simulation is shown as Figure 4.6. It is the motion trajectory of a body in collision with a flexible surface. It exhibits separate parabolas, the heights of which decline gradually and the width narrows gradually. The reason it behaves like this is

that the body is losing some energy after each collision. The lost energy is related to the material characteristics.

A comparison between the calculated and the computer simulation of the impact region is shown as Figure 5.7 and Figure 5.8. This is a plot of the position of the body determined from the simulation. The horizontal axis represents the time after contact. The vertical axis represents the position of the colliding body. The curve and dots represent the simulation values. The calculated values match the curve with good accuracy. Please see Appendix 1.(note: system of units is arbitrary but must be consistent).

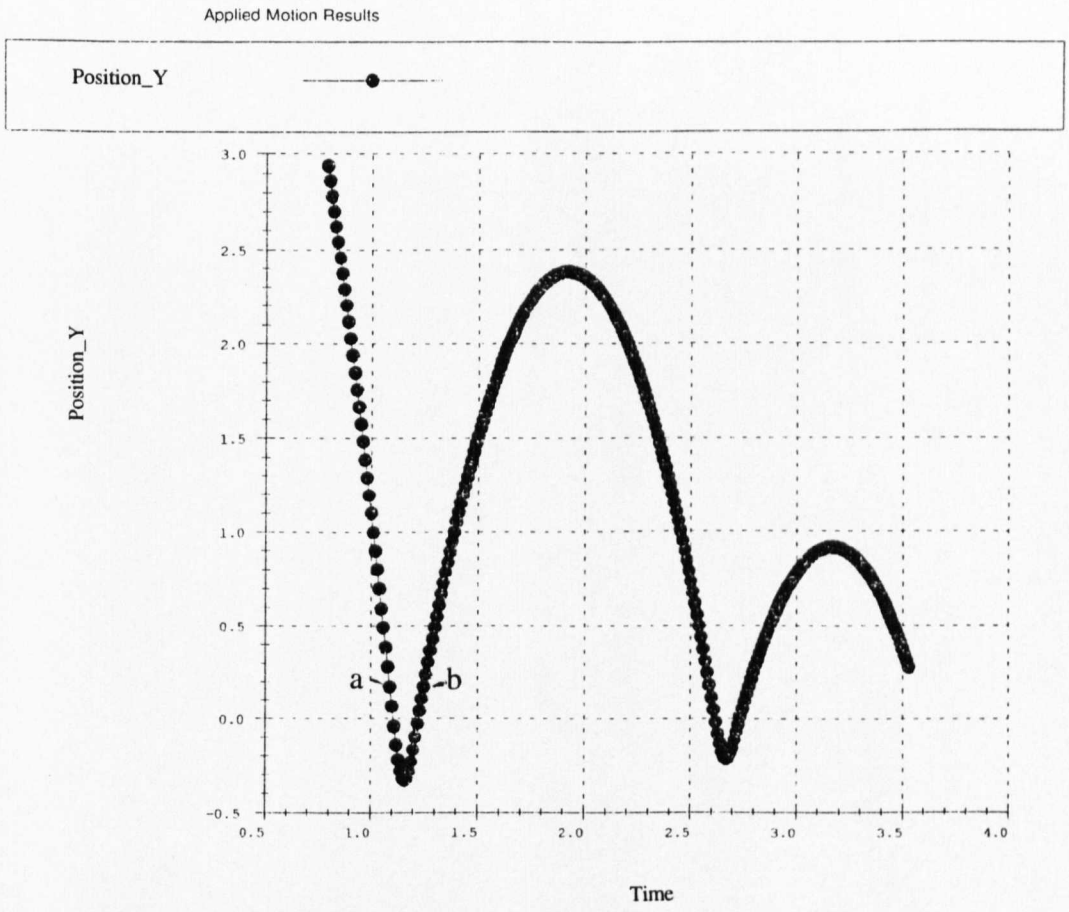

Figure 5.7 Time-position of the colliding body during impact and rebound

5.4 Summary

A model of the collision between a body and a surface was set up and the collision between them was successfully simulated. The surface was assumed to be both rigid and flexible. It has been shown that the analysis of two colliding bodies can be satisfactorily modelled using current dynamics software with good agreement. This gives confidence that the more complex modelling of a 3D system of free bodies within an enclosed space can be modelled with some accuracy.

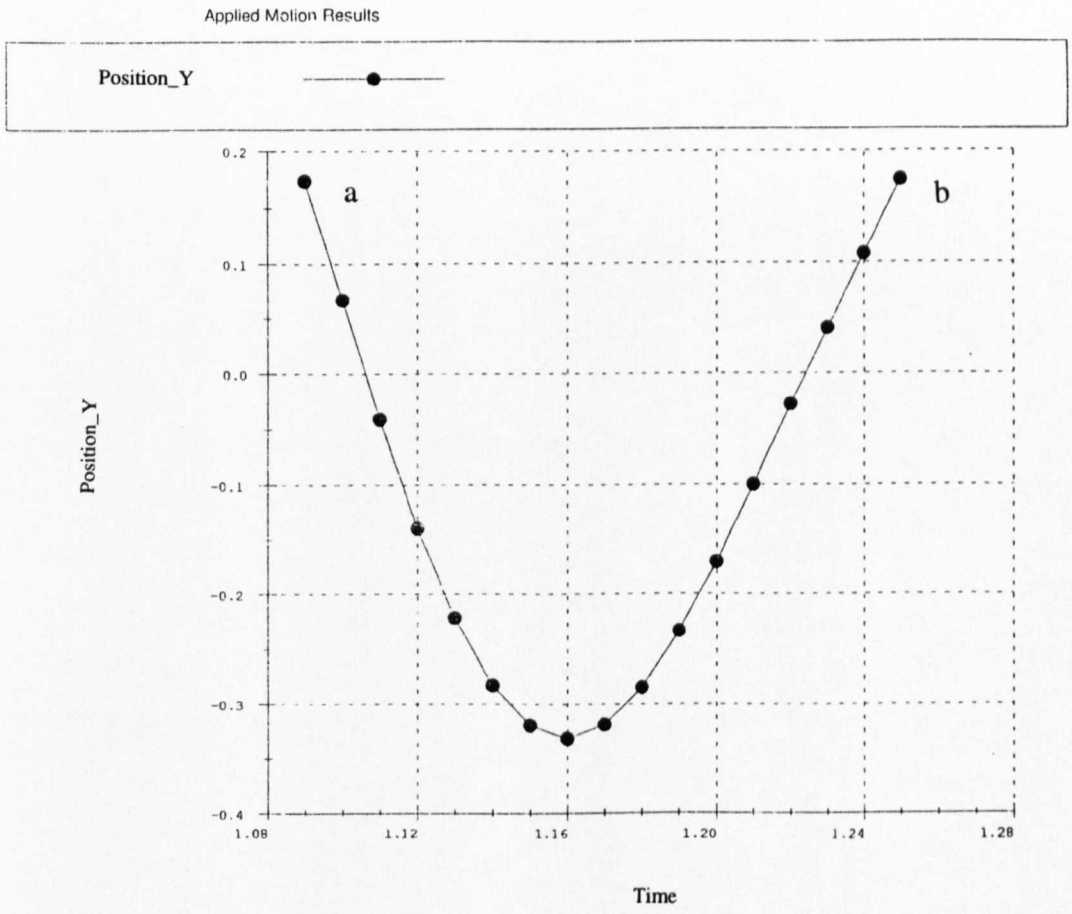

Figure 5.8 A segment graph of Figure 5.7 between points a and b

Chapter 6

Simulation of the Interaction between a Package and Its Contents

6.1 Introduction

Numerous studies investigating the impact behaviour of rigid or semi-rigid containers have already been reported in the literature[24,42,43]. So far, however, most of these investigations have concentrated on methods for evaluating the quality of these containers. Such methods include the Mullen burst test, the puncture test, the short column edge crush test and the fixed and floating test[17,18,19]. There is still a strongly felt need for a further understanding of the mechanical behaviour of a container subjected to an external force or impact, especially when the container has contents[24,43]. Some initial developments of theoretical analysis and simulation methods are presented.

The approach to the problem was to first consider a 2D package-contents systems. Analysis of the movement simulation produced satisfactory results. The 3D model was initiated with two contents within a rigid boundary. Control of the contents required the use of force elements in three directions controlled by conditional statements related to measures that represent the position of one of the contents relative to the boundary and the other content.

Precisely the models were as follows:

1). A 2D model of a moveable packet and two or nine independent moveable contents. The package boundary was rigid and the motion of the contents controlled by conditional spring elements. The results were that it reacted to external forces in

a satisfactory manner with the contents remaining within the packet boundary.

2). A 3D model with a moveable packet and two independent moveable content parts within the rigid boundary. Control of the contents so that they remain within the boundary required the use of force elements in three directions controlled by conditional statements. There related to measures that represent the position relative to the boundary and the other content (Sun[56]).

6.2 The 2D model for movement

A model of two bodies representing the contents within the packet boundary was

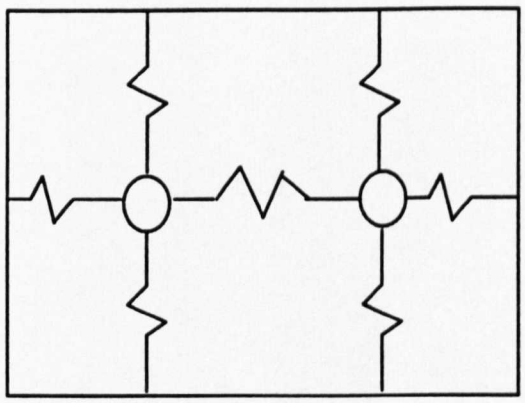

Figure 6.1 The 2D model for movement

developed as shown in Figure 6.1. The packet boundary was made rigid and flexibility ignored. A free joint was used between the bodies and ground. The contents are controlled by two point springs with conditions to eliminate tension introduced. A linear and a angular force was exerted on the packet.

In order to prevent the contents from moving out of the region of the packet, some measures were added to the system to control when the spring forces became active. The model was subject to an impulsive force.

$$F=\rho t \tag{6.1}$$

where ρ is a constant, t stands for time. A series of runs were made with changes in ρ and k the spring stiffness(units are arbitrary). The following values were used.

a). k=10, ρ=2, 4, 6, 20

b). k=4, ρ=2, 4, 6, 20

c). ρ=2, k=2, 4, 10

The system reacted as would be expected with the facility that content motion can be

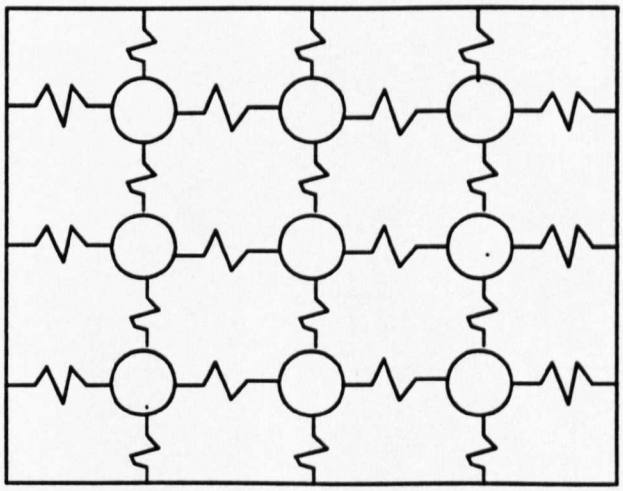

Figure 6.2 The Model with Nine Contents

plotted and evaluated. To obtain not only indications of the forces between the contents and boundary but also between the contents, the number of the contents was increased to nine within the boundary. A primitive, a sphere, was attached to each

content and they were connected with two point springs. The springs become active only when compressed. Follower forces were used between contents and boundary. A follower force is defined by the software that its direction is fixed with respect to a part's local frame. Motion and springs forces were controlled by the measures between contents or contents and boundary. See Figure 6.2.

Separately exerted linear and angular external forces were applied to the model, causing frequent changes to the magnitude and direction of the forces and the subsequent motion of the masses. The behaviour of the contents is similar to rubber balls due to the fact that friction and the flexibility of the contents and boundary were ignored. Figure 6.3 is the reaction of the model to linear force, and Figure 6.4 to angular force.

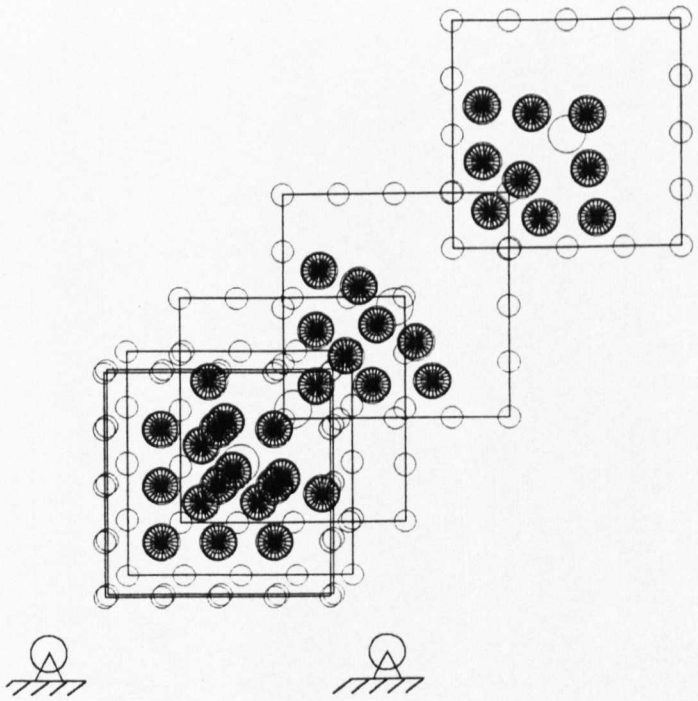

Figure 6.3 The model reacts to linear force

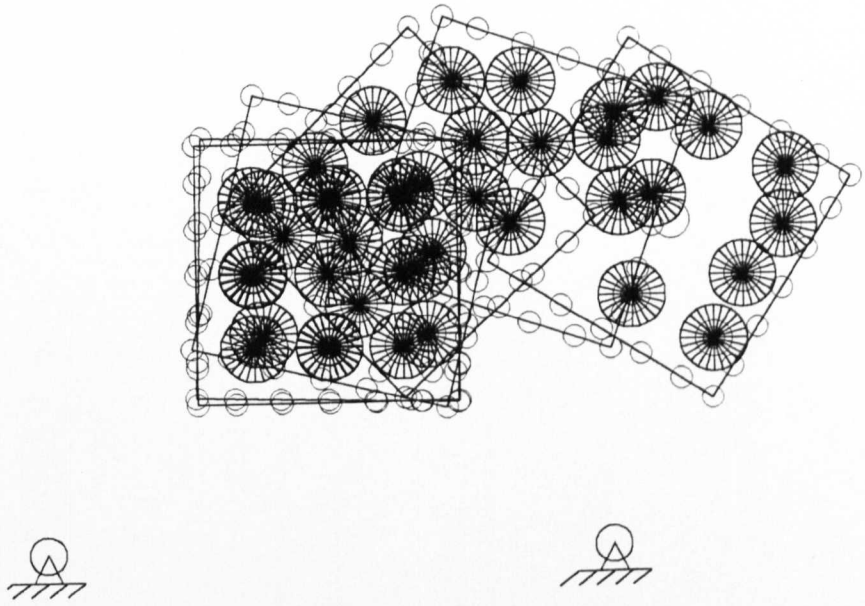

Figure 6.4 The model reacts to angular force

6.3 The 3D Model

A 3D model of a packet with two discrete content items was set up to simulate the behaviour of a more realistic model subject to external force, as shown in Figure 5.5. The packet has a simple rectangular box shape. A planar joint connects it to ground, to ensure that the packet moves on a plane. Two equal impulsive forces were applied on its two corners to create movement in a straight line or curve by changing the

magnitude of one of them. Two contents were created inside the box. In order to make the simulation more arbitrary and observer interaction quicker, the contents were fixed at points apart from the surfaces of the box and were acted upon separately by impulsive forces at the start of the motion. A free joint was created between the contents and ground. The friction force between bottom of the box and the surface must be accounted for if the model is to react as realistically as possible.

At the first glance the model seems simple and rigid, but it can give a good indication of the motion compared with a complex model, furthermore, this model can be treated as a flexible container as long as the interaction force between packet and contents is properly controlled as demonstrated in the 2D model (Sun[56]).

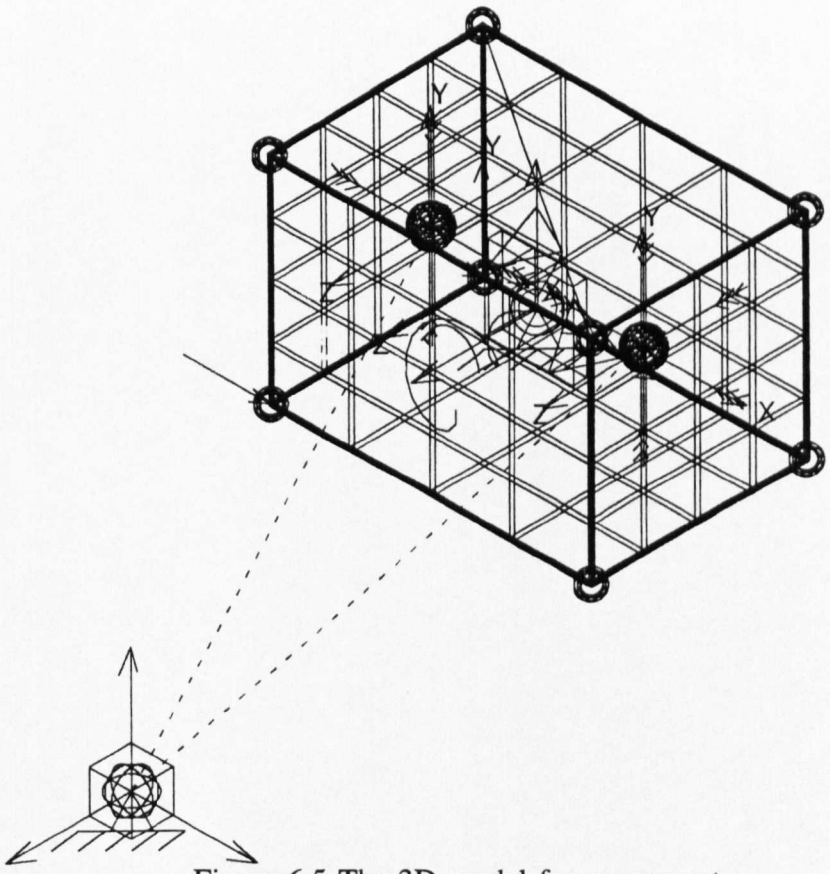

Figure 6.5 The 3D model for movement

6.3.1 Simulation of the 3D model

The collisions can be simulated using springs and six spring forces were fixed on each body using a polynomial function with the variable of a position measure. There are fixed forces along X-axis, Y-axis and Z-axis of the world coordinate system. These forces act separately between the contents and each of the six surfaces of the box. They become active only when the contents touch the relative surface and the magnitude of the force is proportional to the distance of the contents exceeding the surface limit. That means the force is related to the deformation of the surface, if the stiffness of the packet is properly selected, the packet can become as soft as necessary. This was done by creating a series of measures upon which the forces are conditional. These forces not only give the values of the interaction between contents and packet but also are the factors that keep the contents within the package after the start of the simulation.

When the system moves in a straight line the above forces can keep the contents inside the packet, but with rotation around the Y-axis, the contents will move out of the packet and the system loses control. This happens for two reasons, one is that the fixed forces do not change direction as the system rotates, they are not the normal forces any more in this situation. The other reason is that the local coordinate system doesn't change direction along with the rotation, this makes the measures which control the forces incorrect. To solve the first problem two components forces along the X-axis and Z-axis of the WCS were set up to replace the fixed force. They are separately controlled by the sine and cosine of the rotating angle. The second problem was solved by coordinate system realignment. The equations below can be derived as:

$$x' = x\cos\theta - z\sin\theta$$

$$y' = y$$

$$z' = x\sin\theta + z\cos\theta$$

Figure 6.6 shows how the model reacted to a linear force.

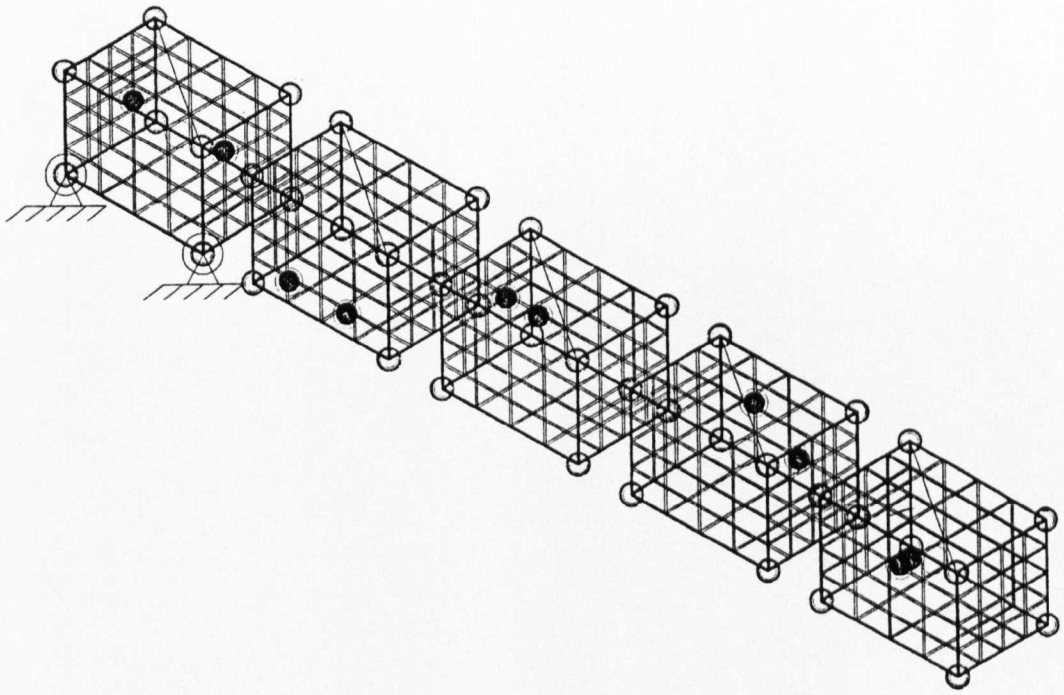

Figure 6.6 The 3D model react to a linear force

6.3.2 Modelling frictional forces

Friction force between the packet and the surface is important in this simulation, because it is the unique external force acting on the model after the initial impact. The frictional forces encountered in physical system are usually nonlinear. The characteristics of the frictional forces between two contacting surfaces depend on such factors as the composition of the surfaces, the pressure between the surfaces and their relative velocity, so that an exact mathematical description of the frictional force is difficult. However, for practical purposes, most frictional forces can be divided into there basic categories: viscous friction, static friction and coulomb friction. Here just static and coulomb friction are considered.

Viscous friction represents a retarding force with a linear relationship between the applied force and velocity. Viscous friction is most commonly called "damping". The mathematical expression of viscous friction is:

$$F_v = cq_{dt} \tag{6.2}$$

where:

c is the damping coefficient

q_{dt} is the relative velocity between the sliding surfaces.

Static friction represents a retarding force F_s that tends to prevent motion from beginning. It is represented graphically in Figure 5.7 and its magnitude is given by

$$F_s = U_s N \tag{6.3}$$

where U_s is defined as the coefficient of static friction and N is the normal force

between the contacting surfaces.

Coulomb friction is a retarding force F_c and has a constant amplitude with respect to velocity, see Figure 6.8.

It is related to the normal force between contacting surfaces and its magnitude is given by

$$F_c = U_k N \tag{6.4}$$

where U_k is defined as the coefficient of sliding friction and N is the normal force between the contacting surfaces.

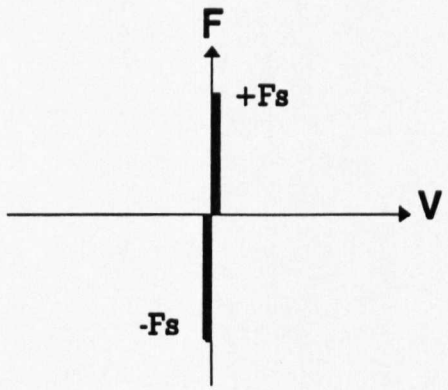

Figure 6.7 The Static Friction

In general, both static and coulomb friction exist together. When combining them there will be two force discontinuities(see Figure 6.9). One is in the static friction and another discontinuity is during the transition from static to coulomb friction. According to Douglas[55] the force discontinuity will cause numerical integrators to either take tiny steps to insure the correct solution or even lock up in extreme cases. To help speed up solution time, discontinuities need to be eliminated by replacing them with piecewise continuous functions. This will not affect model results much but will speed up the solution time dramatically.

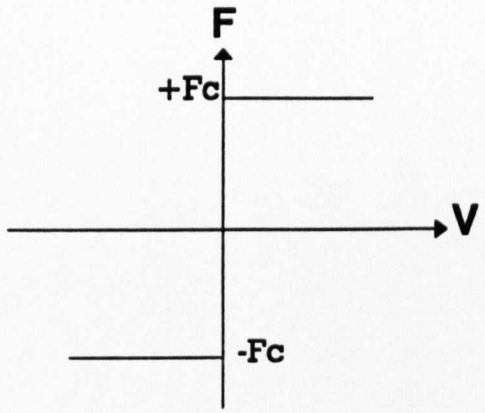

Figure 6.8 The Coulomb Friction

Figure 6.10 shows a comparable model of combined static and coulomb friction that provides good results and doesn't have any discontinuities. The slope shown in Figure 6.10 is exaggerated to clearly show the model. The steeper the slope the closer this model approximates the model of Figure 6.9.

According to [55], the expression for the piecewise continuous function of Figure 6.10 is given below:

$$F_{sc}=(U_kN)(bound(q_{dt}/V_{latch},-1.0,1.0))(1+2(U_{ratio}-1.0))/(1.0+(q_{dt}/V_{latch})^2) \quad (6.5)$$

where q_{dt} is the velocity of the degree of freedom.

U_{ratio} is the ratio of U_s/U_k.

V_{latch} is the velocity where the static friction transfers to coulomb.

This model is complex at first glance. The first section computes the coulomb friction component of the friction force and scales the entire function. The second portion uses the bound function to provide the transition at q_{dt} equal to zero. The bound function limits the first value between the values of the next two values; that is:

if q_{dt}/v_{latch}<-1.0 then bound returns -1.0

if q_{dt}/V_{latch}>1.0 then bound returns 1.0

otherwise bound returns q_{dt}/V_{latch}

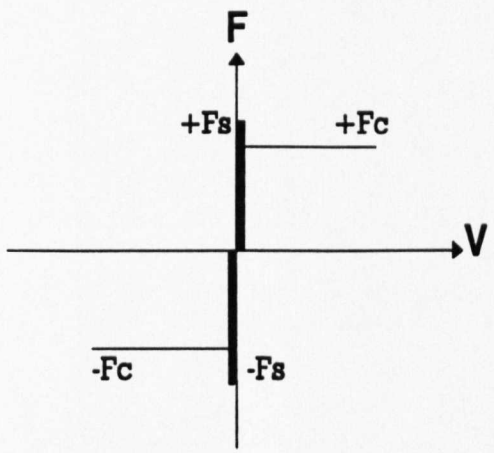

Figure 6.9 Static and Coulomb Friction

The third expression is a mathematical function providing the smooth transition from the force peak of the static friction model to the lower constant value of the coulomb

model.

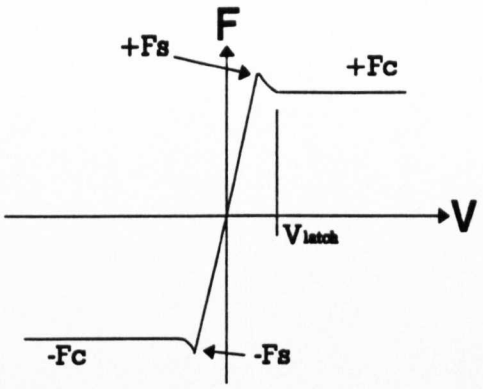

Figure 6.10 The Comparable Model

6.3.3 Implementing friction in Applied Motion

Having discussed the theory above, now applying friction to the 3D model. The normal force of the package on the ground will be determined by its weight. The complex function described on the previous section will be implemented as a computed measure.

Below is the step-by-step procedure for building the 3D model sliding across a surface with friction.

(1) Create a part as the package using the plate mass primitive(see Figure 6.5). Attach this part to the ground with a planar joint. Reorient the rotational joint of the planar joint along the global z-axis. Place a position motion driver on the rotational axis that has a constant value of zero. This locks the rotational degree of freedom about z-axis of the package

(2) Create DOF measures on the planar joints translational x and y axes defined as follows in Table 6.1.

Table 6.1. DOF measures

Measure	Description	Measure	Description
Y_{pos}	DOF position of y-axis	X_{pos}	DOF position of x-axis
Y_{dt}	DOF velocity of y-axis	X_{dt}	DOF velocity of x-axis

(3) Create Design Variable Measures relating to the friction model defined as follows in Table 6.2.

Table 6.2. Design Variable Measures

Design variable	Description	Minimum	Maximum	Current
Latch_vel	V_{latch}	0	1	0.05
Coef_fri	U_k	0	1	0.2
ratio	U_{ratio}	0	3	1.2
stiffness	ground stiffness	100	1.0e6	1.0e6
damping	ground damping	0	1.0e5	1.0e5

(4) Create measures for these Design Variable Measures with Table 6.3 below:

Table 6.3. Design Variable Measures

Design var.	latch_vel	coef_fri	ratio	stiffness	damping
Measure	Vlatch	mu	us_uk	K	C

(5) Create two computed measures. Call the first one "normal" and is the weight of the package. Call the second one "friction" and is the computed friction force using the complex friction equation 6.5 discussed in the last section.

(6) Apply the normal force to the y-axis of the planar joint. Select the force function as a polynomial and a function of the measure "normal" with the first order polynomial coefficient equal to -1.

(7) Apply the frictional force to the x-axis of the planar joint. Select the force function again as polynomial and a function of the measure "friction" with the first order of polynomial coefficient equal to 1.

With the introduction of these modifications the simulation ran successfully and gave confidence that it could be developed further. The data available subsequent to the run is very extensive. Figure 6.11 is the plot of the velocity along X-axis of a point on the packet and Figure 6.12 is the normal and friction force acting on the model.

The internal forces between the contents which could cause problems with their integrity in a real situation is obtained. Analysis of the results is continuing and the model being further developed. Figure 6.13 shows how the 3D model package moves in a curve as the result of an impulsive force.

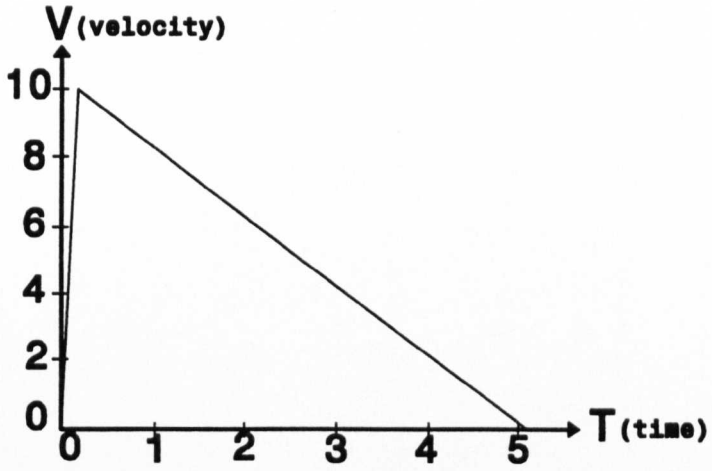

Figure 6.11 The Velocity Along X-axis

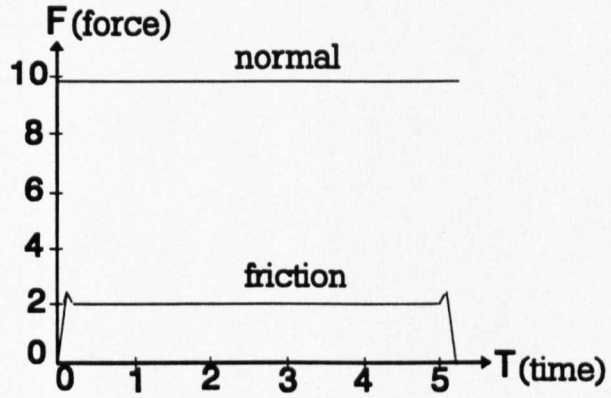

Figure 6.12 Normal and friction forces

6.4 Summary

Two 2D models and a 3D model were created for investigating the impact behaviour of package systems subject to external forces. Techniques for modelling the interaction between package and contents, and the movement of package with contents after impact were developed. The use of state of the art mechanism simulation software provides the means for analysing the kinematics and dynamics of complex systems with confidence in the accuracy of the simulation.

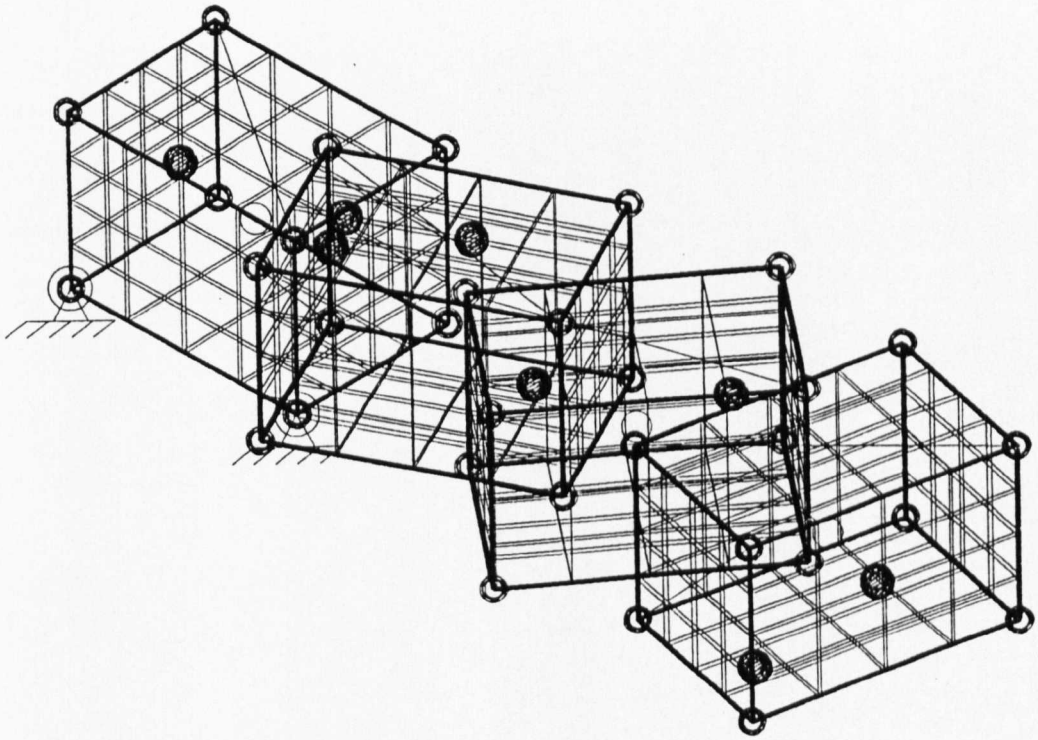

Figure 6.13 3D model reaction to an impulsive force

Chapter 7

A Model of Product-Cushion-Package System

7.1 Introduction

In any industrial society, products must be transported from one location to another. The product-cushion-package system has to survive the rigours of the handling and transportation environment. If the product reaches its destination damaged, it must be repaired or replaced. As a result, the producer will suffer economically and in prestige. Package systems must be designed to minimize any damage during handling and distribution. Packaging material has to be saved and waste has to be avoided.

The product-cushion-package system also must withstand impacts and vibrations. Sensitive products are typically cushioned in polymer materials with good damping properties. This cushion dampens the mechanical loadings on such a system. The present study outlines methods to simulate the mechanical loadings on such a system. It is hoped that these results make it possible to minimize the size of cushion structures and to assist in selection of the appropriate packaging materials.

7.2 Mechanical loadings and cushioning

The product-cushion-package system must withstand dynamic and static loadings. Figure 7.1 shows a model of this system. The product is fixed in the centre of the package by springs connecting it to surfaces. The package is put above a rigid plane surface and then released to strike this surface after a free fall. The height of drop and the attitude of the package are predetermined.

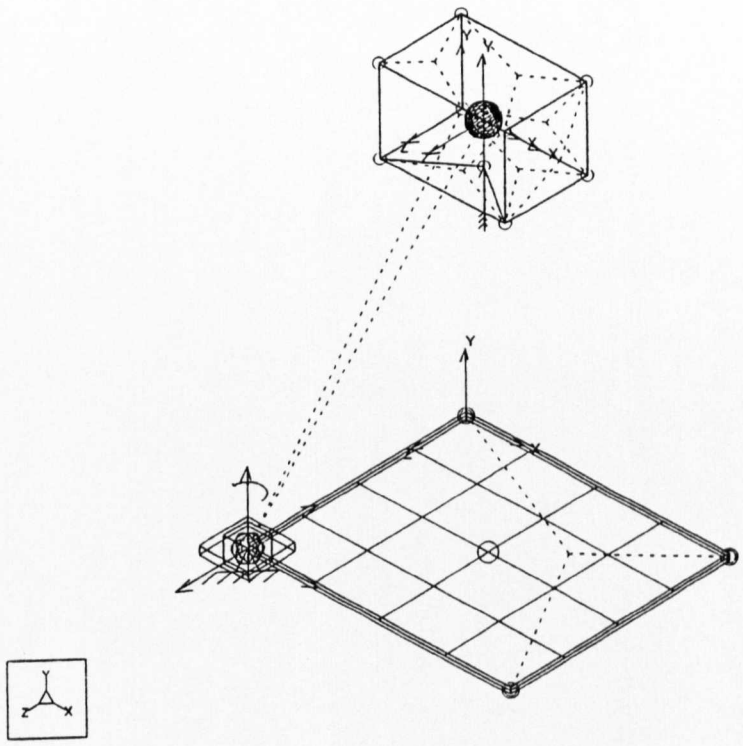

Figure 7.1 A Product-Cushion-Package System

The dynamic properties of a product-cushion-package system, such as acceleration, velocity, and impact forces can be determined by the putting measures into the simulation procedure. Figure 7.2 shows the flat impact.

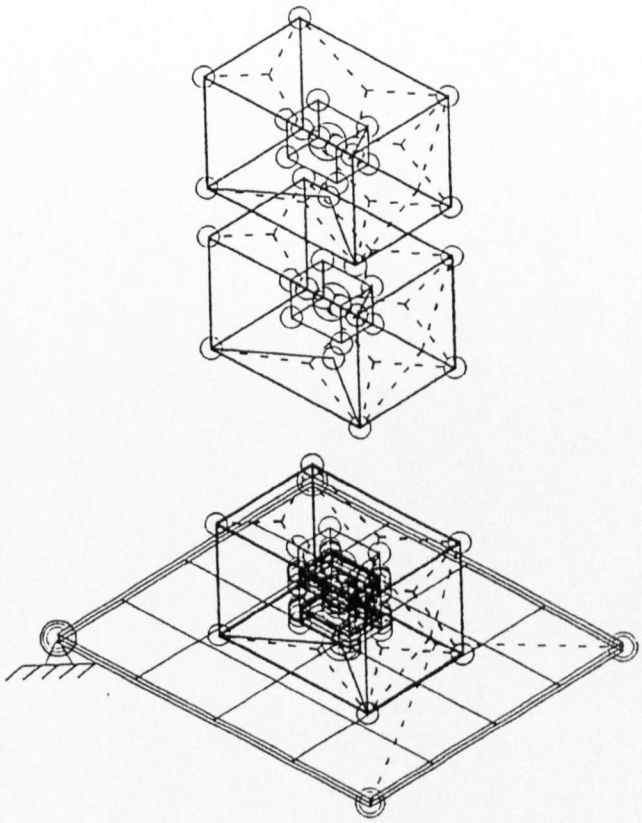

Figure 7.2 The Flat Impact of the System

Figure 7.3 illustrates the edge impact. The impact force between the edge and ground and the cushioning force between the contents and cushion are shown in Figure 7.4. This shows the cushioning force is about a half of the impact force. The solid line represents the impact force, and the dotted line represents the cushioning force. The two forces are damped to zero in about 1 second. The impact occurs at t=3.1s.

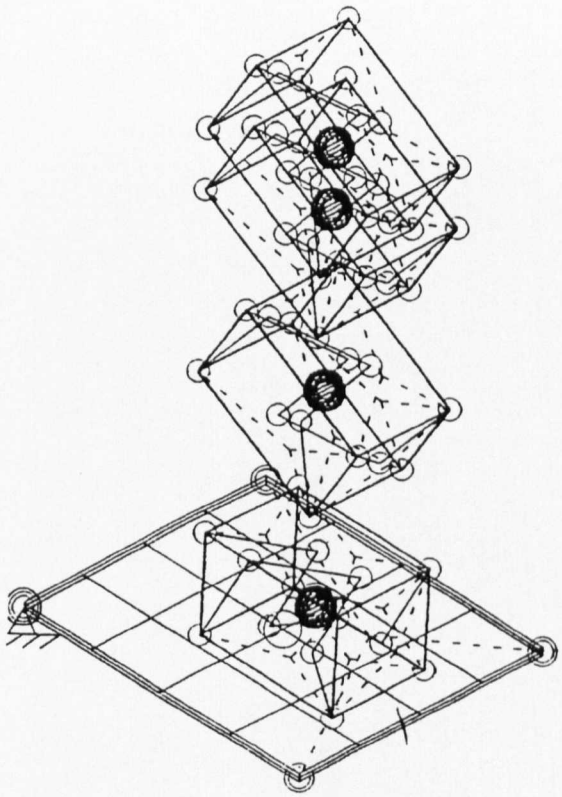

Figure 7.3 The Edge Impact of the System

Figure 7.5 is the corner impact, Figure 7.6 shows the cushioning forces of the contents, and Figure 7.7 shows the impact forces in three directions. The solid line represents the force in y direction, the dotted line represents the force in x direction, and the short dotted line represents the force in z direction.

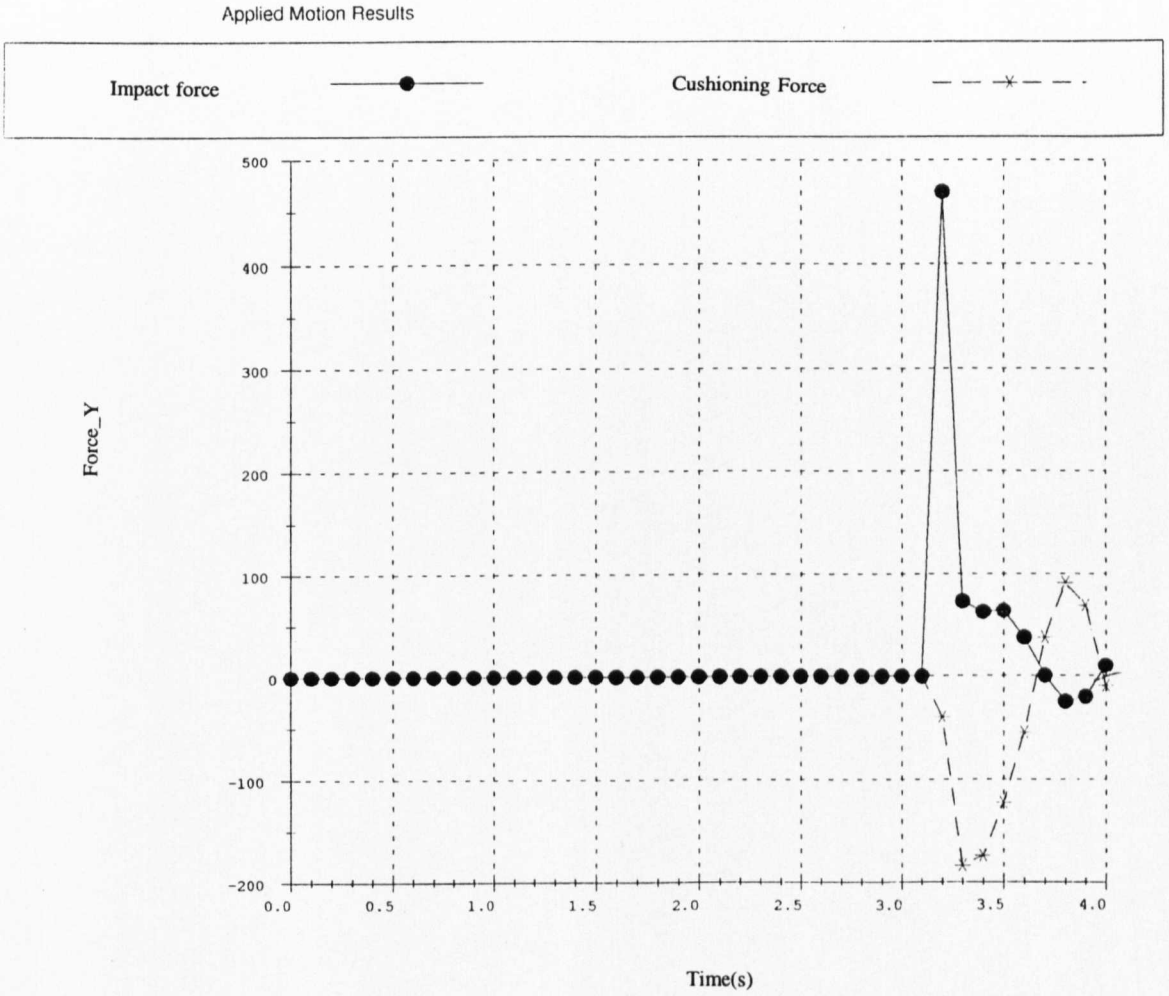

Figure 7.4 The Impact Force and Cushioning Force

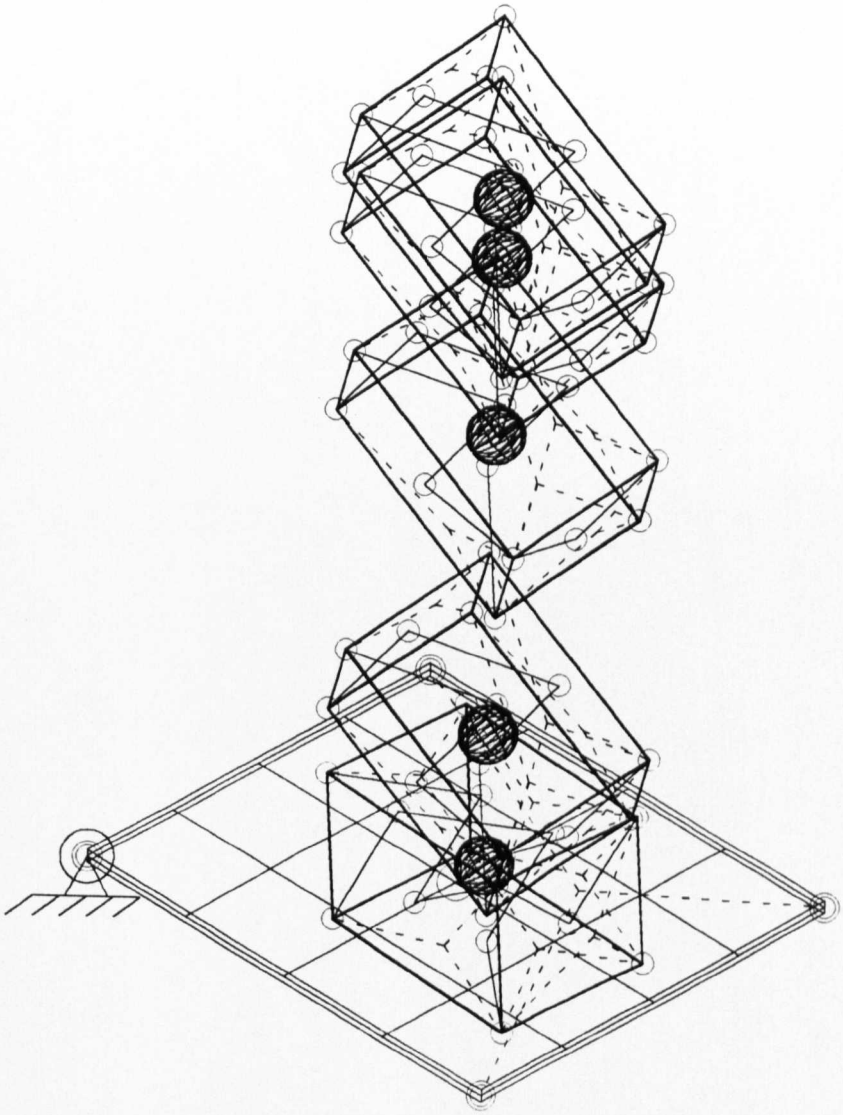

Figure 7.5 The Corner Impact of the System

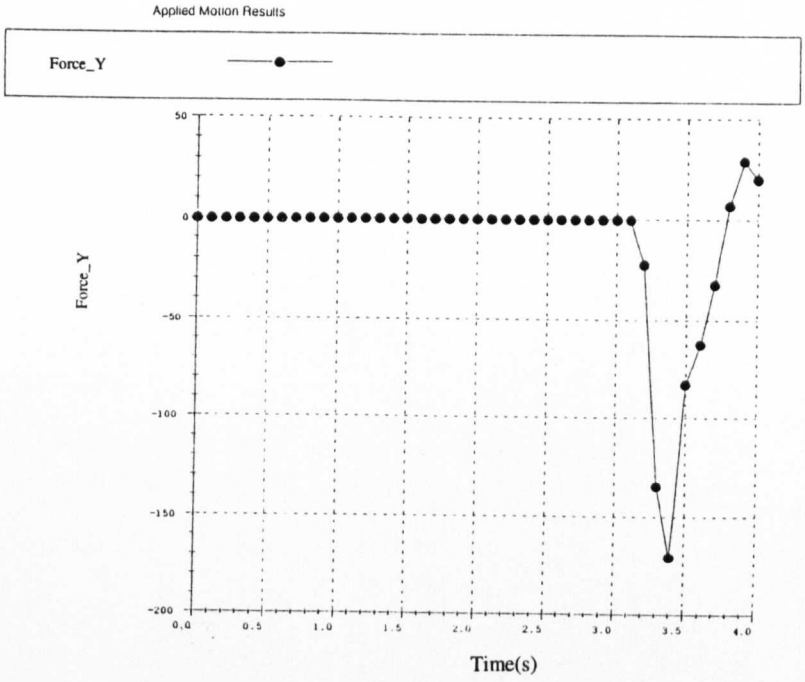

Figure 7.6 The Cushioning Forces

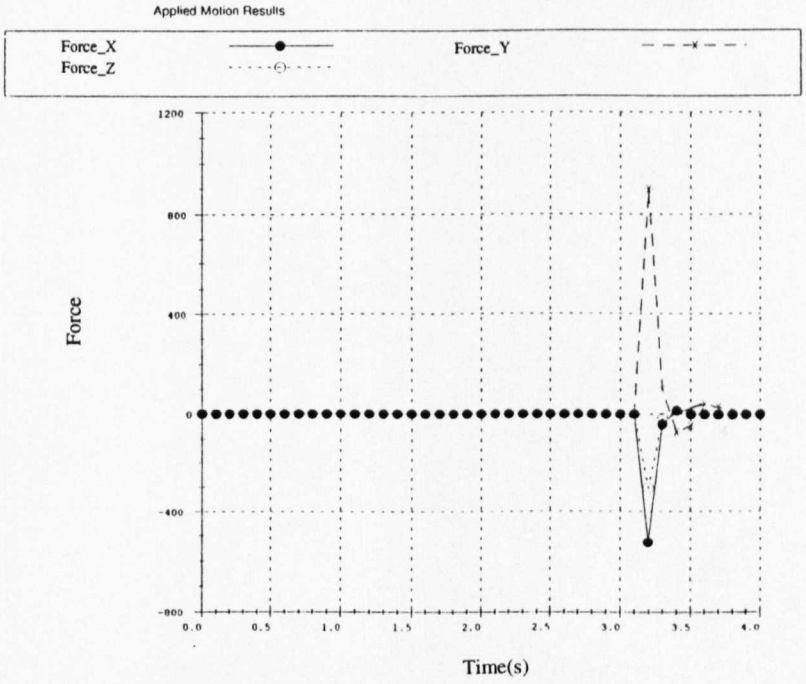

Figure 7.7 The Impact Forces in Three Direction

7.3 The "G factor" of cushioning

Selecting the best type of cushioning and the right amount for a particular packaging application is very important. First the fragility of the item to be packaged must be known; then the hazards it will be exposed to must be considered; and finally the characteristics of the cushioning materials that are available must be understood; so that people can choose the most economical material that will do the job. Starting with the item itself, it is essential to know how much abuse it can take without being seriously damaged. This measure has been translated into a "*G* factor" according to Hanlon[1]. The G factor is related to the minimum force required for damage, and is given as the number of *g*(acceleration of gravity, or $9.81 m/sec^2$). This is another way of expressing the minimum drop height that would break the item without any cushioning, in terms of the number of seconds it takes to reach the ground; or to put it another way, the number of times its own weight that it takes to crush an item is its *G* factor.

The G factor can be determined with a shock machine or an instrumented impact test. However, fairly accurate results can be obtained by a simple trial-and-error method. Use a package similar in dimensions and material to the anticipated final design, with a cushioning material whose peak deceleration versus static stress curves are known. Figure 7.8, 7.9 and 7.10 are presented by Hanlon[1]. During a series of drop tests, the thickness of the cushioning is decreased with each test until damage occurs. The peak acceleration on the curve before failure gives a measure of the product's approximate fragility.

In Figure 7.8, a random selection of materials is used to illustrate the different behaviour of various materials. Other thicknesses, drop heights, and temperatures will move the curves up or down, but will not greatly affect their positions from left to right.

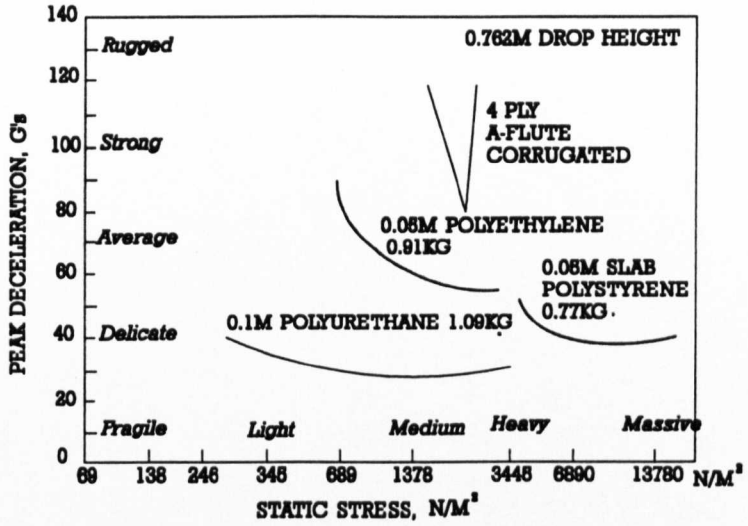

Figure 7.8 Cushioning Effectiveness

Figure 7.9 illustrates the dynamic cushioning of polyurethane for various thicknesses[1]. If the fragility of a particular item is such that it can withstand 50 G's and the weight per unit area of bearing surface is 1035 N/m^2(0.15 psi), the intersection will be above the curve for 50.8mm(2-in) thickness, as shown. Any curve below this point may be used. Creep, which is defined as the deformation of the material over time, becomes a significant factor in the dotted portions of the curve, and may result in as much as 75 percent loss of thickness.

Figure 7.10 shows the dynamic cushioning of expanded polystyrene of various thicknesses[1]. The point where the fragility of the item intersects the dead weight can be found. The curve that comes closest, but dips below this point, indicates the most efficient thickness of 19.07 kg/m^3 (1.2 lb/ft^3) density material for a 762mm (30-in)

drop height. If the height is reduced by half, static stress can be doubled. If the density is increased, it improves the load-bearing capacity only slightly, but it also reduces the shock absorption by a small amount.

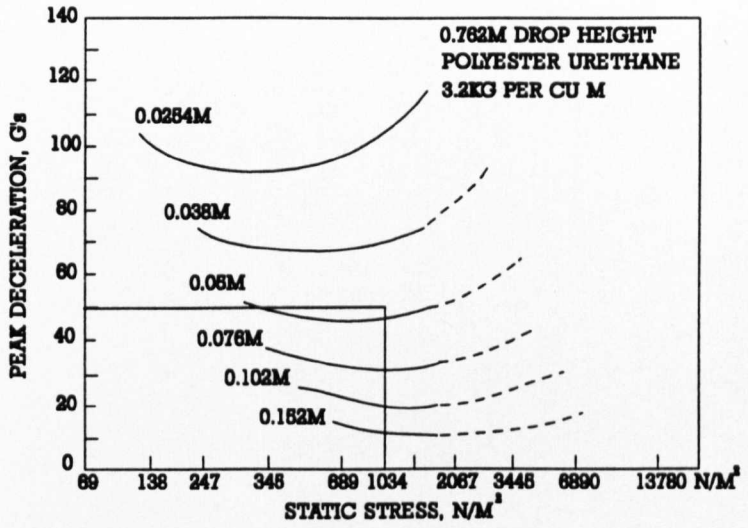

Figure 7.9 Polyurethane Curves

The weight of the object being packaged and the area to be supported by the cushioning also need to be known. If the area is not the same on all sides, the safest thing is to take the smallest area. Dividing the weight by the area W/A gives the static stress in kilogram per square metre.

The next factor is the thickness of a particular cushioning that will be necessary to satisfy the requirements. This information is shown in the G vs. W/A curves which are supplied by the manufacturers of the various materials. A few of these curves are

given for reference in Figure 7.8. Draw a horizontal line from the G factor (fragility) of the item to be packaged, and a vertical line up from the W/A figure derived from the weight and area, and note the point where they intersect. Any curve which passes below this point indicates that the material can be used in that thickness.

A sample problem may help to illustrate this:

Weight=66.75 N

Bearing area=0.254× 0.254 m^2

Fragility=50 G

Potential hazard=0.762m drop

W/A=66.75/0.254×0.254=1034 N/m^2

Referring to Figure 6.9 for polyurethane foam, 3.2 kg/m^3 density, the curve for 0.05m thickness dips below the point where 1034 N/m^2 intersects the line from 50G, indicating that this will satisfy the requirements.

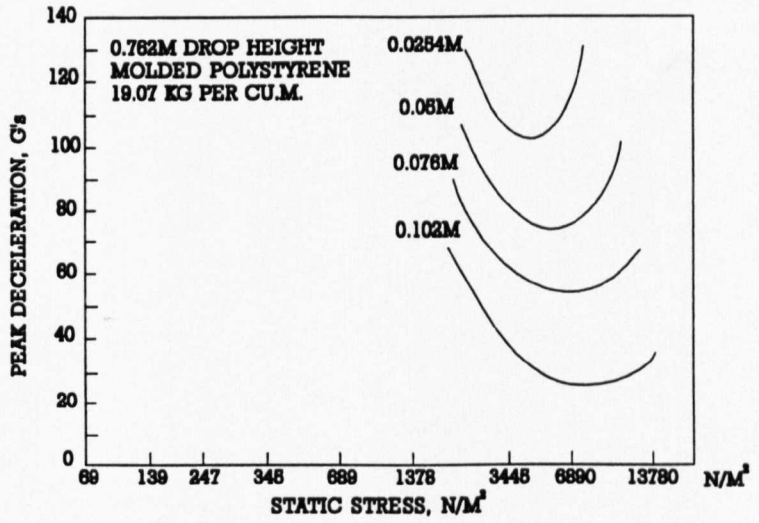

Figure 7.10 Polystyrene Curves

Other points to be considered are: (1) the effects of abrasion of the cushioning material on the item; (2) the settling of the cushioning material from repeated impacts; (3) resonance or periodic vibrations along with harmonics, which are rarely a serious problem, but may help to explain some of the unpredicted failures that occur every once in a while; (4) the mass of the cushioning itself; this is a negligible factor, but for precise calculations one-third of the weight of the cushioning should be added to the weight of the article; (5) internal damping of shock vibrations; this is a plus factor and varies with different materials, but it can be ignored for all but sophisticated investigations; and (6) temperature and humidity, which may alter the protective qualities of certain materials. Plastics tend to stiffen at low temperatures and soften at elevated temperatures. Cellulosic materials are affected by moisture, and if this is expected to be a factor, the supplier of the cushioning should be consulted for data under these conditions

7.4 Methods of cushioning

There are a number of ways of isolating an object from the effects of impact in transit. (1) The most common way of protecting a fragile item is by blocking and bracing it with resilient materials that will absorb the shock energy and direct it to toward the strongest part. This is sometimes called "compression packing" to differentiate it from "suspension-type packing". (2) "Flotation" is a method of surrounding an object with small pieces of cushioning material that can shift or flow to fill up voids and distribute the impact forces over the entire surface of the object. (3) Wrapping individual pieces in sheet material of various types is a frequently used method of packing small objects. (4) Stuffing consists of preparing a base of resilient material, placing the item on this base, and filling the surrounding voids with gobs of the same material. (5) A suspension system is another way of protecting a product, by holding it away from the sides of the enclosure. This can be done with straps, tapes, slings, or other supports which will act as flexible restraints. (6) Enclosures

which conform to the shape of object will distribute the shock force over the maximum area. (7)Foam-in-place is a technique for making a enclosure by using the item and the container itself as the mold for the foam material.

The choice of a suitable type of packing will depend on the type of item to be packed, its value, shape, and the quantity and frequency of shipment. A single large item of great value will require an entirely different treatment from a large number of inexpensive pieces. If there is a variety of sizes and shapes, it is usually better to work with sheet stock that can be used as wrapping material, and can also be crumpled and stuffed into empty spaces in the container. If there are many pieces of the same shape, then a custom container or specially designed supports will save time in packing. In a high-volume operation, flowable dunnage material provides a convenient method, and although it is wasteful of material, it usually makes up for this in labour saving.

The economics of packing fragile objects is often difficult to calculate. It is not enough to simply compare material cost. The labour of packing is often more significant than the material costs. There is also the question of bulk or cube. This may affect transportation cost, and it will certainly make a difference in storage space. With the variety of materials and methods that are available, a thorough investigation of all the different techniques will be beneficial to manufacturers.

7.5 Materials of cushioning

A great variety of natural and synthetic materials is used for cushioning. Paper in different forms can be used as wrapping material and stuffed into empty spaces. Wood shavings or excelsior are also widely used. These cellulosic materials will absorb moisture and may develop mildew. They will also react with strong chemicals, and they should never be used to pack oxidizing materials such as nitric

acid.Vermiculite can be used to pack strong chemicals. It is absorbent to a limited degree, but more important, it is inert to acids, and most other hazardous liquids.

7.5.1 Loose fill cushioning: All type of amorphous materials are included under the term "loose fill". Such things as crumpled paper, excelsior, and foam sheeting are considered loose fill materials.

7.5.2 Paper and paper product: Cellulose wadding is an inexpensive form of crepe paper that is available in various thicknesses with different backings, facings, and embossing. This material will absorb about 16 times its own weight in water, and up to 12 times its weight in oil. Old newspapers provide a cheap source of packing material.

7.5.3 Bubble sheet: As a wrapping material, air bubble sheet is suitable for products that are not very delicate. Only if many layers are used, 2 in. or more in thickness, does it provide adequate protection for fragile objects. It is not recommended for heavy items, as the bubbles start to break when the loading gets much beyond 0.1 psi. Compared with other loose fill and wrapping materials, it offers several advantages. Being light in weight, it provides dunnage with a minimum increase in shipping weight. It is dust-free, nonabsorbent, and will not support the growth of mold or mildew.

7.5.4 Free-flowing cushioning: Flowable dunnage comes in the form of peanuts, shells, rings, tubes, and spaghetti. The reason for these different shapes is to provide a cushioning material that will conform to different-shaped objects, and at the same time interlock to form a cohesive mass that will not shift or settle out. In practice, a small amount of material is put in the bottom of the shipping container. The items are placed on the top of this, with space all around. More dunnage is then added until the box is overfilled by 5 to 7 percent, or until it takes fairly heavy pressure to close the

container.

7.5.5 Foam blocking: Molded pieces of polystyrene foam can be made to fit around objects or to support corners and edges of large items. Slab material which is used for building insulation can also be cut with a hot wire for this purpose. It should be designed to distribute the load over the largest possible area. The support should be against the strongest part of the item, and should be clear of the weakest parts. The support area must not be too small in relation to the thickness of the foam, or the cushion may buckle instead of compressing uniformly. A cushion will buckle when its area is less than the square of 1.33 times the thickness, or to put it another way, a square block of foam should be at least one-third longer and wider than it is high.

7.5.6 Foam-in-place cushioning: For products that are heavy, with irregular shapes and high value, in short production runs that are labour-intensive, the foam-in-place technique has been very successful in reducing damage. Although this type of cushioning does not have the resiliency of some other cushioning materials. It is suitable for certain types of industrial and military equipment, in the range of 20 to 45 kg.

7.6 A Finite Element Model Proposition

To design a product-cushion-package system it is necessary to calculate the effects of external loadings on this system. One method to accomplish this is the Finite Element technique. The complex geometry of the system can be modelled successfully by using this method. Constitutive equations that describe the non-linear response of the system can be implemented in Finite Element programmes.

At first the effect of the static load on the system has to be determined. Then the impact load is simulated, and finally these two effects are superimposed to determine

the total deformation and stress of the product-cushion-package system. In Figure 7.11 the mesh of Finite Element is shown. The shaded area is the product, and the unshadowed area is the cushioning. It is assumed that the structure is statically loaded by its own weight.

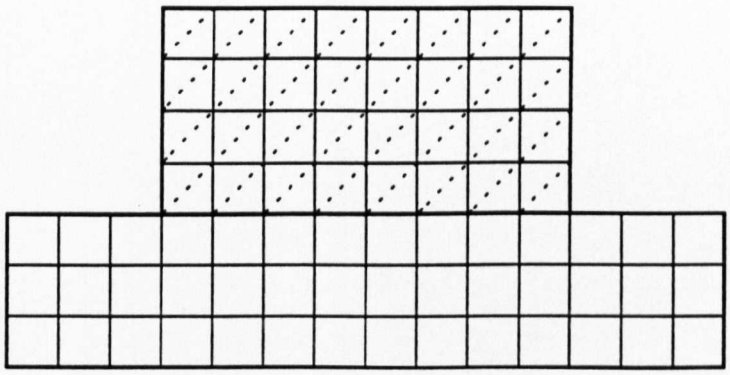

Figure 7.11 Finite Element Model

7.7 Summary

The simulation of a model of product-cushion-package system is examined in this chapter, with the drop tests of different positions, such as flat, edge and corner drop. The acceleration of the product which is an important indication of the susceptibility to damage was observed and the impact forces were obtained. The "G factor" which is related to the minimum force required for damage has been discussed and the determination of it for different materials was presented. Different methods and materials of cushioning have also been discussed.

Chapter 8

Analysis of a Packaging System

8.1 Introduction

In any industrial society products must be transported from one location to another. The product-cushion-package system has to survive the rigours of the handling and transportation environment. Mechanical damage is a common occurrence in the transportation of packaged articles. The causes of failures are generally inadequate protective cushioning, lack of ruggedness of the outer pack container, or occasional abnormal weakness of the packaged article. The first of these problems is investigated in this chapter.

The approach to the problem has been investigated by both theoretical analysis and computer simulation of the drop test, which is broadly used in packaging design. The main aim of this study is to develop techniques of evaluating the susceptibility to damage of a package and product subject to handling and distribution hazards. To minimize the size of package, and to choose the appropriate packaging material, with a view to making recommendations to handling machinery designers that will improve the accuracy of orientation and secure the integrity of the package and products. Attention is concentrated on the cushioning properties which were divided into six types. The different function of the six types cushioning is discussed and simulated.

The acceleration of a product in a cushioning package is crucial for estimating the safety of the product. The performance measure for the problem has been translated into a "G factor" as mentioned before, which has been discussed broadly in literature. It is still necessary to have a further understanding of the influence of the acceleration on the response of the packaged article, and the acceleration-time relationship with

different cushioning characteristics, different velocity damping and friction. As a consequence the techniques for modelling the product-cushion-package system will be developed. Some application of the cushioning is also presented. In the meanwhile the techniques for modelling the product-cushion-package system are developed.

Numerous studies investigating the impact behaviour of rigid or semi-rigid containers have already been reported in the literature. So far, however, most of these investigations have concentrated on methods for evaluating the quality of these containers. There is still a strongly felt need for a further understanding of the mechanical behaviour of containers subjected to external force or impact, especially with contents inside. One of the major influences in reducing the incidence of mechanical failures of packaged articles has been the use of the drop test. This test requires a large number of samples before a reliable estimate of quality can be made. An adequate number of tests is prohibitive when the packaged article is costly. In

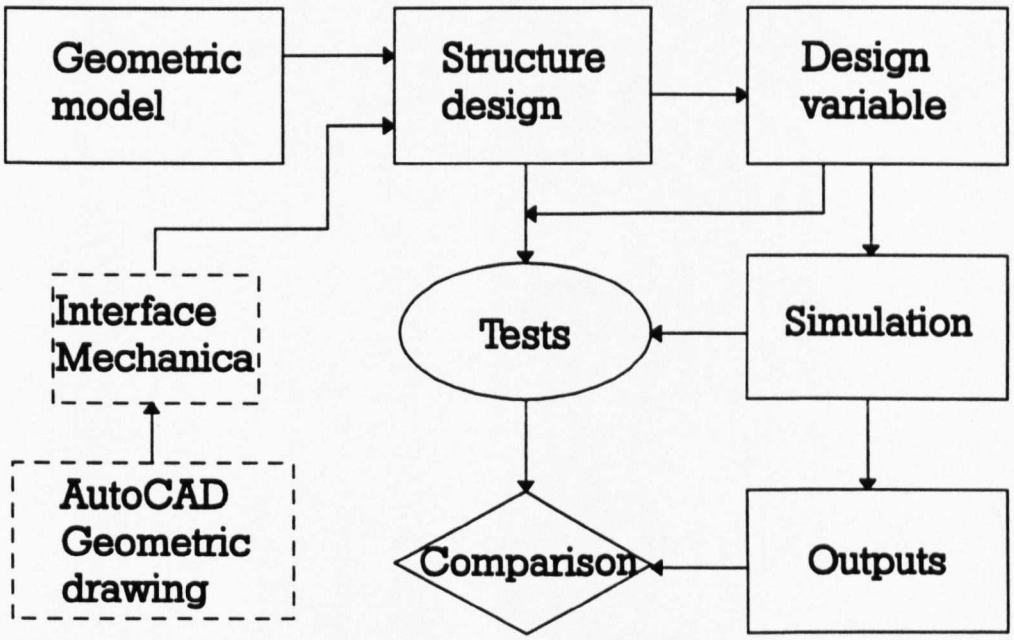

Figure 8.1 The structure of the operating sequence for design/simulation

such cases it is important, and in any case it is useful, to supplement the drop test data with measurements and simulation. Simulating the situation can also overcome the difficult that it might be impossible for a real drop test to be carried out, such as when a specified impact position is required or, very high distance defined. With simulation The characteristics of contents and package can be selected arbitrarily and changed easily. The drop test then becomes only a check instead of playing an integral role in design procedure.

8.2 Design procedure of the packaging system

The objectives of this study were to define the packaging design procedure, to develop the techniques of evaluating the probability of damage to the package and product when subject to handling and distribution hazards, to minimize the size of the package and choose the appropriate packaging material. In order to evaluate the susceptibility to damage to the product, three factors which refer to external hazard, the package size and the cushioning characteristics were taken into account The structure of the operating sequence for design and simulation is shown in Figure 8.1.

Commercially available software MECHANICA APPLIED MOTION was used for pre/post processing such as generating the model and defining the design variable, and simulating the drop test. A geometric model can be also be created by AutoCAD. Data exchange between AutoCAD and MECHANICA can be implemented using an interface called "MECHANICAL".

8.3 The model for analysis

The survival of a packaged article in a drop test depends upon a large number of factors descriptive of the mechanical properties of the cushioning medium and the packaged item. However, the important properties can be grouped as the following

factors:

(1) The magnitude of the maximum acceleration that the cushioning permits the packaged item to reach.

(2) The specification of the container.

(3) The form of the acceleration-time relationship.

(4) The strengths, natural frequencies of vibration and damping of the structural elements of the packaged article.

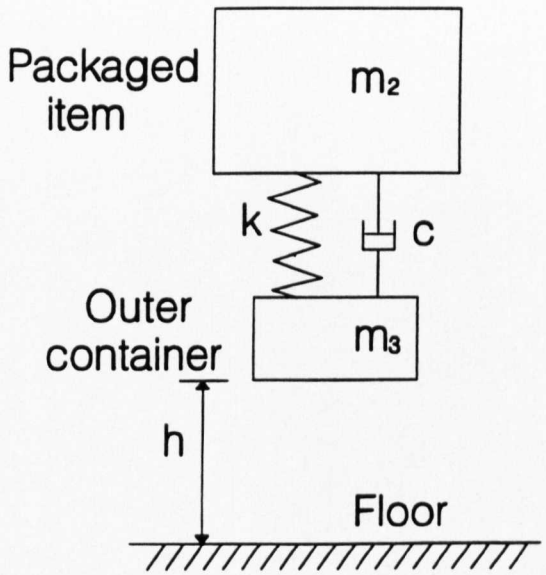

Figure 8.2 The model of packaging cushioning system

This chapter is concerned primarily with methods for predicting maximum acceleration of the packaged article with emphasis on linear and non-linear cushioning, the different types of acceleration-time relation, and the influences of different cushioning and damping and friction on acceleration.

Essentially, a package consists of the packaged article, the cushioning medium and outer container. The idealized package-content-cushioning system is illustrated in Figure 8.2. The major components of the system are as follows:

(1) The cushioning is represented by a spring which may have a linear or non-linear load-displacement characteristic and which dissipates energy through velocity damping or dry friction and permanent deformation. The mass of the cushioning (m_1) is assumed to be small in comparison with m_2.

(2) The whole packaged item is represented by a mass m_2.

(3) The container is represented by the mass m_3. The impact of m_3 on the floor is assumed to be rigid and during contact the relative displacement between m_3 and the initial position of the floor is assumed to be small in comparison with the relative displacement between m_2 and m_3.

8.4 Cushioning with linear and non-linear elasticity

What is of major concern in this study is the maximum acceleration that the cushioning permits the packaged article to attain. In many instances this will be the most important information necessary for judging the suitability of a cushioning system.

In order to develop the methods of simulation some further analysis is required. The mass of the cushioning is omitted and the cushioning is assumed to have no damping or friction. The mass of the outer container m_3 is neglected. The spring rate k_2 of a linear spring is a constant. The force P acted on m_2 through a linear spring is:

$$P=k_2x \tag{8.1}$$

Where x is the displacement of m_2 measured downward from its position on first contact of the spring with the floor. For a nonlinear spring, P will be some other function of x:

$$P=P(x) \tag{8.2}$$

To write the equation of motion for the mass m_2 , consider the forces acting on it at any instant. These are the spring force P and the weight m_2g, where g is the acceleration of gravity. When x is positive (i.e., a downward displacement of m_2 from its position at first contact of m_3 with floor) the spring exerts an upward force P on m_2, opposing the weight. The total downward force on m_2 is thus m_2g-P. By the second law of motion, the product of m_2 and its acceleration at any instant is equal to the applied force:

$$m_2\ddot{x}=m_2g-P \tag{8.3}$$

where $\ddot{x}$ represents the acceleration of m_2. equation (8.3) is the law governing the motion of m_2 as long as the spring or m_3 is in contact with the floor. When m_3 is not in contact with the floor, it can exert no force on the mass so that, in writing the equation of motion that governs before or after contact, the free-body drop should be:

$$\ddot{x}=g \tag{8.4}$$

Equation (8.4) holds from the instant the package starts to fall until the instant it strikes the floor, and from it the package velocity can be found at the instant of first contact. Integrating equation (8.4) with respect to time,

$$\dot{x}=gt+A \tag{8.5}$$

where $\dot{x}$ is the velocity and A is a constant of integration whose value is found from the initial condition that when $t=0$ (the instant of release), $\dot{x}=0$. Thus $A=0$ and

$$\dot{x}=gt \tag{8.6}$$

Integrating again,

$$x=\frac{1}{2}gt^2+B \tag{8.7}$$

The value of the integration constant B is found from the initial condition that $x=-h$ (the height of drop) when $t=0$. Hence $B=-h$ and:

$$x=\frac{1}{2}gt^2-h \tag{8.8}$$

At the instant of contact, $x=0$ and from equation (8.8), the time at first contact is given by $t_0^2=2h/g$. Substituting this value of t in equation (8.5) we find, for the velocity at first contact is found as:

$$[\dot{x}]_{x=0}=\sqrt{2gh} \tag{8.9}$$

These are the initial conditions for finding the values of the integration constants in the solution of equation (8.3).

First multiply both sides of equation (8.3) by dx/dt:

$$m_2 \frac{dx}{dt} \frac{d}{dt} \left(\frac{dx}{dt} \right) + P \frac{dx}{dt} = m_2 g \frac{dx}{dt} \tag{8.10}$$

or:

$$\frac{1}{2} m_2 \frac{d}{dt} \left(\frac{dx}{dt} \right)^2 + P \frac{dx}{dt} = m_2 g \frac{dx}{dt}$$

Multiplying by dt and integrating once:

$$\frac{1}{2} m_2 \dot{x}^2 + \int^x P dx = \int^x m_2 g dx + L \tag{8.11}$$

Where L is a constant of integration whose value is determined by the initial conditions that $\dot{x}^2 = 2gh$ and $x = 0$ at the instant of contact. Hence:

$$L = m_2 gh + \int^0 P dx$$

Substituting the above value of L in equation (8.11),

$$\frac{1}{2}m_2\dot{x}^2+\int_0^x Pdx=m_2g(h+x) \tag{8.12}$$

It can be observed that equation (8.12) is an energy equation in which the terms have the following meanings:

$1/2m_2\dot{x}^2$ is the instantaneous kinetic energy of m_2,

$\int_0^x Pdx$ is the energy stored in the spring at any instant.

$m_2g(h+x)$ is the potential energy of the mass at its initial height $h+x$ above the instantaneous position x.

Hence equation(8.12) expresses the law of conservation of energy.

Ordinarily, h is very much larger than x so that it can be written, with good accuracy,

$$\frac{1}{2}m_2\dot{x}^2+\int_0^x Pdx=m_2gh \tag{8.13}$$

To the same approximation, equation (8.3) becomes:

$$m_2\ddot{x}+P=0 \tag{8.14}$$

Equation(8.14) and its first integration, equation(8.13), are convenient forms for calculating events at any time during contact. For calculating only maximum displacement and acceleration, the equations become simpler. Let

W_2=weight of the packaged article(m_2g),

d_m=maximum displacement of the packaged article,

G_m=absolute value of maximum acceleration of the packaged article in terms of number of times gravity,

P_m=maximum force exerted on packaged article by cushioning.

This study is limited to the practical regions where P>0 when x>0. Then it may be seen from equation(8.13) that x is a maximum when $\dot{x}$ is zero, hence,

$$\int_0^{d_m} P dx = W_2 h \tag{8.15}$$

and from equation (8.14),

$$G_m = \frac{P_m}{W_2} \tag{8.16}$$

Where P_m is the maximum value of P. If $P(x)$ is a monotonic function, P_m may be obtained from equation (8.2) by substituting d_m for x:

$$P_m = P(d_m) \tag{8.17}$$

The general procedure is to calculate d_m from equation (8.15), P_m from equation (8.17) and then G_m from equation (8.16).

For cushioning with a linear load-displacement relation as equation (8.1), and substituting it in equation (8.15), and performing the integration, there is:

$$d_m = \sqrt{\frac{2hW_2}{k_2}} \tag{8.18}$$

From equation (8.18) and equation (8.17),

$$P_m = \sqrt{2hW_2k_2} \tag{8.19}$$

and from equation (8.19) and equation (8.16),

$$G_m = \sqrt{\frac{2hk_2}{W_2}} \tag{8.20}$$

Equation (8.20) holds only if there is space available for a displacement d_m and if the cushioning is linear and capable of transmitting a force P_m. Also from equation (8.20) and equation (8.18),

$$d_m = \frac{2h}{G_m} \tag{8.21}$$

and

$$k_2 = \frac{W_2G_m^2}{2h} = \frac{2hW_2}{d_m^2} \tag{8.22}$$

Example: Find the properties of the linear cushioning required so that the maximum acceleration will be *50g* (*g* is gravity of acceleration) in a *1.5m* drop of *a 10*kg. article. From equation (8.21), necessary travel, $d_m=(2*1.5)/50=0.066m$. From equation (8.22), spring rate, $k_2=(10*9.8065*50^2)/(2*1.5)=81720.8N/m$. From equation (8.16) the maximum force $P_m=10*9.8065*50=4903.3N$. The result by computer simulation using Mechanica software is $d_m=0.051m$, $P_m=4200N$. The differences are mainly due to the approximations made during derivation.

8.4.1 Six types of cushioning

It is rare that a packaging system has linear characteristics. Departure from linearity may be due to non-linear geometry, such as in the tension spring package, non-linear characteristics of materials or abrupt change of stiffness. So, the linear and non-linear characteristics of cushioning can be divided into six classes. most of them are associated with simple functions having one or two adjustable parameters and can be simulated on the computer. The software used is RASNA MECHANICA Applied Motion. The model is set up as Figure 8.2. The characteristics of the packaged item, cushioning, and the environment of the test are defined by the features of the software. The six classes are as follows:

Class A-Linear Elasticity. This has already been dealt with. With the load-displacement function is as given in equation (8.1). Figure 8.3 is the output of the model with the cushioning function as in equation(8.1).

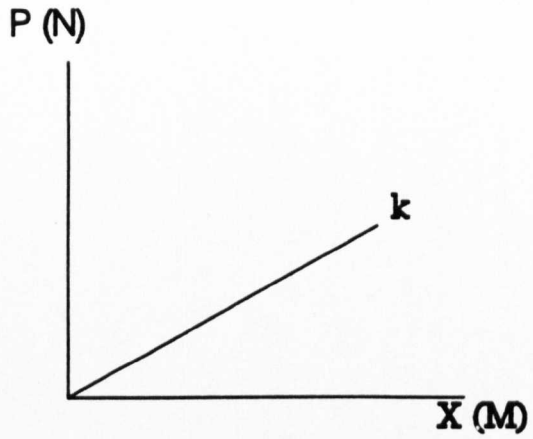

Figure 8.3 Linear elasticity

Class B-Cubic Elasticity. This includes cushioning which does not bottom in the anticipated range of use, but the slope of the load-displacement function generally increases with increasing displacement as in the curved full line of Figure 8.4 . A suitable load-displacement function is:

$$P=k_0x+rx^3 \tag{8.23}$$

k_0 is the initial spring rate of the cushioning, as shown by the slope of the dashed straight line in Figure 8.4, and r determines the rate of increase of the spring rate. The same function can be used if the slope of the curve decreases gradually with increasing load as shown by the curved dashed line. In this case the parameter is negative. The result of the simulation using cushioning with the function as in equation (8.23) coincides with Figure 8.4.

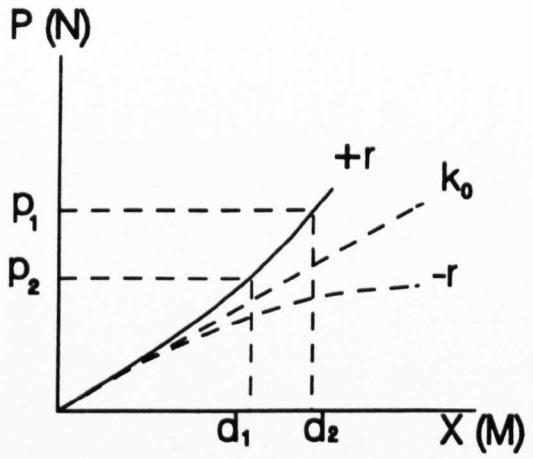

Figure 8.4 Cubic elasticity

Substituting equation (8.23) in equation(8.15) and performing the integration,

$$\frac{k_0 d_m^2}{2} + \frac{r d_m^4}{4} = W_2 h \tag{8.24}$$

Let

$$d_0 = \sqrt{\frac{2W_2 h}{k_0}} \tag{8.25}$$

That is, d_0 is the displacement that would take place if the elasticity were linear (see equation(8.18)) with a constant spring rate k_0 equal to the initial spring rate of the cubic elasticity. Also let

Then, from equation (8.24), (8.25) and (8.26)

$$B=\frac{4W_2hr}{k_0^2} \tag{8.26}$$

Then, from equation (8.24), (8.25) and (8.26)

$$\frac{d_m}{d_0}=\sqrt{\frac{2}{B}\left(-1+\sqrt{1+B}\right)} \tag{8.27}$$

Equation (8.27) is plotted in Figure 8.5 by Mindlin[19] which shows the maximum displacement d_m compares with the "equivalent linear displacement d_0" as the parameter B is varied. Note that B depends on the weight of the packaged item, the height of drop and the shape of the load-displacement curve(as determined by k_0 and r).

Mindlin[19] also compared the maximum acceleration G_m with the maximum G_0 that would be obtained if the load-displacement curve were linear with spring rate k_0. The latter acceleration is given by

$$G_0=\sqrt{\frac{2hk_0}{W_2}} \tag{8.28}$$

and the former is obtained by finding P_m from equation (8.17) and then from equation (8.16),

$$\frac{G_m}{G_0}=\sqrt{\frac{2}{B}(1+B)\left(-1+\sqrt{1+B}\right)} \tag{8.29}$$

Equation (8.29) is plotted in Figure 8.6 by Mindlin[19].

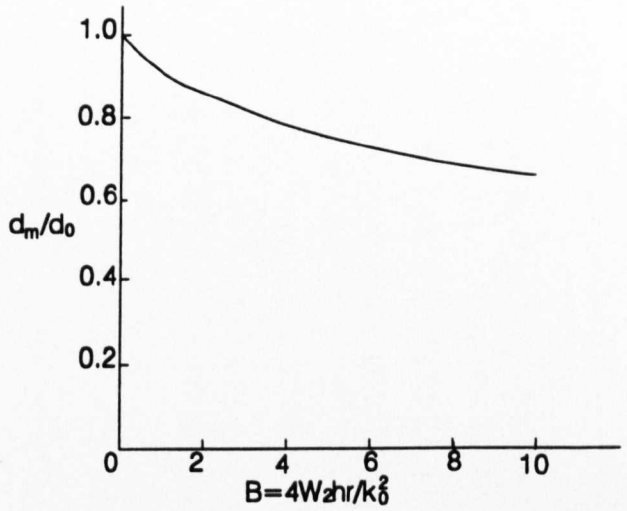

Figure 8.5 Maximum displacement for cushioning with cubic elasticity

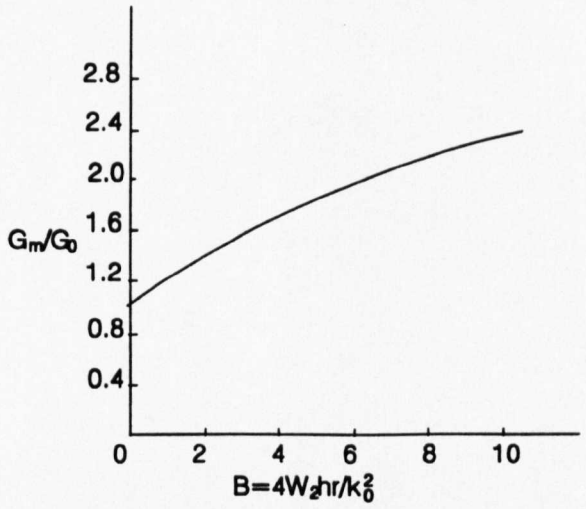

Figure 8.6 Maximum acceleration for cushioning with cubic elasticity

Class C-Tangent Elasticity. Cushioning that bottoms, but not very abruptly, can be represented by the load-displacement function:

$$P=\frac{2k_0 d_b}{\pi}\tan\frac{\pi x}{2d_b} \tag{8.30}$$

Referring to Figure 8.7, k_0 is the initial spring rate and d_b is the maximum available displacement. The figure shows how the stiffness of the cushioning(i.e., the slope of the curve) increases as the displacement approaches the maximum available (d_b) at hard bottoming. The shape of the curve is typical of load-displacement curves for a great variety of packages with distributed cushioning.

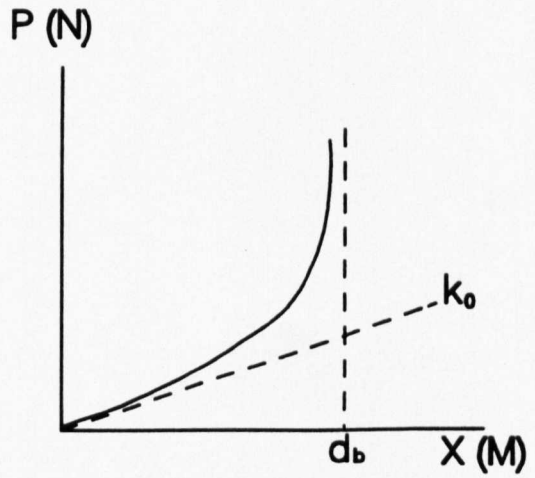

Figure 8.7 Tangent elasticity

Considering the example in section 8.4 where a spring with $k=81720.8N/m$ and a displacement of $0.051m$ were required to limit a $10kg$ article to an acceleration of $50g$ in a $1.5m$ drop with linear cushioning. If only $0.035m$ were available instead of

$0.051m$, and the cushioning had tangent elasticity starting with a spring rate of $81720.8N/m$, from the simulation the maximum acceleration is $G_m=295g$. By entering $d_b/d_0=0.69$ into the curve of G_m/G_0 versus d_b/d_0 in reference[19], then $G_m=280g$. The two maximum acceleration are quite close.

Class D-Bi-linear Elasticity. This is characterized by a load-displacement curve consisting of two straight line segments. The load displacement function is ,

$$\begin{aligned} P&=k_0x & 0\le x\le d_s \\ P&=k_ax-(k_a-k_0)\,d_s & x\ge d_s \end{aligned} \tag{8.31}$$

As shown by Figure 8.8. It is useful especially in situations where very abrupt bottoming is possible.

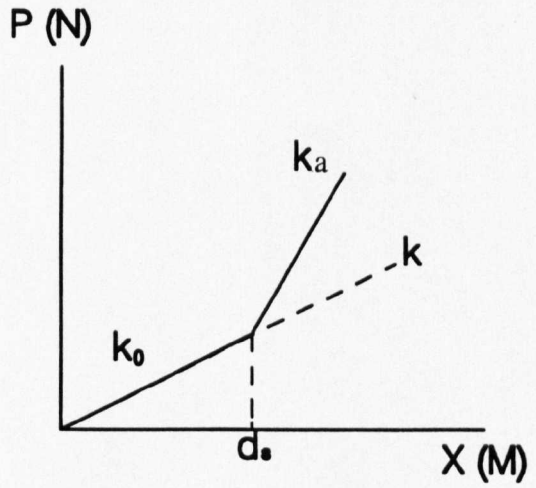

Figure 8.8 Bi-linear elasticity

Class E-Hyperbolic Tangent Elasticity. Where the mechanism of the cushioning is such as to limit the maximum force that can be transmitted over a considerable displacement range, this load-displacement function is useful. P_0 is the asymptotic value of the force and k_0 is the initial spring rate(see Figure 8.9).

$$P=P_0 \tanh \frac{k_0 x}{P_0} \tag{8.32}$$

Class F-Anomalous Elasticity. In occasional instances the load-displacement curve of the cushioning cannot be matched accurately enough by any of the five preceding functions. In such cases a numerical integration procedure can be used.

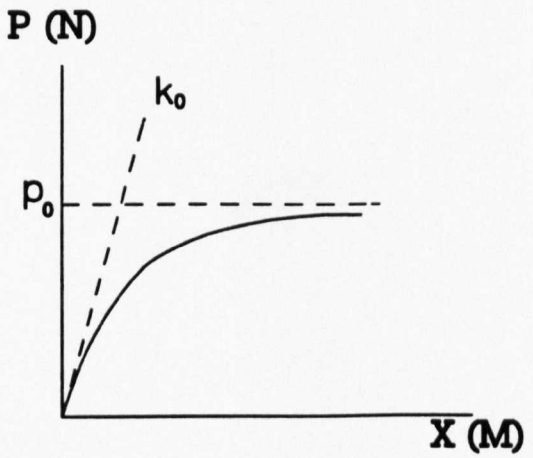

Figure 8.9 Hyperbolic tangent elasticity

8.4.2 An Application

A large vacuum tube, weighting *12.2kg*, was packed in a carton which was supported on corrugated cardboard spring pads in another carton. Then they were packed in *12.7kg* of excelsior in a carton. The tube is rated at *50g* and the package was tested for a drop of 1 metre. This model was set up as Figure 8.10 as presented by Sun[57]. The cushioning was simulated by a spring with cubic elasticity characteristics presented by equation 8.23. Selecting k_0=*4900N/m*, $r=2*10^7 N/m^3$ for the corrugated spring pads and k_0=*3500N/m*, $r=5*10^6 N/m^3$ for excelsior.

Load was applied to the tube and the displacement was obtained by static analysis using simulation software. The load-displacement curve (Figure 8.11) is plotted from the results in the below table.

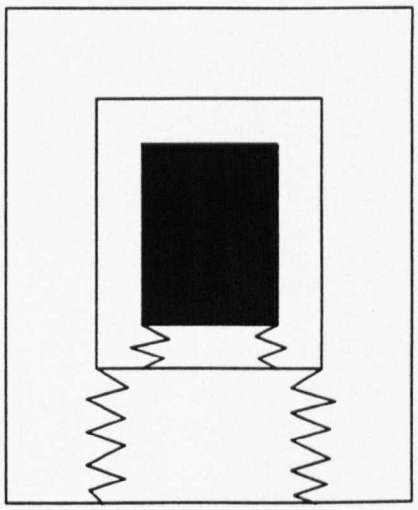

Figure 8.10 The model of tube package

Table 8.1 Load-displacement values

P(N)	0	45	90	135	180	225	270	315	360	405	450	495	540	585	630
d(cm)	0	0.92	1.76	2.31	2.75	3.11	3.42	3.70	3.95	4.17	4.38	4.57	4.75	4.94	5.08

The procedure for estimating the effectiveness of the cushioning is as shown below according to Mindlin[19]. First, select the point on the load-displacement curve for which the load is equal to the weight of the packaged item multiplied by the allowable G_m. Call this load P_2 and the corresponding displacement d_2. Second, select another point (d_1, P_1) about half way toward the origin from (d_2, P_2). See Figure 8.4. Then calculate

$$k_0 = \frac{\frac{P_1}{d_1} d_2^2 - \frac{P_2}{d_2} d_1^2}{d_2^2 - d_1^2} \tag{8.33}$$

and

$$r = \frac{\frac{P_2}{d_2} - \frac{P_1}{d_1}}{d_2^2 - d_1^2} \tag{8.34}$$

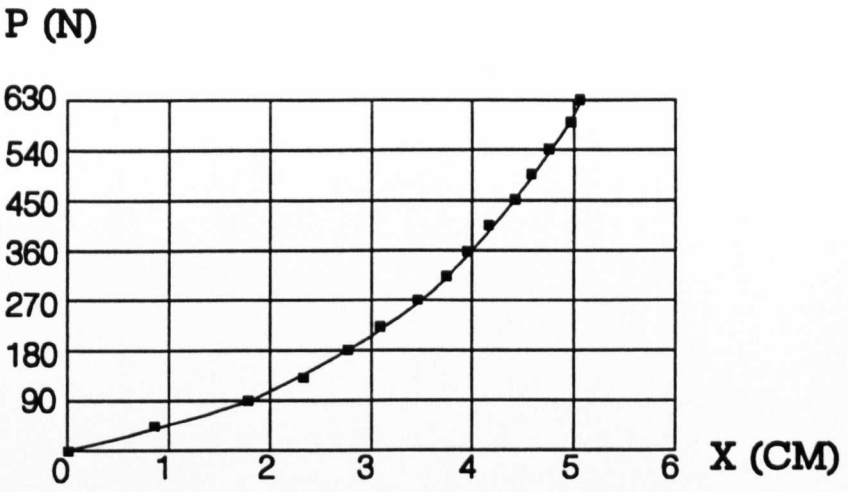

Figure 8.11 Load-displacement curve for cubic elasticity cushioning

If selecting $P_2=12.2*50=610N$, and from the curve, $d_2=5cm$. Also from the curve, select $d_1=2cm$ and $P_1=110N$. Substituting these values in equation (8.33) and (8.34), we find $k_0=4119\ N/m$ and r=$3345181N/m^3$. From equation (8.26) and (8.28), we find B=9.6 and $G_0=25.9$. Entering Figure 8.6 with $B=9.6$ we find $G_m/G_0=2.2$. Hence G_m= $25.9*2.2=56.9$, This is close enough to the $50g$ rating of the tube to call the cushioning safe insofar as maximum acceleration is concerned.

The maximum displacement, obtain by entering Figure 8.5 with $B=9.6$ and finding $d_m/d_0=0.68$. Then $d_m=0.68*2h/G_0=5cm$. By simulating the drop test of the model, the maximum of acceleration of the tube is $480m/s^2$, see Figure 8.12, so $G_m=49$. $d_m=9cm$ from Figure 8.13. The maximum acceleration from the calculations and simulation are both close to $50g$, and it can be seen that the package is much larger than necessary since approximately $19cm$ of cushioning thickness is supplied to accommodate $5cm$ of displacement.

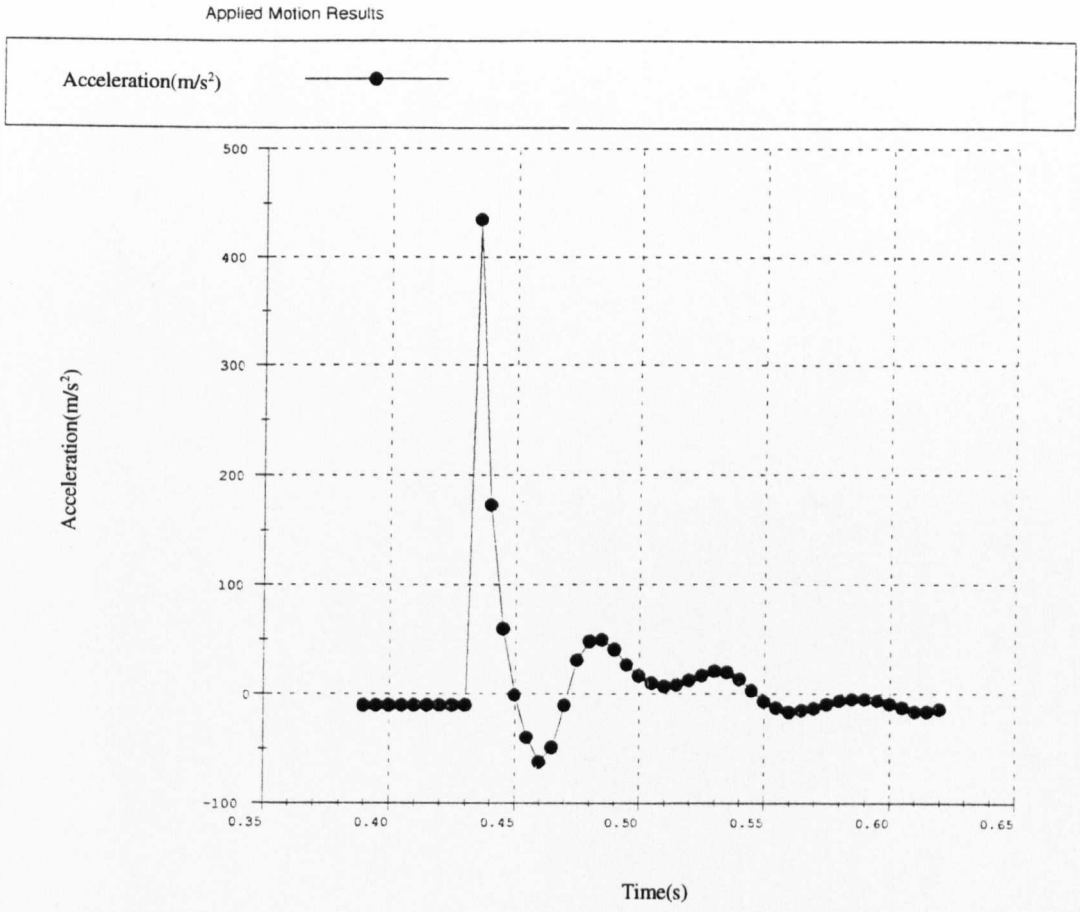

Figure 8.12 Acceleration of packaged vacuum tube from simulation

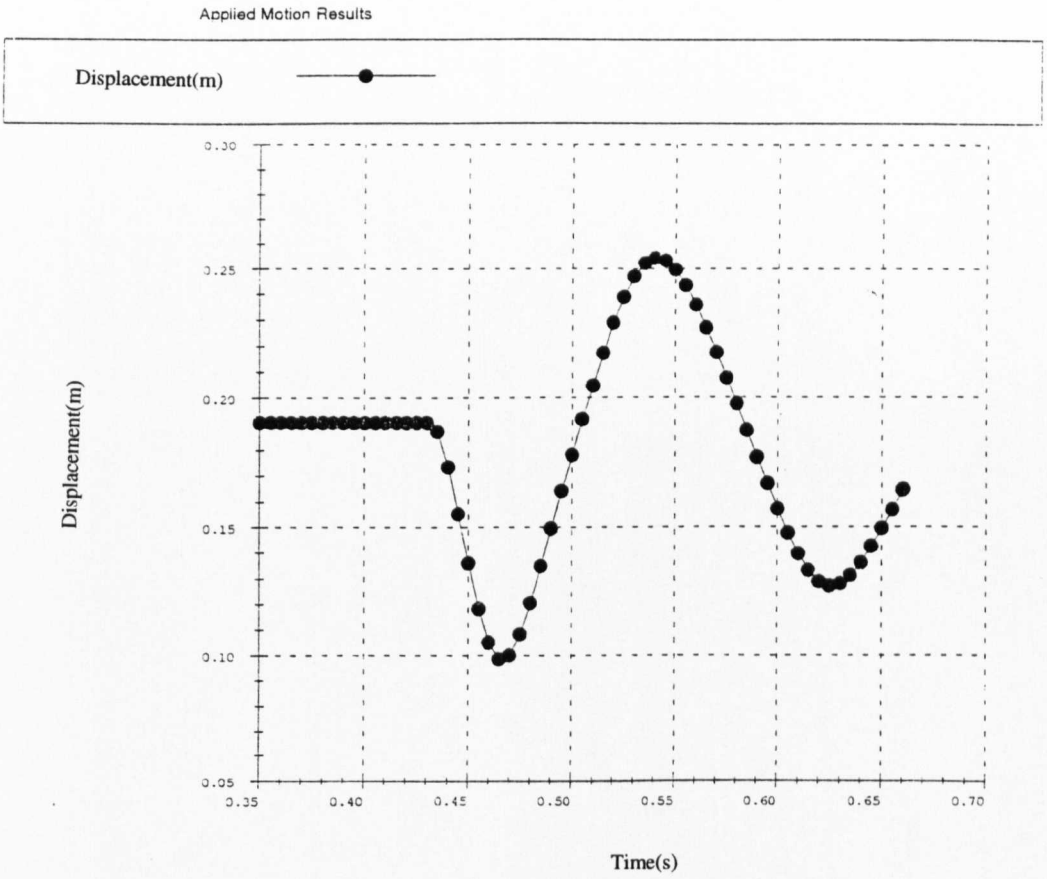

Figure 8.13 Displacement of packaged vacuum tube from simulation

Figure 8.14 to Figure 8.18 are the load-displacement relationships from simulation of the packaging system with different cushioning properties. These figures match those from the equations. The simulation of static and impact of the packaged vacuum tube and its load-displacement relationship are shown in Figure 8.19.

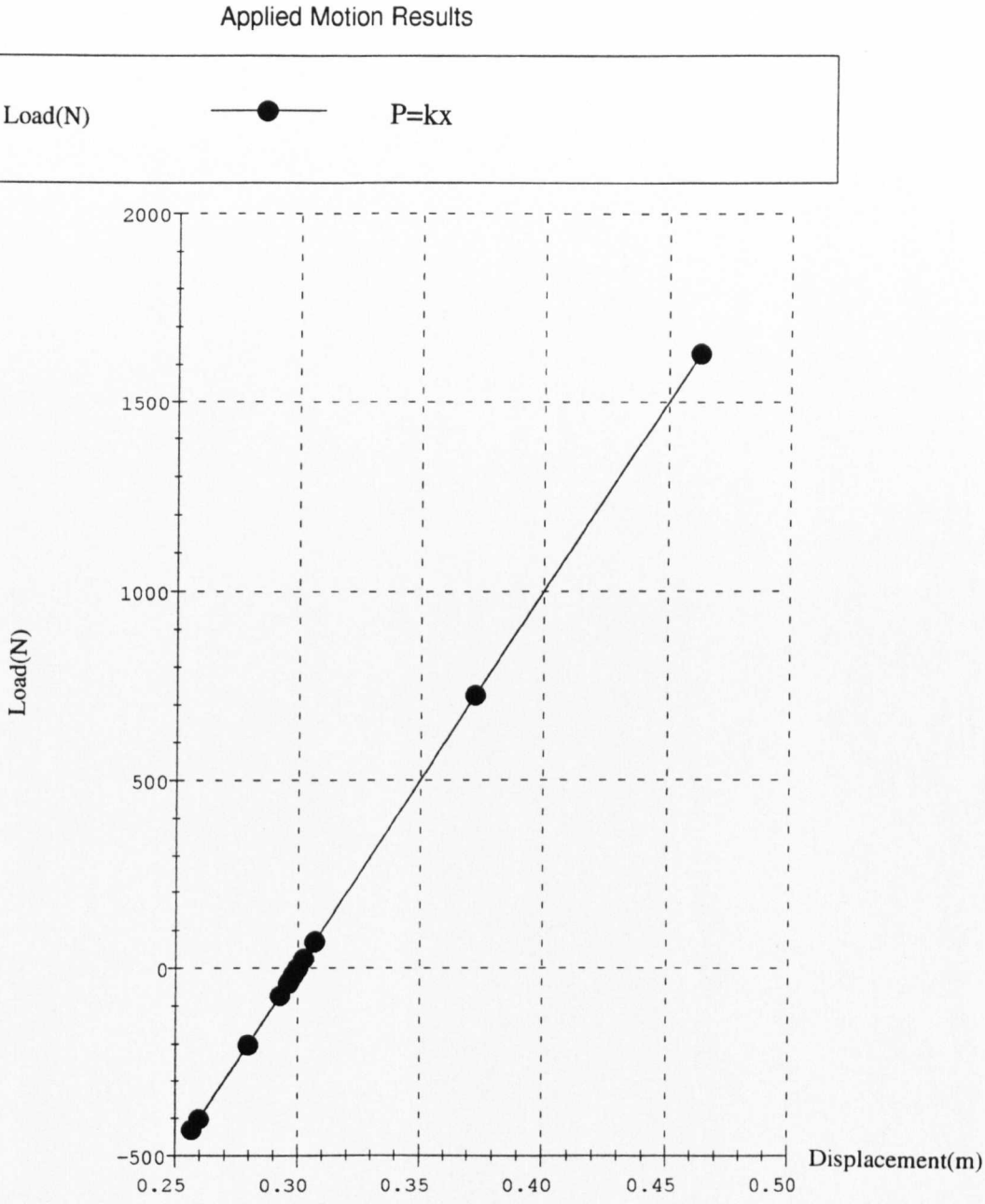

Figure 8. 14 Load-displacement relationship of linear cushioning

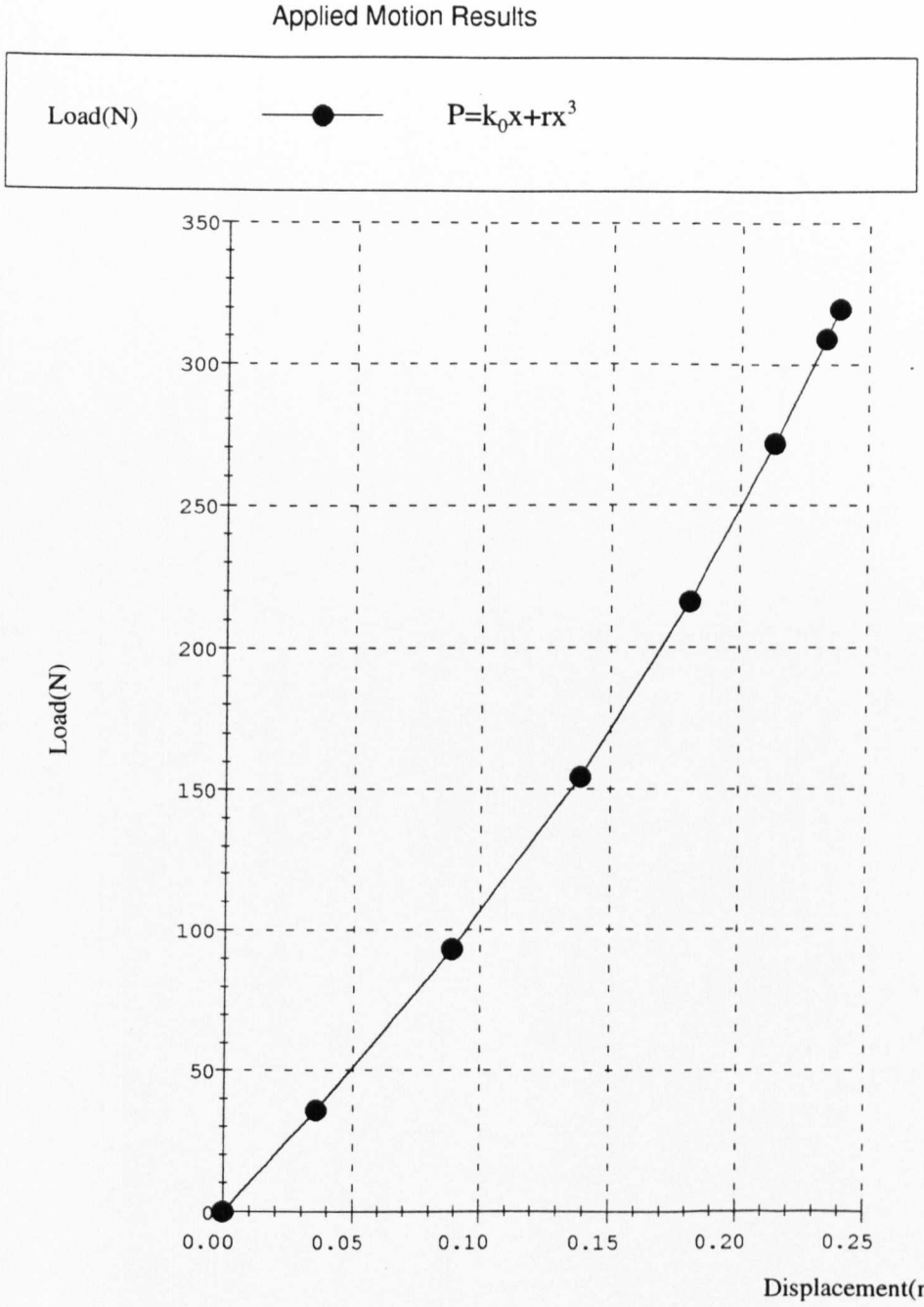

Figure 8.15 Load-displacement relationship of cubic cushioning

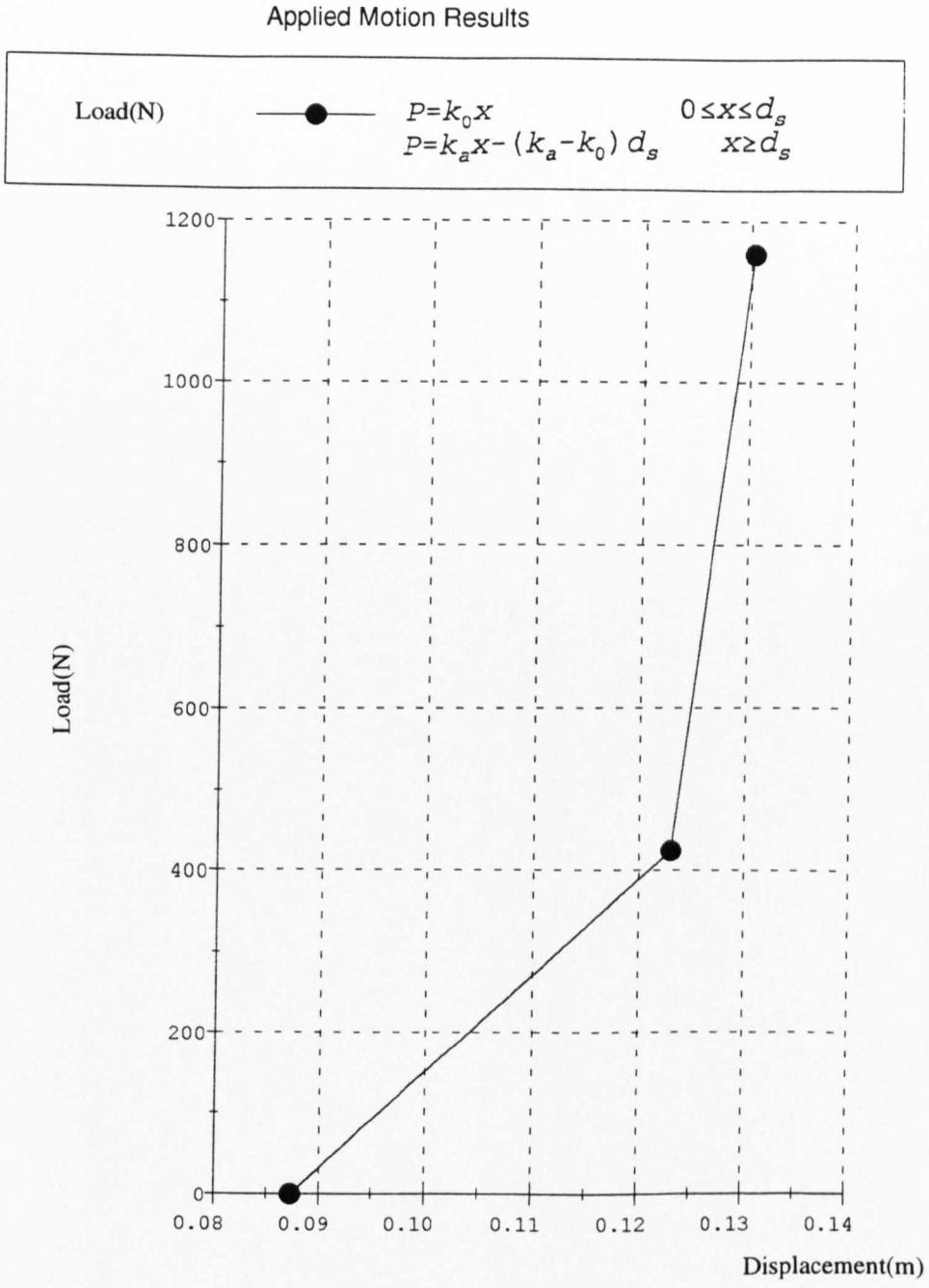

Figure 8.16 Load-displacement relationship of bi-linear cushioning

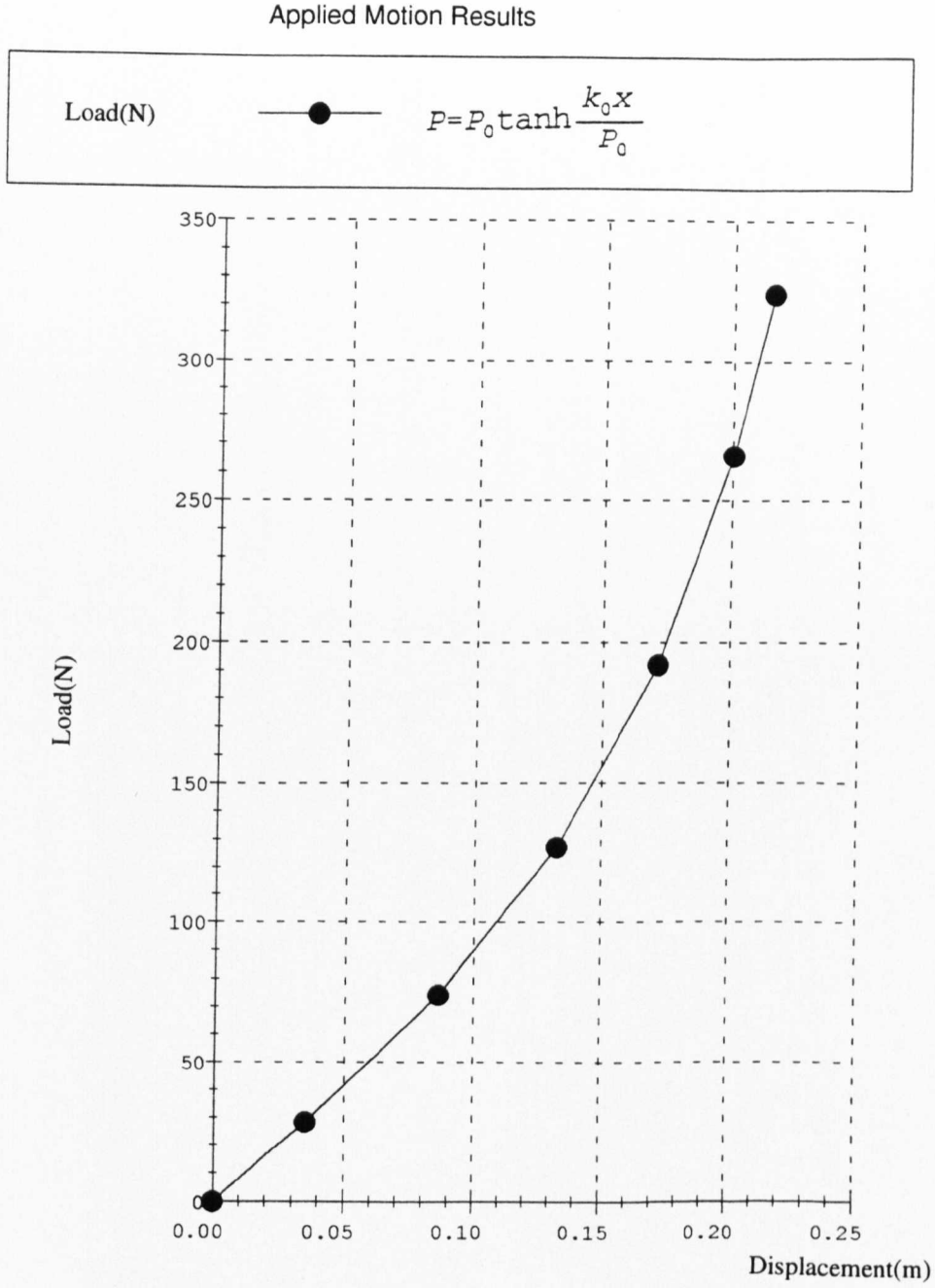

Figure 8.17 Load-displacement relationship of tangent cushioning

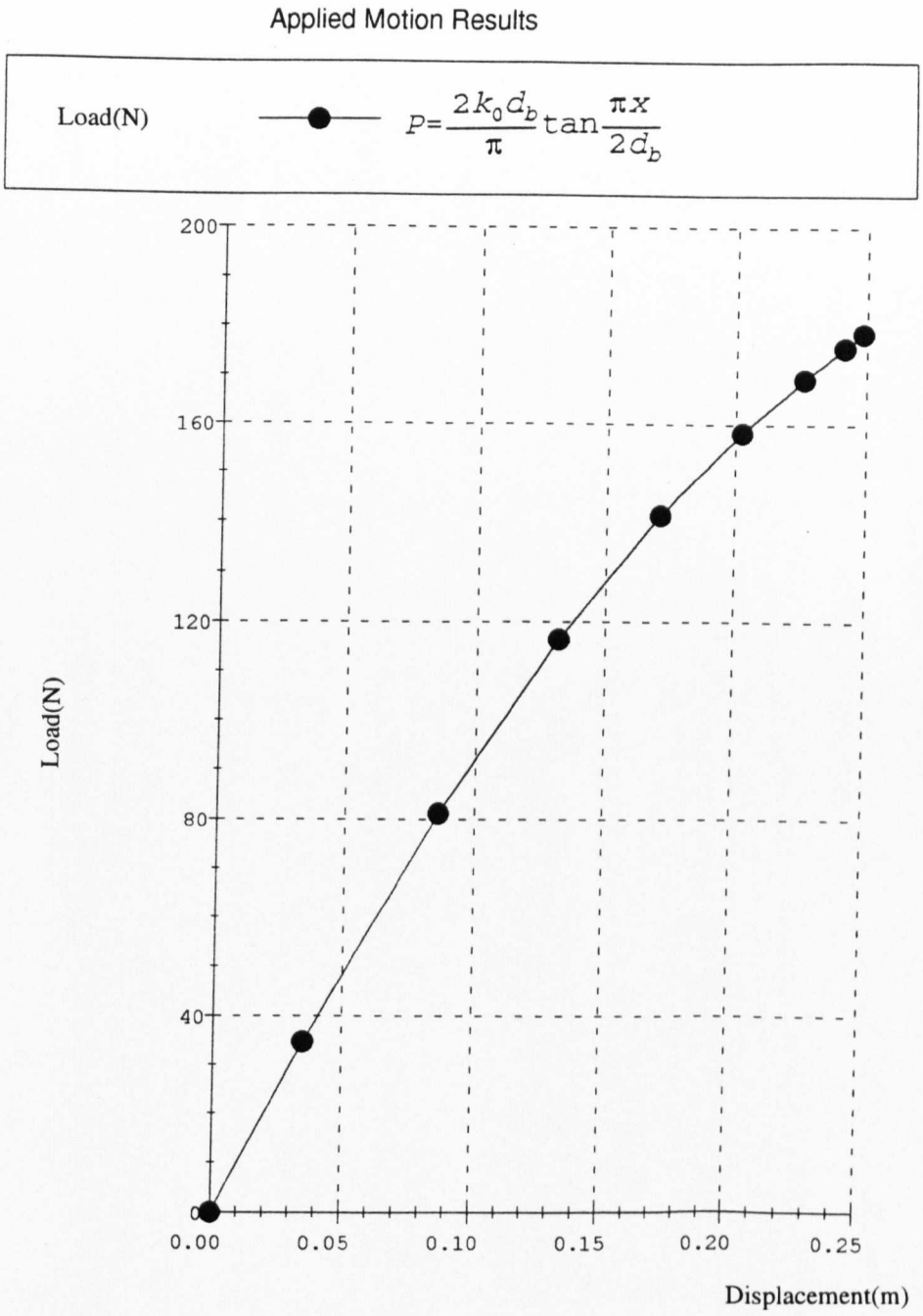

Figure 8.18 Load-displacement relationship of hyperbolic tangent cushioning

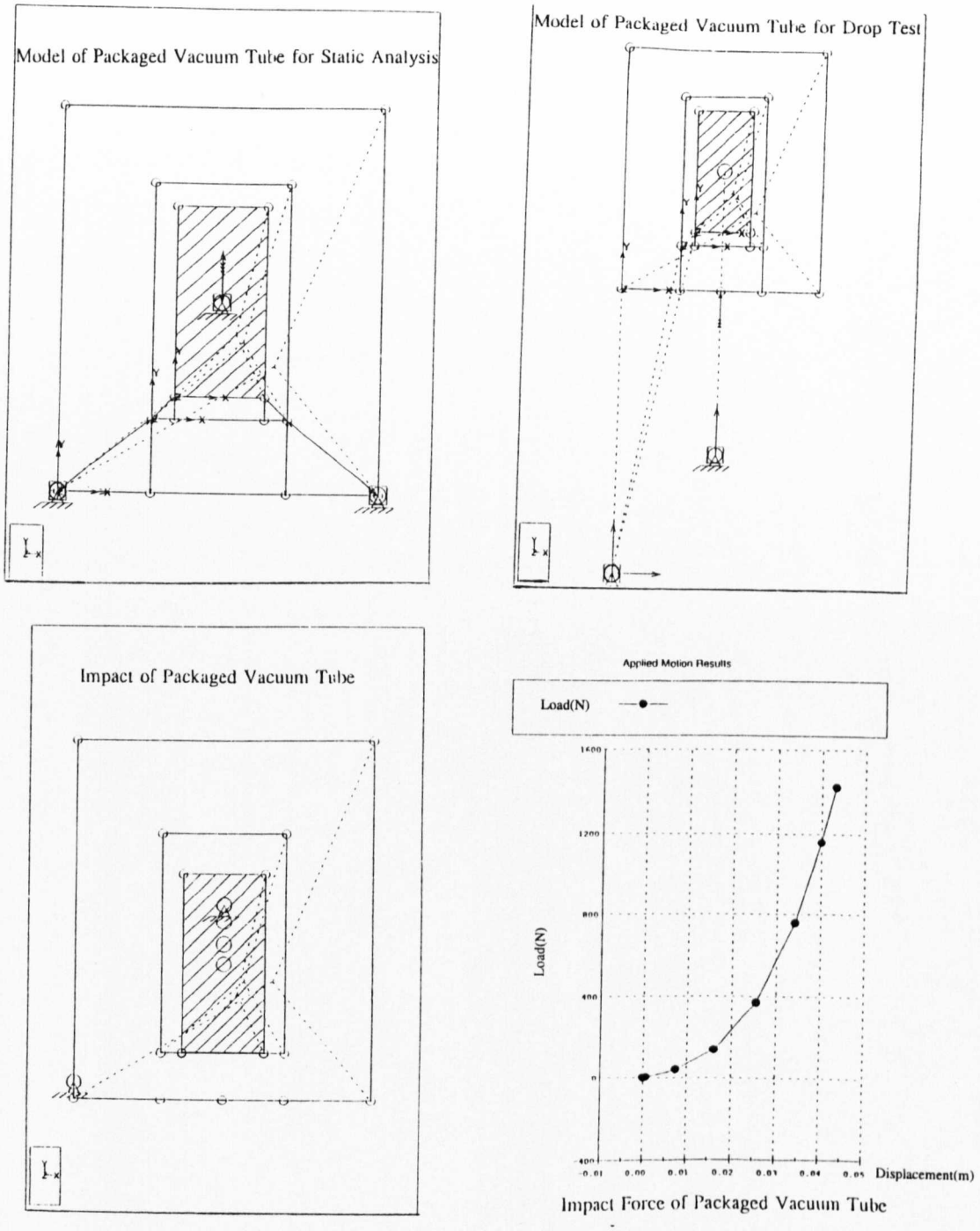

Figure 8.19 Simulation of the packaged vacuum tube

This section presents a method of finding the maximum acceleration and displacement of a packaged article for cushioning with non-linear elasticity. It also develops a model of simulation for a drop test. With the model, it is possible to vary the parameters of the structure and to compare different designs of a product-cushioning-package system, to suit different handling and transportation environments and different specifications of product. It is also possible to perform tests for very special packaging systems such as that used for an expensive product. Eventually it will indicate the ultimate design for the system.

8.5 Acceleration with linear cushioning

This section is concerned primarily with the motion of the packaged article with emphasis on linear and non-linear cushioning. The acceleration-time relationship under different cushioning characteristics, different velocity damping and friction.

The equation of motion for a mass m_2 controlled by a linear spring of rate k_2 and no damping is:

$$m_2\ddot{x}+k_2x=m_2g \tag{8.35}$$

Considering the initial conditions:

$$[x]_{t=0}=0 \qquad [\dot{x}]_{t=0}=\sqrt{2gh} \tag{8.36}$$

The solution of (8.35) is:

$$x=\sqrt{\frac{W_2^2}{k_2^2}+d_m^2}\ (\sin(\omega_2 t-\alpha))+\frac{w_2}{k_2} \tag{8.37}$$

where

$$\omega_2=\sqrt{\frac{k_2}{m_2}}=2\pi f_2=\frac{2\pi}{T_2} \qquad \alpha=\tan^{-1}\frac{g}{w_2\sqrt{2gh}}=\tan^{-1}\frac{w_2}{k_2 d_m} \tag{8.38}$$

ω_2 is the circular frequency and f_2 is the frequency and T_2 is the period of vibration of mass m_2 on the spring, d_m is the maximum displacement of m_2, w_2 is the weight of m_2. When neglecting the static displacement and differentiating equation (8.37) twice with respect to t, the acceleration is:

$$\ddot{x}=-\omega^2{}_2 d_m \sin\omega_2 t=-\omega_2\sqrt{2hg}\sin\omega_2 t \tag{8.39}$$

So the absolute magnitude of the maximum acceleration is:

$$G_m=\frac{|\ddot{x}|_{max}}{g}=\frac{\omega_2^2 d_m}{g}=\sqrt{\frac{2hk_2}{w_2}} \tag{8.40}$$

Equation (8.39) shows that the acceleration varies sinusoidally with time. The acceleration-time curve of the content from the model simulation are shown in Figure 8.20. The acceleration rises to maximum in a time $\pi/2\omega_2$ (=*0.07*sec.), at which time the displacement also reached its maximum value. The computer simulation developed using RASNA MECHANICA Applied Motion, enables the characteristics of the packaged item, cushioning, and the environment of the test to be defined by features in the software.

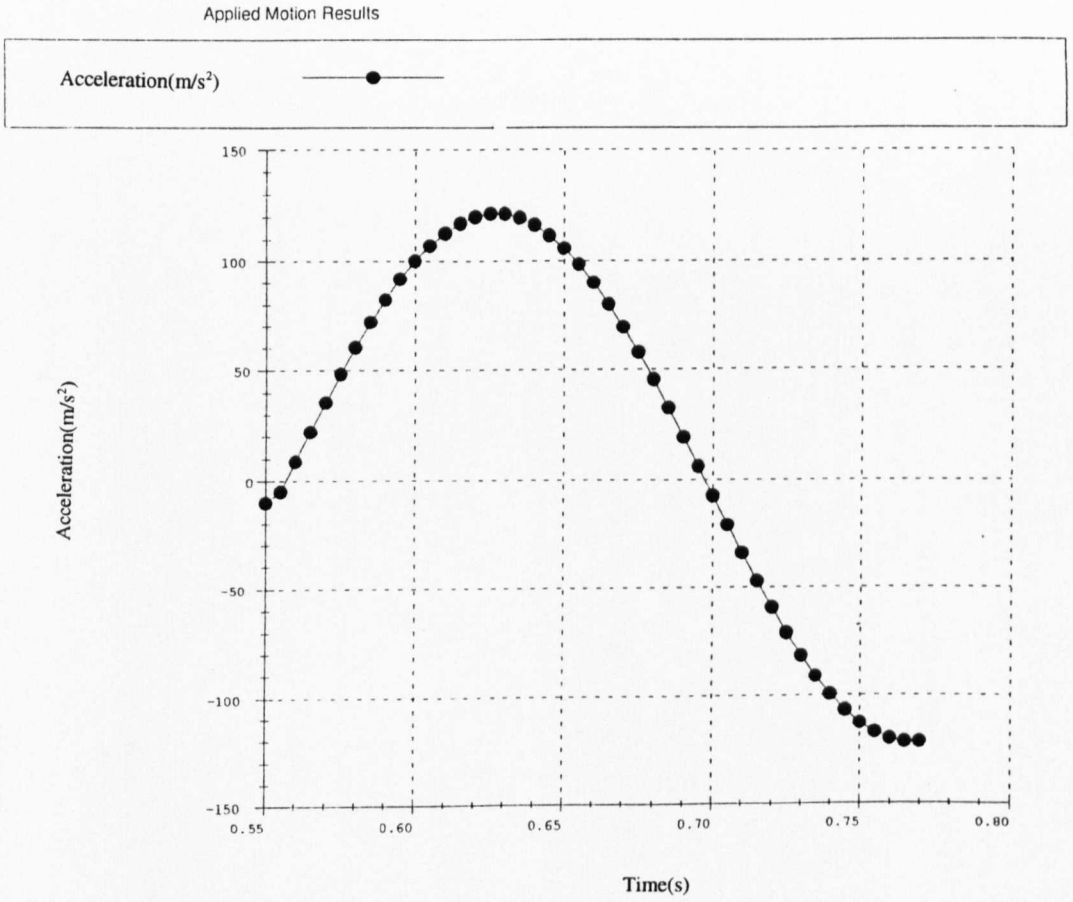

Figure 8.20 Acceleration-time curve for linear cushioning from simulation

8. 6 Acceleration with damping

In order to prevent large amplitudes and to reduce the maximum acceleration in a drop test, damping is necessary in the product-cushioning-package system. But there is an optimum amount of damping for a particular system.

Considering the model in Figure 8.2 with linear cushioning and damping proportional to velocity the equation of motion of m_2 during contact of the package with floor is:

$$m_2\ddot{x}+c_2\dot{x}+k_2x=m_2g \tag{8.41}$$

where c_2 is the damping coefficient of the cushioning. Considering g is very much smaller than $\ddot{x}$, the m_2g term can be neglected and the equation can be written as:

$$\ddot{x}+2\beta_2\omega_2\dot{x}+\omega_2^2x=0 \tag{8.42}$$

$$\omega_2=\sqrt{\frac{k_2}{m_2}} \qquad \beta_2=\frac{c_2}{2m_2\omega_2} \tag{8.43}$$

where ω_2 is the circular frequency of vibration of m_2 without damping and β_2 is the fraction of critical damping. $\beta_2=0$ means no damping and $\beta_2=1$ means, according to [2], just enough damping so that there will be no oscillation if the packaged item is displaced and released.

The solution of equation (8.42) is:

$$\ddot{x}=-\frac{\omega_2\sqrt{2gh}}{1-\beta^2_2}e^{-\beta_2\omega_2 t}\cos(\omega_2 t\sqrt{1-\beta_2^2}+\gamma) \tag{8.44}$$

where

$$\tan\gamma=\frac{2\beta^2_2-1}{2\beta_2\sqrt{1-\beta_2^2}} \tag{8.45}$$

If G_0 stands for the maximum number of g's (multiples of gravitation acceleration) without damping and G_m with damping. At t=0 :

$$\frac{G_m}{G_0}=2\beta_2 \tag{8.46}$$

After t=0,

$$\frac{G_m}{G_0}=e^{-\beta_2\omega_2 t} \tag{8.47}$$

See Appendix 2 for reference. The value of G_m/G_0 from equation(8.46) and (8.47) is plotted against β_2 in Figure 8.21.

By simulating the drop test of the model, the acceleration-time relationship of m_2

were found as a damped sinusoid (as shown in Figure 8.12).

Table 8.2 Acceleration with damping

C_2	0	8	16	24	32	40	48	54	78	89.44	110
β_2	0.00	0.08	0.18	0.27	0.36	0.45	0.54	0.58	0.87	1.00	1.23
G_m/G_0	1.00	0.88	0.81	0.78	0.79	0.85	0.98	1.09	1.53	1.72	2.05

The influence of damping on maximum acceleration in Figure 8.21, presented by Mindlin[19], shows that as the damping is increased from zero, the maximum acceleration first decreases to a minimum of *78%* of G_0 and then increases to G_0 at β_2=*0.6*. For β_2<*0.6* the maximum acceleration occurs after *t=0*. For damping β_2>*0.6* the maximum acceleration occurs at the instant of contact and increases in direct proportion to β_2.

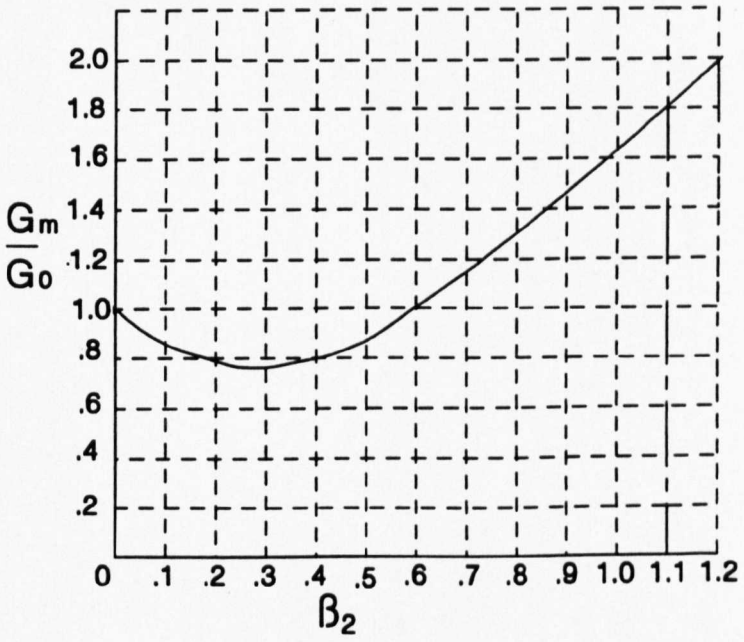

Figure 8.21 Influence of velocity damping on maximum acceleration

8.8 Summary

The study and simulation of a packaging system were described in this chapter, and some conclusions are as follows:

1 A computer aided design and simulation procedure was presented for analysing the packaging system using MECHANICA software.

2 A package-cushion-product system was developed for both the theoretical derivation and simulation of a drop test.

3 Six types of linear and nonlinear cushioning characteristics were identified. The simulation of these cushioning system achieved satisfactory results compared with theoretical work.

4 The methods for simulating the acceleration-time relationships of a packaged product with linear and nonlinear elasticity and different damping were presented. The influence of the cushioning and the damping on the product was discussed.

5 The friction force within the system and the influence of it on the product were simulated and discussed.

6 An application of the discussed model was evaluated and found to be satisfactory. With the model it is possible to vary the parameters of the structure and to compare different design of product-cushioning-package systems to suit different handling and transportation environments with different specification of the product. It is possible to perform simulations for very special packaging system such as that for an expensive product. Hence to be able to choose the optimum design for the system.

Chapter 9

Conclusion and Further Work

9.1 Conclusions

The work carried out in this study has sought to develop a better understanding of the kinematics and dynamics of packages with discrete contents and the structural behaviour of corrugated fibreboard. The primary objective of the project was to complete a successful simulation of a packaged system, by which the size of the cushion structure could be minimized and the cushion and package materials can be selected appropriately.

1. A Finite Element simulation of the structural properties of corrugated fibreboard has been developed using commercial software. A simplified model was set up and the simulation of stress, strain, deformation and buckling have been carried out.

2. A series of tests of corrugated fibreboard and container elements have been carried out with regard to buckling and compression. The results from the simulation and tests have been compared and give encouragement that this approach is feasible.

3. A comprehensive technique for modelling the collision behaviour of a body colliding with a surface has been developed using Mechanica software 'Applied Motion'. This makes it possible to investigate and evaluate the load/deformation created by internal/external forces and relate this to material properties.

4. Some initial development of theoretical analysis and simulation methods were required to simulate the movement of 2D and 3D package-contents systems and are presented. The system reacted to external forces including friction in a satisfactory

manner. Giving the possibility for further computer simulation of real package system.

5. A model of a product-cushion-package system which demonstrated the impact parameters such as acceleration, velocity and impact forces has been developed and the measure of the susceptibility to damage to the content has been discussed.

This project has developed computer simulation techniques which would be useful in the packaging industry to maintain integrity of packages and contents subject to handling and distribution hazards. The model of the drop test of a product-cushion-package system can perform a series of simulations with the possibility of optimising the cushioning with reference to the drop height, orientation of the package, package materials, and the characteristics of the cushioning. The model of the corrugated fibreboard and container element presents the ability with computer simulation to evaluate the materials properties of the board and investigate factors such as buckling and deformation, which are crucial considerations in the stacking of packages. Finite Element analysis of complete containers using knowledge developed from this work has proved accurate in predicting bulge in large heavy duty containers and has enabled competitive designs to be developed.

9.2 Further Work

In order to complete a comprehensive packaging design procedure, some further work needs to be carried out.

1. Further Finite Elements modelling of the structure of corrugated fibreboard to investigate geometry and the composition of the board elements to determine the overall material properties of the board.

2. Finite Element modelling of the real structure of a corrugated fibreboard container, taking into account the method of construction including the different joints, to determine the structural properties.

3. Set up a geometric database for corrugated fibreboard and container with regard to different flute type, liner and medium thickness and properties. That can be used for Further Finite Element analysis.

4. The drop tests for a package with cushion and packaged article to be carried out with a fully instrumented rig to compare the results with those from analysis and simulation to investigate the accelerations of the packaged article.

5. To develop a knowledge based system for material selection for package and cushion regarding to their structure and size.

References

1 Hanlon, J.F. "*Handbook of Package Engineering*", 2nd ed., McGrawHill, New York, 1984

2 Foxboro, Y. A. "*The Corrugated Industry Today and Tomorrow*", Paper, December 1983, pp. 21-26.

3 Covell, P. "*Boxes Built to Help Handling*", Materials Handling News, April 1987, pp. 27-32.

4 Morris, R. M. "*The Status of Rules 41*", Paperboard Packaging, August 1978, pp. 72-75.

5 Scott, R. A. "*Towards an International Standard Method for the Edgewise Compression Test of Corrugated Board*", Appita 40, November 1987, pp. 436-438.

6 King, F. W. "*Fefco Standard Grades of Board*", ICCA Proc., International Technical Conference on Corrugated Cases, May 1975, pp. 51-53

7 McKee, R.C., Gander, J.W., Wachuta, J.R., "*Compression Strength Formula for Corrugated Boxes*", Paperboard Packaging, Vol. 48, August 1963, P149-159.

8 Uniform Freight Classification Committee, "*Uniform Freight Classification 6000E*", Chicago, Uniform Freight Classification Committee, 1988, ?????

9 Jonson, G. "*Utilizing Linear/Medium Weight in Corrugated Board for Best Box Performance*", Boxboard Containers, June 1985, pp. 23-25.

10 Boonyasarn, A. "*The Effect of Cyclic Environments on the Compression Strength of Boxes Made from High Performance Corrugated Fibreboards*", M.S. Thesis, School of Package, Michigan State University, Lansing, 1990

11 Cavlin, S., and Fellers, C., "*A New Method for Measuring the Edgewise Compression Properties of Paper*". Svensk Papperstidning, No. 9, 1975, pp. 329-332.

12 Stott, R. A., "*A Comparison of Edgewise Compression Test Methods*", Appita, Vol.29, 1975, pp. 29-32.

13 Eriksson, L. E., "*A Review of the Edge Crush Test of Corrugated, Part I*", Boxboard Containers, Vol. 86, March 1979, pp. 34-39

14 Eriksson, L. E., "*A Review of the Edge Crush Test of Corrugated Board-Part II*", Boxboard Containers, Vol. 86, 1979, pp. 64-67.

15 Kroeschell, W.O., "*The Edge Crush Test of Corrugated Board:Development of TAPPI Test Methods T 811 and T 823*", Tappi, Vol. 67, 1984, pp. 56-59

16 Stockmann, V. E., "*Edgewise Compressive Strength of Paper: A Physical or Structural Property?*" Tappi Annual Meeting Preprint, p15, Mar. 1976, pp. 257-264.

17 Peterson, W. S. and Schimmelpfenning, W.J., "*Panel Edge Boundary Conditions and Compressive Strengths of Tubes and Boxes*", Tappi. Vol. 65, No. 8, August 1982, pp. 108-110.

18 McKee, R. C., Gander, J. W., and Wachuta, J. R., "*Flexural Stiffness of*

Corrugated Board". Paperboard Packaging, December 1962, pp. 111-118

19 Mindlin, R. D., "*Dynamics of Package Cushioning*", Bell System Technical Journal, P353, 1945.

20 Weiner, H. M., "Military Package in the United States", Inst. of Packaging Journal, October 1959, pp.24-38.

21 Maltenfort, G. G., "*The Structural Aspects of Corrugated Board*". Tappi, Vol. 53 No. 7, July 1970.

22 Singh, S. P., Crofts, B., and Burgess, G. "*The Effect of Handling on the Compression Strength of Corrugated Fibreboard Containers*", Journal of Testing and Evaluation, February 1991, pp. 374-378.

23 Singh, S.P., Burgess, G., and Langlois, M. "*Compression of Single-Wall Corrugated Shipping Containers Using Fixed and Floating Test Platens*", Journal of Testing and Evaluation, October 1991, Vol. 20, pp. 318-320.

24 Sayir, M. B., Hausler, K. and Partl, M. "*Impact Behaviour of Corrugated Sheets of Fibre-reinforced Cement*", Composites, November 1992, pp. 441-452.

25 Butler, N. "*Impact Strength of Containers for Carrying Radioactive Materials*", The Nuclear Engineer, Vol. 33, No. 5, 138-145.

26 Fox, T. S., "*Shipping Containers and Cartons Shown to Fail Only in Compression when Loaded Internally*, Part I", Paperboard Packaging, March 1978, pp. 23-36.

27 Fox, T. S., "*Shipping Containers and Cartons Shown to Fail Only in Compression when Loaded Internally, Part II*", Paperboard Packaging, March 1978, pp. 23-36.

28 Fox, T. S., "*Shipping Containers and Cartons Shown to Fail Only in Compression when Loaded Internally*, Part III", Paperboard Packaging, March 1978, pp. 23-36.

29 Peterson, W. S., "*Unified Container Performance and Failure Theory*", Tappi, Nov. 1980, pp. 115-121

30 Peterson, W. S., "*Component Properties and Container End Use Performance-Part One*", Southern Pulp and Paper Manufacturer, October 1979, pp. 16-19.

31 Peterson, W. S., "*Component Properties and Container End Use Performance-Part Two*", Southern Pulp and Paper Manufacturer, November 1979, pp. 20-24.

32 Peterson, W. S., "*Component Properties and Container End Use Performance-Part Three*", Southern Pulp and Paper Manufacturer, December 1979, p 38-42.

33 Peterson, W. S., "*Component Properties and Container End Use Performance-Part Four*", Southern Pulp and Paper Manufacturer, January 1980, pp. 23-37.

34 Konning, J.W., "*Compressive Properties of Linerboard as Related to Corrugated Fibreboard Containers: A Theoretical Model*" , Journal-Tappi, Vol. 58, 1975, pp. 105-108.

35 Plooy, A.B.J., "*Comments on Selected Publications Regarding the Prediction of Corrugated Box Compression Strengths*", Paper Southern Africa, April

1990, pp. 22-36.

36 Carlsson, L., Fellers, C., and Jonsson, P., "*Bending Stiffness of Corrugated Board Under Special Consideration of Asymmetrical and Multiply Construction*", Das Papier, Vol. 39, 1985, pp.153-156

37 Geibler, E. and Weber, H., "*Computer-aided Package Design for Sensitive Products*", Packaging Technology and Science, Vol 4,1991, pp. 311-314.

38 Pommier, J. C., Poustis, J., Fourcade, E. and Morlier, P., "*Determination of The Critical Load of A Corrugated Cardboard Box Subjected to Vertical Compression By Finite Element Methods*". International Paper Physics Conference,1991, pp. 437-447.

39 "*Packaging Specifications*", Pira International, November 1993.

40 Wang, C. T., "*Applied Elasticity*", McGraw-Hill Publishing Company LTD, New York, London, 1953

41 Maltenfort, G. G., "*How Are We Progressing with The Corrugated Column Crush Tests?*". Package Engineering 7(6). pp. 75-81, 1961.

42 Maltenfort, G. G., "*The Structural Aspects of Corrugated Board*". Tappi, Vol. 53 No. 7, July 1970.

43 Maltenfort, G. G., "*Optimum Package Dimensions Save Board, Part One*". Package Engineering, June 1961.

44 Maltenfort, G. G., "*Optimum Package Dimensions Save Board, Part Two*".

Package Engineering, July 1961.

45 Maltenfort, G. G.,"*Put Strength in Corrugated Box Without Wasting Any Board*". Package Engineering, October 1969.

46 Marcondes, J. A., "*Procedure to Determine Optimum Dimensions of Packages*", Packaging Technology and Science, Vol. 4, 1991, pp. 139-144.

47 Maltenfort, G. G., "*Compression Strength of Corrugated Containers: Part I*", Fibre Containers, July 1956, pp. 44-57.

48 Maltenfort, G. G., "*Compression Strength of Corrugated Containers: Part II* ", Fibre Containers, September 1956, pp. 60-74.

49 Kellicutt, K. Q., and Landt, E. F., "*Basic Design Data for The Use of Fibreboard in Shipping Containers*". Forest Products Laboratory Report 1911, 1958.

50 Pommier, J. C., and Poustis, J., "*Carton Encasement Material Performance Results*", Revue A.T.I.P., Vol.40, 1986, pp. 397-400

51 Stockmann, V.E., "*Measurement of Intrinsic Compressive Strength of Paper*", Tappi, July 1976, pp. 93-97.

52 Moody, R.C.,"*Edgewise Compressive Strength of Corrugated Fibreboard as Determined by Local Instability*", Forest Prod. lab. Res, Paper 46, 1965, pp. 1-8.

53 Setterholm, V.C., and Gertjejansen,R.O., "*Method for Measuring the Edgewise*

Compressive Properties of Paper", Tappi, May 1965, pp. 309-313.

54 Douglas, N.B., "*Modelling Impacts with Applied Motion*", Applied motion papers

55 Douglas, N. B. "*Modelling Friction in Applied Motion*", Applied Motion Application, Sep. 1992.

56 Sun, J.Y., Newlyn, H. A., "*Simulation of the Impact behaviour of a Package with Dicrete Contents*", Advances in Engineering Software, Vol.31, December 1995, pp. 129-131

57 Sun, J. Y., Newlyn, H. A., and Knight, J. A. G., "*A Model of Product Cushion-Package System*", Proceeding of 8th Symposium on INCOM'95 held by IFAC, October 11-13, 1995, Beijing, China, pp277-280

58 Teper, W.W., Sauve,R.G. "*Simplified Method for Predicting Impact Loads of Solid-walled Transportation Packagings for Radioactive Materials*", Journal of Pressure Vessel Technology, Vol.111, 1989, pp. 138-143

59 Mannheim,C.H., Passy,N. "*Interaction Between Packaging Materials and Foods*", Packaging Technology and Science, Vol. 3, 1990.

60 Guild, F.J., "*The Prediction of Three-Dimensional Properties of Composite Laminates Using the Finite Element Analysis Methods*", Composite Structure, 6 Edited by I. H. Marshall (Eleevier Applied Science), London, 1991, pp. 811-825.

61 Maltenfort, G. G., "*Axial Corrugating: A Follow-Up*", Paperboard Packaging,

July 1983, pp. 45-48.

62 Maltenfort, G. G., "*Compression Strength of Corrugated Containers: Part III* ", Fibre Containers, October 1956, pp. 52-59.

63 Timoshenko, S., "*Theory of Plates and Shells*", McGraw-Hill Book Company. Inc. New york and London, 1940.

64 Guise, B., "*Packaging in Corrugated Containers*", Food Processing, december 1983, pp. 35-38.

65 Ihara, T., Shaw, M.C., and Bh*ushan, B.,"A Finite Element Analysis of Contact Stress and Strain in an Elastic Film on a Rigid Substrate-Part Two: Zero Feriction*", Journal of Tribology, October 1986, pp. 534-539.

66 Shrivastava, S., and Tang, J., "*Large Deformation Finite Element Analysis of Non-Linear Viscoelastic Membrances with Reference to Thermoforming*", Journal of Strain Analysis, Vol. 28, No. 1, 1993, pp. 31-51.

67 Smaili, A.A., "*A Three-Node Finite Element Beam Element for Dynamic Analysis of Planar Manipulators with Flexible Joints*", Mech. Mach. Theory, Vol. 28, No. 2, pp. 193-206.

68 Contrl, P., and Schrefler, B.A., "*A Geometrically Nonlinear Finite Element Analysis of Wrinkled Membrance Surfaces by A No-Compression Material Model*", Communications in Applied Numerical Methods, Vol. 4, 1988, p.5-15.

69 Huh, H., and kwak, Y. K., "*Finite Element Stress Analysis of the Reinforced Tire Contact Problem*", Computers and Structures, Vol. 36, No. 5, 1990, pp.

871-881.

70 Chang, Y. B., Yang, T. Y., and Soedel, W., "*Dynamic Analysis of A Radial Tire by Finite Element and Model Expansion*", Journal of Sound and Vibration, 96(1), 1984, pp. 1-11.

71 Alaylioglu, A., "*A Finit Element Code for thin Plate Dynamics*", Mathematics and Computers in Simulation, Vol. 30, 1988, pp. 429-440.

72 Quinn, D. W., "*A Finite Element Method for Computing Sound Propagation in Ducts*", Mathematics and Computers in Simulation, Vol. 29, 1987, pp. 51-64.

73 Chang, Y. B., Yang, T. Y., and Soedel, W., "*Linear Dynamic Analysis of Evolutional Shells Using Finite Element and Model Expansion*", Journal of Sound and Vibration, 86(4), 1983, pp. 523-538.

74 Murakoshi, H., Ide, H., and Nishihata, S., "*An Approach to Vehicle Pull Using a Tire Finite Element Model*", Tire Science and Technology, TSTCA, Vol. 20, No. 4, October-December, 1992, pp. 212-229.

75 Saran, M. J., and Wagoner, R. H., "*A Consistaent Implicit Formulation for Nonlinear Finite Element Modelling With Contact and Friction:part II Numerical verification and Results*", Journal of Applied Mechanics, June 1991, Vol. 58, pp. 507-512.

76 Lin Y. H., and Trethewey, M. W., "*Finite Element Analysis of Elastic Beams Subjected to Moving Dynamic Loads*",Journal of Sound and Vibration, Vol. 136, 1990, pp. 323-342.

77 Potts, D. M., Dounias, G. T., and Vaughan, P. R., "*Finite Element Analysis of the Direct Shear Box Test*", Geotechnique, Vol. 37, No. 1, 1987, pp.11-23.

78 Ali, S., and Page, A. W., "*Non-linear Finite Element Analysis of Masonry Subjected to Concentrated Load*", Proc. Instn Civ. Engrs, Part 2, 1987, Vol. 83, pp. 815-832.

79 Germain, Y., Chung, K. and Wagoner, R. H., "*A Rigid-viscoplastic Finite Element Program for Sheet Metal Forming Analysis*", International Journal of Mechanical Sciences, Vol. 31, No. 1, 1989, pp. 1-24.

80 Bennett, P.G., and McKinlay, P.R., Appita Conference, pp. 149-163

81 Rhodes, J., "*Microcomputer Design Analysis of Plate Post-Buckling Behaviour*", Journal of Strain Analysis, Vol 21, No 2 1986, pp. 71-76.

82 Wang, J.T., and Ngo, T., "*Modelling of Passenger Side Airbags with A Complex Shape*", General Motors Research Publication No. GMR-6152, Jan 1990, SAE Paper No.900545.

83 Akasaka, T., Kabe, K., Koishi, M., and Kuwashima, M., "*Analysis of the Contact Deformation of Tread Blocks*", Tire Science and Technology, TSTCA, Vol. 20, No. 4, October-December, 1992, pp. 230-253.

84 Kaga, H., Okamoto, K., and Tozawa, Y., "*Stress Analysis of a Tire Under Vertical Load by a Finite Element method*", Tire Science and Technology, TSTCA, Vol. 5, No. 2, May 1977, pp. 102-118.

85 Abdelhamid, M. K., McConnell, K.G. "*A Computer Method for Simulation*

Service Loads", Experiment Mechanics, March 1986. pp. 41-47.

86 Anosova,J.P. "*Computer Simulations in the General Three-body Problem, the Theoretical Bases of the Studies*", Celestial Mechanics and Dynamical Astronomy, Vol 48, pp. 357-368.

87 Yang, K. H., Wang, H. "*Two-D model of Airbag Development*", ASCE Engineering Mechanics Specialty Conference on Mechanics Computing, 1990, New York.

Appendix

Appendix 1. Time-Position Relationship of the Colliding Body

The governing equation on impact is:

$$\ddot{y}+\frac{c}{m}\dot{y}+\frac{k}{m}y=g \tag{A1}$$

in which m=2.6 kg, c=2 kg/s, k=200 kg/s^2, let a=c/m and b=k/m. A particular solution for equation (A1) is:

$$y=\frac{mg}{k}=0.01275 \tag{A2}$$

Since $a^2-4b<0$, so the general solution for equation (A1) is:

$$y=e^{\alpha t}(C_1\cos\beta t+c_2\sin\beta t) \tag{A3}$$

The solution for equation (A1) is:

$$y=e^{\alpha t}(C_1\cos\beta t+c_2\sin\beta t)+0.01275 \tag{A4}$$

where $\alpha=-a/2=-c/2m=-3.84$, $\beta=(4b-a^2)^{1/2}/2=27.47$. Using the boundary conditions the values of c_1, c_2, α and β can be decided.

When t=0 and y=0: $c_1=-0.01275$,

When t=0, $\dot{y}=(2hg)^{1/2}=10.8\text{m/s}^2$, h=60mm is the height of the body above the surface initially, and g is the acceleration due to gravity. By differentiating the both sides of equation (A4) , gives:

$$\dot{y}=\alpha e^{\alpha t}(c_1\cos\beta t+c_2\sin\beta t)+e^{\alpha t}(-c_1\beta\sin\beta t+c_2\beta\cos\beta t) \quad \text{(A5)}$$

Substituting the above values into equation (A5), and produces c_2=0.39.

When ẏ=0, the body reaches the lowest point, and the time spent from the body touching the surface to the lowest point can be calculated by equation (A5) and is found to be t=0.0533 second. The position of the body at every moment after impact can be calculated from equation (A4) and are shown in Table A1.

Table A1 Time-position of the colliding body

t(s)	0	0.01	0.02	0.033	0.04	0.05	0.06
y(mm)	0	0.1276	0.1935	0.2652	0.3092	0.3253	0.3626
t(s)	0.07	0.08	0.09	0.10	0.11	0.12	0.13
y(mm)	0.2992	0.2533	0.1931	0.1113	0.0520	0	-0.0304

When on rebound the governing equation is:

$$\ddot{y}+\frac{c}{m}\dot{y}+\frac{k}{m}y=g \quad \text{(A6)}$$

The solution of it is the same as equation (A4). The initial conditions are t=0, $y=y_{max}$=0.325mm, and t=0, ẏ=0. Using the times shown in Table A1, the position of the body have been calculated and found to be very well matched with the output of the simulation shown in Figure 5.7.

Appendix 2. G_m and G_0 Relationship

If t=0, There is:

$$e^{-\beta_2\omega_2 t}=1 \tag{A7}$$

$$\ddot{x}=\frac{-\omega\sqrt{2gh}}{\sqrt{1-\beta_2^2}}\cos(\gamma) \tag{A8}$$

From equation (8.37),

$$\cos(\gamma)=\frac{2\beta_2\sqrt{1-\beta_2^2}}{\sqrt{4\beta_2^2(1-\beta_2^2)+(2\beta_2^2-1)^2}}=2\beta_2\sqrt{1-\beta_2^2} \tag{A9}$$

Substitute equation (A9) into equation (A8), there is:

$$\ddot{x}=-2\omega_2\beta_2\sqrt{2gh} \tag{A10}$$

So

$$2\beta_2=-\frac{\ddot{x}}{\omega_2\sqrt{2gh}}=-\frac{\ddot{x}}{\sqrt{\frac{2g^2hk_2}{m_2g}}}=-\frac{\ddot{x}}{g\sqrt{\frac{2hk_2}{w_2}}}=\frac{(-\frac{\ddot{x}}{g})}{G_0}=\frac{G_m}{G_0} \tag{A11}$$

After t=0, when maximum acceleration occurs there is:

$$\ddot{x}=\frac{\omega_2\sqrt{2gh}}{\sqrt{1-\beta_2^2}}e^{-\beta_2\omega_2 t} \qquad \text{(A12)}$$

Since $\omega_2=(k_2/m_2)^{1/2}$, $(1-\beta_2^2)^{1/2}\approx 0$, equation (A12) becomes:

$$\ddot{x}=\sqrt{\frac{2ghk_2}{m_2}}e^{-\beta_2\omega_2 t}=g\sqrt{\frac{2gk_2}{mg}}e^{-\beta_2\omega_2 t}=gG_0e^{-\beta_2\omega_2 t} \qquad \text{(A13)}$$

Appendix 3. Publications from This Work

1. J.Y.Sun, H.A.Newlyn, "*Simulaion of the Impact Behaviour of A Package with Discrete Contents*". Journal of Advances Engineering Software, Vol. 31 December, 1995, pp. 129-131.

2. J.Y.Sun, H.A.Newlyn, and J.A.G.Knight, "*A Model of Product-Cushion-Package System*", Proceedings of 8th Symposium on INCOM'1995 held by IFAC,October 11-13, 1995, Beijing, China, pp.277-280.

3. J.Y.Sun, H.A.Newlyn, "*Modelling of Dynamics of Packaging System*", Proceedings of 11th National Conference on Manufacturing Research. 12-14 September 1995, Leicester, UK, pp.433-437

4. H.A.Newlyn, J.Y.Sun, "*Computer Simulation of Impact of Packaging System*", won the best presentation prize on the 2nd ProMechanica UK User Conference, Coventry, March 1995, UK